MATERIALS SCIENCES CORPORATION

NASA CR-145039

(MSC/TFR/601/1025)

FATIGUE OF NOTCHED FIBER COMPOSITE LAMINATES

PART II: ANALYTICAL AND EXPERIMENTAL EVALUATION

By

S. V. Kulkarni, P. V. McLaughlin, Jr.,
and R. B. Pipes

Prepared under Contract No. NAS1-13931

for

NASA
National Aeronautics and
Space Administration

FATIGUE OF NOTCHED FIBER COMPOSITE LAMINATES

PART II: ANALYTICAL AND EXPERIMENTAL EVALUATION

By S. V. Kulkarni, P. V. McLaughlin, Jr.,
and R. B. Pipes

Prepared under Contract No. NAS1-13931

by

MATERIALS SCIENCES CORPORATION
Blue Bell, PA 19422

for

NATIONAL AERONAUTICS AND SPACE ADMINISTRATION

FOREWORD

This report summarizes the work accomplished by the Materials Sciences Corporation under NASA Contract NAS1-13931. Mr. G. L. Roderick (US AAMRDL, Langley Directorate) was the NASA Project Engineer.

The authors would like to gratefully acknowledge the many helpful suggestions made by Mr. G. L. Roderick and Dr. B. Walter Rosen (Materials Sciences Corporation) during this program.

TABLE OF CONTENTS

TABLE OF CONTENTS (contd.)

SYMBOLS

a	-	half width of notch;
A_f	-	fiber cross-sectional area;
$B_{1...4}$	-	function of n^*, r, $\gamma_{1,2}$, $\beta_{1,2}$, G_R;
c	-	superscript indicating compressive stress;
$C_{1...9}$	-	constants;
d	-	fiber or yarn-bundle spacing;
E_f	-	fiber Young's modulus;
E_x	-	longitudinal modulus of laminate;
E_{xf}	-	E_x/V_f;
E_R	-	ratio of E_x at $N > 1$ to E_x at $N = 1$;
E_{11}, E_{22}	-	lamina moduli in fiber and transverse directions, respectively;
G_{xy}	-	axial shear modulus of laminate in xy coordinate system;
G_f	-	fiber shear modulus;
G_R	-	ratio of shear stiffness at $N > 1$ to the shear stiffness of $N = 1$;
G_{12}	-	axial shear modulus of lamina;
G_{90}	-	modified shear modulus of 90° lamina;
G'_{90}	-	contribution of fiber bending stiffness to the modified shear modulus G_{90} of the 90 degree lamina;
H	-	laminate thickness;
h	-	lamina thickness;
h^*	-	fiber or yarn-bundle diameter;
j	-	number of layers in the laminate;

SYMBOLS (Continued)

j_{90} - number of 90° layers in the laminate;

ℓ - m/2;

m - size of overstressed intact region;

m* - number of fibers or yarn-bundles in overstressed region in a 0° layer (m/d);

n - notch width (2a);

m' - m^*E_R;

n* - number of fibers or yarn-bundles in notch region in a 0° layer (n/d);

N - number of cycles;

N_f - fatigue lifetime;

Q - function of G_R, r;

R - $\sigma_{min.}/\sigma_{max.}$, stress ratio;

S - cyclic maximum stress/static failure strength

S_{11} - cyclic maximum axial stress/static failure axial strength;

S_{12} - cyclic maximum shear stress/static failure shear strength;

S_{22} - cyclic maximum transverse stress/static failure transverse strength;

S_{12}^e - effective S_{12} due to combined stress state;

t - superscript indicating tensile stress;

u_0, U_0 - non-dimensional and dimensional axial displacement inside the core region, respectively;

u_1, U_1 - non-dimensional and dimensional axial displacement in the overstressed region, respectively;

u_2, U_2 - non-dimensional and dimensional axial displacement in the average uniformly stressed region, respectively;

SYMBOLS (Continued)

V_f	-	fiber volume fraction;
x, y	-	laminate coordinate system;
x', y'	-	off-axis laminate coordinate system;
α	-	non-dimensional axial "crack" length (including plastic zone), inelastic length;
$\beta_{1, 2}$	-	functions of m*, n*, r, Q;
γ_{ult}	-	axial shear failure strain;
$\gamma_{1, 2}$	-	functions of m', n*, and r;
Δ	-	function of m*, r, E_R;
ζ	-	non-dimensional axial crack length;
θ	-	lamina orientation;
κ	-	shear coefficient;
σ_x, σ_g	-	applied gross laminate stress in x direction;
σ_{gf}	-	σ_g/V_f;
σ_A	-	applied laminate stress at which axial crack propagates to infinity;
σ_C	-	applied laminate stress at which axial crack is initiated at notch tip;
σ_{SCFM}	-	maximum composite overstress in material adjacent to notch;
σ_T	-	applied laminate stress at which transverse crack propagates from notch tip;
σ_{xy}	-	laminate in-plane shear stress;
σ_x^t	-	unnotched laminate tensile strength;

SYMBOLS (Continued)

σ_x^c - unnotched laminate compressive strength;

σ_Y - applied stress at which axial plasticity is initiated at the notch tip;

σ_{11}, σ_{22}, σ_{12} - stress components in lamina;

τ° - shear yield stress and strength of the unnotched laminate in the xy coordinate system;

τ_{12}° - lamina in-plane static shear strength;

τ_y - non-dimensional in-plane shear stress;

ξ - non-dimensional distance in x-direction.

FATIGUE OF NOTCHED FIBER COMPOSITE LAMINATES
PART II: ANALYTICAL AND EXPERIMENTAL EVALUATION

by S. V. Kulkarni, P. V. McLaughlin, Jr.,
and R. B. Pipes*

Materials Sciences Corporation

SUMMARY

This report describes the analytical/experimental correlation study performed to develop an understanding of the behavior of notched Boron/epoxy laminates subjected to tension/tension fatigue loading.

It is postulated that the fatigue induced property changes (stiffness as well as strength) of the laminate can be obtained from the lamina fatigue properties. To that end, the Boron/epoxy lamina static and fatigue data (lifetime, residual stiffness and strength) were obtained initially. The longitudinal and transverse tension data were determined from the [0] and [90] laminate tests while the in-plane shear data were obtained from the $[\pm 45]_s$ laminates.

Subsequently, notched $[0_2/\pm 45]_s$ Boron/epoxy laminates containing a 0.64 cm diameter center circular hole in a 3.81 cm wide coupon were subjected to static tension and tension/tension fatigue (R = 0.1, S = 0.8 and 0.667 at 30 Hz) loadings. The objectives of the static tests were to obtain the notched strength and mode of failure while those of the fatigue tests were to determine lifetime, damage propagation and residual strength. The failure in static tension occurred in a transverse crack propagation mode. The fatigue tests indicated substantial interlaminar damage propagation with the 0° surface layers separating from the ± 45° sub-surface layers in the region of the projection of the notch diameter. No through-the-thickness axial cracking was observed. Residual strength tests demonstrated

*Associate Professor, University of Delaware and Affiliate Staff Member, Materials Sciences Corporation.

that the laminate still fails in a transverse crack propagation mode with an increase in the residual strength.

The mini-mechanics model used herein for the static failure analysis of notched laminates is based upon composite heterogeneous behavior and experimentally observed failure modes under both static and fatigue loading. The modes of failure treated are:

(i) axial cracking in the load direction; and

(ii) transverse cracking across the specimen.

The 'mechanistic wearout' fatigue analysis uses this static failure model and embodies the concept that material properties in the notch region are continually changing with cyclic loading and that, if these properties are known at a given time, they could be used in the static failure analysis to compute residual strength and preferred mode of crack propagation.

During fatigue loading of a notched laminate, high axial and shear stresses exist near the notch root. These stresses will cause the material in the vicinity of the notch to be degraded much more rapidly than throughout the rest of the laminate. Consequently, it is appropriate to consider a failure analysis which considers a spatial variation of material properties (degraded properties in the vicinity of the notch and virgin material properties throughout the rest of the laminate). Such a variation has been incorporated into the failure analysis.

In accordance with the modified fatigue model, laminate fatigue behavior was predicted from lamina fatigue data. Predictions were compared with the experimental notched-laminate fatigue data for $[0_2/\pm 45]_s$ Boron/epoxy laminates containing a 0.635 cm diameter circular hole. The specific phenomena of interest are:

(i) the initiation of fatigue damage and its growth as a function of load cycles;

(ii) fatigue life and mode of failure; and

(iii) the residual strength after a predetermined number of cycles and the corresponding mode of failure.

Certain of the predicted phenomena were observed experimentally. Principal among these is the increase in residual strength after fatigue loading, and both axial and transverse damage growth.

Correlation of theory and experiment was hampered by the following factors:

(i) delamination of the 0° surface layers in the region of the longitudinal projection of the notch diameter;

(ii) lack of statistically significant data base for lamina fatigue properties in general; and

(iii) absence of lamina axial compression fatigue data in particular.

The principal deficiency appears to be the lack of a capability to predict growth of delaminations. Therefore, the interplay of stacking sequence and various failure modes (transverse, axial, and off-axis through-cracks and delaminations) should be investigated analytically and experimentally in detail.

INTRODUCTION

The utilization of composite materials for primary aerospace structural applications requires adequate safety margins and lifetime under all anticipated environments. This necessitates a sound understanding of the fracture and fatigue behavior of these materials as well as a broad experimental data base to completely characterize them. Since the latter is an expensive undertaking, an analytical model of the fatigue behavior of composite laminates is a desirable tool. To that end, a "mechanistic wearout" framework was developed in Reference 1 for predicting the growth of cracks and ultimate failure of fiber composite laminates containing through-the-thickness notches or holes under fatigue loading, provided that certain basic information is given about the fatigue behavior of a unidirectional layer of the material. The objectives of the present program are to evaluate this fatigue failure model and to expand the model, as required, to develop a semi-empirical capability for the fatigue analysis of notched fiber composite laminates. In order to accomplish these objectives, the present program was comprised of an experimental study of notched Boron/epoxy laminates, an experimental/analytical correlation effort, and an analytical development phase. The program addressed the need to utilize a limited data base to predict the behavior of notched composite laminates subjected to a tension/tension fatigue loading spectrum.

The philosophy underlying the fatigue model is the "wearout" concept; namely, that repeated application of load results in material degradation and hence in changed residual properties. When the residual strength is reduced to the level of the applied loads, fatigue failure occurs. Thus, the basic ingredients of the fatigue failure model in Reference 1 for notched composite laminates are:

(i) a 'mechanistic wearout' approach to fatigue which requires: (a) the experimental characterization of lamina fatigue behavior; (b) the subsequent utilization of these lamina fatigue data to obtain changes (degradation) in laminate properties in the vicinity of the notch with number of cycles; and (c) the prediction of residual strength and preferred mode of failure from a static failure model by using these 'new', degraded laminate properties; and

(ii) a mini-mechanics failure analysis of notched laminates (Ref. 3) which is based upon composite heterogeneous behavior and experimentally observed failure modes (Ref. 2) under both static and fatigue loadings; these modes of failure (as illustrated schematically in Figure 1) are: (a) axial cracking in the load direction; (b) transverse cracking across the specimen, and (c) cracking at an angle to the load axis along a fiber direction.

The capability of the static failure model to predict failure stresses and modes for notched Boron/epoxy laminates has been investigated in Reference 3 and satisfactory correlation was obtained with the experimental data. The fatigue model, however, had not been experimentally verified. To that end, an experimental program was undertaken to obtain:

(i) lamina fatigue data (lifetime, residual stiffness and strength) for longitudinal and transverse tension and in-plane shear;
(ii) notched laminate static data; and
(iii) notched laminate fatigue data (lifetime, damage propagation and residual strength).

The lamina fatigue data are a prerequisite for analytically predicting the notched laminate fatigue behavior while the notched laminate static data are utilized to determine the unknown parameters in the analysis. The analytical predictions of the fatigue model are compared with the experimental notched laminate fatigue data.

During fatigue loading of a notched laminate, high axial and shear stresses near the notch root will cause the material in the vicinity of the notch to be degraded much more rapidly than throughout the rest of the laminate. Consequently, it was deemed desirable to modify the existing static/fatigue failure model to consider a spatial variation of material properties (degraded properties in the vicinity of the notch and virgin material properties throughout the rest of the laminate).

Salient features of the static/fatigue analysis model of Reference 1 (including the modification to consider the spatial variation of degraded properties) are described subsequently (mathematical details pertaining to the modification of the analysis are presented in Appendix A). This description is followed by a summary of the experimental program, a discussion of the analytical/experimental correlation study, and the conclusions of the present investigation.

STATIC AND FATIGUE FAILURE ANALYSIS OF NOTCHED LAMINATES

STATIC FAILURE MODEL

The unique aspects of the fatigue failure analysis are associated with the modes of failure which are treated in the static failure model. Hence, a brief review of the static model is presented first.

The basic static model for axial and transverse failure of notched composites was developed in References 3, 4, and 5. Modification to the basic model by the addition of an approximate off-axis cracking capability was performed in Reference 1.

The model for the static failure of a notched composite laminate (Ref. 3) is illustrated in Figure 2. The laminate is assumed to be under a tensile stress in the x direction. A notch of width 2a is centered in the specimen at x = 0. It has been observed in Reference 2 that notch shape may not be as important to failure as the size (width) of the notch (this is particularly true when failure occurs by axial crack propagation). Hence, for the purposes of the present investigation, a through-the-thickness notch of any shape and width 2a will be modeled by a slit notch of width 2a.

The central core region wants to "pull out" from the notch area due to the applied tensile loading. This core, however, is restrained by shear stresses between the core and the adjacent intact material. These shear stresses generally result in a region of high shear strain parallel to the loading direction. Immediately adjacent to the notch core, there is an overstressed region of average stress concentration of width 'm'. Everywhere outside the core and overstressed regions, the laminate is uniformly strained. Shear strain due to core pullout is assumed to extend in the 'y' direction over a region three times the size of the overstressed fiber region 'm'. The laminate axial shear stress-strain

curve is approximated as linear elastic-perfectly plastic. The axial shear modulus G_{xy}*, the shear failure stress, τ°, and the shear failure strain, γ_{ult}, are chosen to obtain the best fit to the actual laminate shear stress-strain curve.

In Figure 2, ζ is a nondimensional axial crack length extending from the notch tip (x = 0) to the bottom of the plastic zone. The nondimensional distance from the notch tip to the beginning of the elastic zone is α, and includes the axial crack and the plastic zone. For this reason, α is termed as the "inelastic length" and is a good measure of the extent of damage in the axial direction from the notch tip.

The static failure analysis has the capability of computing α, ζ and maximum overstress in the material adjacent to the notch for a given applied laminate tensile stress so that tendency to axial or transverse crack propagation modes can be monitored. Typical results of the analysis are shown in Figure 3.

The dashed line shows the growth of the axial damage region with increasing tensile stress σ_x. The applied stress at which plasticity is initiated at the notch tip is called σ_y. At some higher stress level σ_c, an axial crack will begin to grow from the notch tip (the shear strain γ having exceeded γ_{ult}). The failure stress of the notched composite in the axial crack propagation failure mode is σ_A ($\alpha \to \infty$).

The solid line in Figure 3 shows the growth of notch tip overstress with applied stress σ_x. As stressing of the composite increases, it is possible that the maximum overstress in the adjacent material, σ_{SCFM}, will increase to the point where it exceeds the unnotched laminate strength, σ_x^t. For this case, transverse crack propagation ensues. The applied

*The 'x-y' coordinate system refers to the laminate while the '1-2' coordinate system refers to the lamina ('1' - fiber direction, '2' - transverse direction)

laminate stress at which transverse cracking occurs is called σ_T. Also, at the initiation of the inelastic region ($\alpha > o$), the stress concentration effects are blunted and σ_{SCFM} grows with applied stress σ_x at a lesser rate than before, until the initiation of the axial crack ($\zeta \geq o$) when σ_{SCFM} actually decreases with increasing σ_x. In the figure, a transverse failure occurs.

In all failures, it has been observed that cracks propagate either along a fiber direction or transversely across the specimen perpendicular to the direction of tensile loading. The mode of failure can be different for fatigue and static loading for the same laminate. In addition, different notch sizes can trigger different failure modes in the same laminate. Other factors which can affect failure mode are ply orientation, constituent material properties, and environment.

Determination of the Average Stress Concentration Region 'm'

Given the laminate mechanical properties (E_x, E_y, G_{xy}, ν_{xy}) and failure stresses and strains (σ_x^t, $\tau°$, and γ_{ult}), the unknown parameter in the analysis is 'm' which defines the extent of the average stress concentration region (see Figure 2; other investigators have also recognized the need to define the dimension of this region; for example, the "intense energy region" of Reference 6, and the distances associated with the 'point stress' and 'average stress' criteria of Reference 7). Accurate determination of 'm' is an important aspect of the predictive capability of the static/fatigue failure model. Various empirical forms for predicting 'm' as a function of the notch size and laminate construction can be postulated. However, for the purposes of the present investigation, the value of 'm' will be determined from the notched laminate static failure data. This value of 'm' will be used subsequently for the fatigue analysis.

In summary, the static failure analysis procedure for notched laminates consists of the following steps:

(i) Determine laminate mechanical properties (E_x, E_y, G_{xy}, ν_{xy}) and the pertinent failure stresses and strains (σ^t_x, $\tau°$, γ_{ult}).

(ii) Define the region of stress concentration 'm' either analytically or from experiment.

(iii) Use the axial/transverse failure model to compute the laminate stresses causing axial crack propagation (σ_A) and transverse crack propagation (σ_T).

(iv) Compare the failure stresses σ_A and σ_T and use the lower value for the predicted failure stress and the dominant failure mode.

FATIGUE ANALYSIS

A semi-empirical, deterministic framework for the prediction and correlation of fatigue crack growth, residual strength, and fatigue lifetime of fiber composite laminates containing notches or holes was developed in Reference 1. The approach is consistent with the 'mechanistic wearout' fatigue philosophy and is reviewed briefly here.

If a structural component fails after a certain number of cycles of a specified cyclic loading, the maximum magnitude of which is less than that required to cause failure of the virgin material, it is apparently clear that repeated loading (a number of cycles, N) has brought about an alteration (generally, a degradation) in the strength and stiffness characteristics of the material. The rate of degradation is likely to be a function of many factors such as maximum stress, stress ratio, frequency, environment, etc.

Given a particular material, with a built-in macroscopic imperfection, and a static failure model, it is possible to perform

a stress and failure analysis for a given set of loading conditions, with the stiffness and strength properties as input data. Degradation of the material will merely alter the basic input property data for the analysis. The stiffness, strength, and ductility are basic material properties and will depend upon material structure, environment, etc. The precise effect of these factors on the moduli and strength can be best established by an empirical approach. Hence, an objective is to obtain the following relationship:

$$\text{Moduli, Strength, Ductility (Ultimate Strain)} = F\,(N, \text{maximum stress, stress ratio, frequency, environment, etc.}) \quad (1)$$

As the number of load cycles increases, local properties will change. There will be stress redistributions and the failure prediction for a notched composite laminate will change. Although the changes are continuous, the suggested approach is to observe the behavior for discrete increments in the number of cycles.

Fatigue failure in notched fiber composite laminates occurs as a result of growth of cracks along preferred directions in the laminate as load cycling proceeds. This crack growth is influenced by local material properties which change as a result of the repeated loads. When the local material properties and the geometry of the damaged regions are redefined after any number of cycles, the residual static strength can be found from the failure model outlined in the preceding section. If the residual strength so computed is less than the maximum cyclic stress, the fatigue lifetime of the notched composite has been exceeded.

The most direct way to determine laminate tensile and shear behavior under cyclic loads is simply to perform fatigue tests on unnotched specimens. This method, though straightforward, would require a large number of tests for each laminate layup geometry in both the axial xy and off-axis x'y' systems. The results would

only be applicable to the specific laminate tested; each new laminate would require additional tests. Therefore, a method of generating laminate fatigue behavior from lamina properties was developed and is as follows:

(i) The laminate stress state which exists in the notch vicinity (axial tension and shear) is determined by utilizing the static failure model.

(ii) A constant strain laminate analysis is performed on the laminate for these stresses utilizing initial static lamina properties. From this laminate analysis, the stress state in each layer of the laminate is computed.

(iii) From data on fatigue behavior of a unidirectional lamina, calculations are made of changes in lamina elastic properties and residual failure stresses for some increment in load cycles. It is assumed that, over the range of cycles considered, the individual stresses in each lamina are not changing significantly.

(iv) The changed lamina elastic properties and lamina strengths are re-introduced into the laminate analysis to predict new laminate elastic properties and failure stresses.

(v) A second increment of cyclic loading is selected, and steps (i) through (iv) are repeated.

This procedure can be repeated as necessary to find the residual strength after a required number of cycles, or until the residual strength of the laminate reduces to the stress levels existing at the notch. When the latter occurs, the fatigue lifetime of the material near the notch has been reached.

The lamina fatigue information which would be necessary to generate laminate fatigue properties in the notch vicinity should generally include longitudinal and transverse tension and compression and in-plane shear. However, only the longitudinal and transverse tension and in-plane shear data were generated during the present program.

Interaction Effects of Layer Stress Components in Fatigue

Experimental and analytical results indicate that the primary in-plane stress interactions appear to be between transverse normal stress, σ_{22}, and axial shear stress, σ_{12}. Hashin and Rotem (Ref. 8) have developed a quadratic interaction theory which empirically treats the fatigue of a unidirectional layer under combined axial shear and transverse normal stresses. In their theory, axial stress is assumed to be uncoupled from the other two stress components in fatigue. In the present formulation, the assumption of uncoupled fatigue behavior between the axial stress and other in-plane stress components will be maintained. Due, however, to the complexity of the experimental information which is necessary to fully utilize the Hashin-Rotem theory, a less complicated interaction between σ_{22} and σ_{12} is proposed here.

In the presence of a given cyclic shear stress, the effect of an additional transverse normal stress component will be to accelerate fatigue degradation. This will be done by means of an increased "effective" shear stress level and a resulting "effective" S^e_{12} ($S_{12} = \sigma_{12}/\tau^\circ_{12}$; τ°_{12} is lamina static axial shear strength). It is necessary that S^e_{12} be equal to the actual S_{12} when σ_{22} vanishes. Also, as σ_{22} approaches its failure value in either tension or compression, it is reasonable to assume that its effect is similar to cycling at an effective shear stress close to the static failure shear stress.

The approach taken in Reference 1 is to utilize a quadratic interaction formula as in Figure 4 with a zero minimum for S_{12}. The equation to be used is as follows:

$$\left(\frac{\sigma_{22} + \sigma_{22}^{d}}{\sigma_{22}^{p}}\right)^{2} + \left(\frac{1 - S_{12}^{e}}{S^{p}}\right)^{2} = 1, \qquad S_{12}^{e} \geq 0 \qquad (2)$$

(If $S_{12}^{e} < 0$ from above, set $S_{12}^{e} = 0$)

where

$$\sigma_{22}^{p} = \frac{\sigma_{22}^{c} + \sigma_{22}^{t}}{2}, \quad \sigma_{22}^{d} = \frac{\sigma_{22}^{c} - \sigma_{22}^{t}}{2} \quad \text{and}$$

$$S^{p} = \frac{1 - S_{12}}{[1 - (\sigma_{22}^{d}/\sigma_{22}^{p})^{2}]^{1/2}} .$$

The calculated value of S_{12}^{e} is used in place of S_{12} to predict layer axial shear property degradation from experimentally determined layer fatigue behavior. It is expected that the combined stress state will also cause degradation in transverse tensile properties. Specifically, transverse normal strength and transverse Young's modulus are anticipated to exhibit the greatest changes. It will be assumed that the degradations which occur in transverse normal strengths and transverse Young's modulus occur to the same degree as axial shear strength and axial shear modulus. Specifically, the same fractional reduction will be assumed in E_{22} as G_{12}, and in σ_{22}^{t} as τ°_{12}.

The procedure for determining the effect of transverse normal property degradation in a unidirectional layer is, therefore, as follows:

(i) Determine, from laminate analysis techniques, the values of σ_{12} and σ_{22} in a given layer.

(ii) Compute the effective stress ratio S_{12}^{e} from Equation (2).

(iii) Utilize an experimentally determined axial shear fatigue wearout curve to determine the change in axial shear failure strength and axial shear modulus with number of cycles N.

(iv) Calculate the degradation of transverse Young's modulus and transverse normal strength by assuming that the reductions in these values are fractionally the same as in their shear mode counterparts.

SPATIAL VARIATION OF DEGRADED PROPERTIES

As has been pointed out earlier, the basic ingredients of the fatigue analysis are a viable static failure model and a capability to predict degraded laminate properties as a function of load cycles. In Reference 1, the degraded laminate properties were used throughout the laminate while in reality, the degradation will be predominant near the vicinity of the notch because of stress concentration effects. The rest of the laminate will in fact experience little wearout and it may be appropriate to use the virgin material properties (N = 1). Consequently, it is necessary to modify the analysis to consider the spatial variation of laminate properties. The precise mechanism to incorporate such a variation is rather complex because the stress states around the notch are strongly a function of the coordinates (e.g., primarily axial tension adjacent to the notch along the y-axis to primarily in-plane shear along the x-axis). Also, the magnitude of the stresses and hence, the degree of wearout also decreases as one proceeds farther away from the notch. Furthermore, the spatial variation should be

considered within the framework of the static failure model (Figure 2) without overly complicating the analysis procedure.

Referring to Figures 2 and 5, two distinct regions of different degradation can be identified, namely, the overstressed region represented by 'm' adjacent to the notch and extending from $\zeta = 0$ to $\zeta = \alpha$, and the shear strain concentration region between the notch and this overstressed region. Regarding the extent of the degraded shear region, it should be noted that this region will generally extend beyond $\zeta = \alpha$ and, for a specified fatigue loading (given value of S), it may behave elastically although matrix crazing (as is commonly observed) will indicate some form of visual damage. In other words, appearance of visual damage in the form of matrix crazing does not necessarily indicate the propagation of an inelastic region α in the context of the present model in Figure 2. In the first region, the significant laminate parameters are the longitudinal modulus E_x and tensile strength σ_x^t while in the second region, they are the shear modulus G_{xy}, shear failure stress $\tau°$, and ultimate shear strain γ_{ult}.

Ideally, it is appropriate to discretize the laminate not only along the y-axis (as is presently done in Figure 2), but also along the x-axis, to consider different degrees of degradation. Since this would entail a significant alteration in the existing analysis capability, a simpler approach appears desirable. Specifically, the shear property degradation region is considered to extend beyond $\zeta = \alpha$ between the notch and the overstressed region, while the axial property degradation region is assumed to extend from $\zeta = 0$ to $\zeta = \alpha$. This is illustrated in Figure 5. Corresponding modifications to the analysis have been made and are described in Appendix A.

The two significant parameters which appear as a result of considering a spatial variation of material properties are E_R (ratio of the current modulus E_x in the overstressed region to

modulus E_x at N = 1) and G_R (ratio of current shear stiffness in the shear transfer region between the notch and the over-stressed region to the shear stiffness at N = 1). These modifications have been incorporated into the existing FATLAM-I computer code (renamed as FATLAM-IA).

EXPERIMENTAL PROGRAM

The thrust of the experimental program (conducted primarily* at the Center for Composite Materials of the University of Delaware) was directed towards providing Boron/epoxy lamina static and fatigue data to be used as input into the fatigue analysis to predict degraded laminate properties as a function of load cycles, and generating static and fatigue data (lifetime, damage propagation and residual strength) for notched Boron/epoxy laminates to be utilized for the evaluation of the fatigue failure model. These objectives of the experimental effort are consistent with the static/fatigue failure analysis methodology outlined in the preceding sections and in Reference 1. Specifically, tests were conducted to obtain:

(i) Lamina static longitudinal tension ([0] laminate), transverse tension ([90] laminate) and in-plane shear ($[\pm 45]_s$ laminate) test data.

(ii) Lamina fatigue longitudinal and transverse tension/tension, and in-plane shear test data (lifetime, residual modulus and strength; R = 0.1, 30Hz, different S-levels).

(iii) Unnotched $[0_2/\pm 45]_s$ Boron/epoxy laminate static test data (moduli, strength).

(iv) Notched $[0_2/\pm 45]_s$ Boron/epoxy laminate static test data (notched strength, failure mode).

(v) Notched $[0_2/\pm 45]_s$ Boron/epoxy laminate tension/tension fatigue test data (lifetime, damage propagation, and residual strength; R = 0.1, 30Hz, S = 0.8 and 0.667).

(vi) X-Ray monitoring of damage propagation as a function of load cycles in the notch vicinity (R = 0.1, 25Hz and S = 0.8; conducted at the NASA Langley Research Center).

---

*Some notched laminate fatigue tests and X-Ray monitoring of damage propagation was performed at the NASA Langley Research Center by G. L. Roderick, US AAMRDL, Langley Directorate.

Salient features of the experimental program are discussed subsequently.

SPECIMEN FABRICATION

All test specimens utilized in the current program were fabricated from Boron/epoxy laminates supplied by Composite Materials Corporation (CMC). The Boron/epoxy prepreg was manufactured by the 3M Company from CMC fiber, of 0.004 inch (0.10 mm) diameter, and the 3M SP296 epoxy resin system. All laminates were midplane symmetric, balanced and consisted of eight layers. Panel thicknesses varied from 0.0375 to 0.0458 inches (0.952 to 1.16mm). Test specimen geometries investigated are given in Table 1.

Each laminate was subjected to both visual and ultrasonic "C" scan examination prior to specimen fabrication. Laminates which revealed anomolies in the examinations were excluded from test specimen fabrication. Typical anomolies revealed included fiber wash, gaps between prepreg tapes, foreign matter, delamination and surface indentations.

Load introduction tabs consisting of Scotchply bidirectional laminates 0.13 inches (3.3mm) in thickness were bonded to each laminate. The tabs were bonded to the laminates with Eccobond # 45 adhesive utilizing precision fixtures to insure that the tab was properly aligned with the laminate and to assure parallel tab surfaces in order to give uniform load introduction utilizing friction type grips.

Two machining operations were required in fabrication of the test specimens. The first operation consisted of sawing test coupons from the tabbed laminate. The second operation was machining of the circular notch for notched specimens.

Machining of a 0.25 inch (6.35 mm) circular hole in the Boron/epoxy material requires a capability to accurately locate

the hole, as well as to produce a circular hole free from geometric irregularities or delaminations. Such a facility is shown in Figure 6. It consists of a standard Bridgeport® milling machine, diamond core drill, emulsion cooling, and a positioning fixture.

Subsequent to fatigue testing, and/or prior to static test, each specimen was instrumented with electrical resistance strain gages. Type EA-06-125AC-350 Micromeasurements® foil gages were bonded to the surface of each specimen utilizing M-Bond 200® adhesive. Table 2 indicates the location and orientation of the gage for each test specimen geometry.

TEST SYSTEM

The test system consisted of specially designed grips, Instron friction grips, a servo-hydraulic closed-loop test system, and Datran II strain instrumentation.

Load introduction for fatigue of the 1.5 inches (38.1 mm) wide test specimens required the development of a new grip design. The configuration shown in Figure 7 consists of a clevis and pin arrangement wherein the specimen is clamped between two serrated plates. Load is transferred to the specimen tabs through friction avoiding the need to penetrate the laminate. Two bolts on either side of the specimen act to clamp it between the serrated plates and position it in the grips.

The servo-hydraulic test system shown in Figure 8 consists of two, model 1321 Instron, closed-loop machines with a capacity of ± 5000 kg and a frequency response range of 0-50 Hertz. The machines were equipped with cycle counters and could operate under strain, stroke, or load control. Control functions include square wave, triangular wave, ramp, and sinusoid. In addition, the test system operates under computer (Alpha-LSI) control. The computer is also shown in Figure 8.

Strain gage data were obtained in the test program through implementation of the Datran II system. The Datran II consists of a scanner, ten channel bridge, and printer. Up to ten channels of strain can be recorded at a rate of ten per second.

All tension/tension fatigue tests in this program were performed under load control. The load function was sinusoidal with a frequency of thirty (30) Hertz (cycles per second). The ratio of minimum stress amplitude to maximum stress amplitude was R = 0.1.

LAMINA STATIC TESTS

Properties determined in the lamina static characterization included longitudinal tensile strength, σ_{11}^{t}; longitudinal modulus, E_{11}; transverse tensile strength, σ_{22}^{t}; transverse modulus, E_{22}; Poisson's ratio, ν_{12}; in-plane shear strength, τ°_{12}; and in-plane shear modulus, G_{12}. The in-plane shear properties of the Boron/epoxy composite were determined by employing the $[45/-45/45/-45]_s$ tensile coupon specimen. It has been well established (e.g. in Reference 9) that the response of this specimen can be utilized to determine in-plane shear properties of the lamina. Experimental results for longitudinal and transverse tension and in-plane shear are tabulated in Tables 3, 4, and 5, respectively. Typical failure specimens for each of these tests are illustrated in Figures 9, 10, and 11.

LAMINA FATIGUE TESTS

In order to examine the fatigue properties of the lamina, the test specimens utilized in the static characterization were subjected to sinusoidal loadings. In this manner, fatigue properties in the longitudinal tension, transverse tension, and in-plane shear modes were determined.

The longitudinal tension fatigue results are summarized in Table 6. Data are presented for sinusoidal loadings of ratio of maximum stress to ultimate strength (S) ranging from 0.55 to 0.80. Residual strength and stiffness data are tabulated for

specimens subjected to predetermined numbers of cycles (N) and subsequent static testing. Only the specimens denoted by "FF" failed during the fatigue loading. Typical longitudinal fatigue failure samples are shown in Figure 12.

The lamina transverse tension fatigue data are summarized in Table 7. The results presented include residual strength and residual tangent and secant moduli. Fatigue failures are again denoted by the symbol "FF". In addition, certain of the samples which experienced fatigue failures were subjected to residual strength and stiffness measurements. These specimens are noted in the table. A significant conclusion which may be drawn from these results is that the transverse fatigue results exhibit great scatter. This may be attributed to the very fragile nature of the $[90_8]$ test specimen. Typical transverse tension fatigue failures are shown in Figure 13.

The lamina in-plane shear fatigue data are tabulated in Table 8. Data presented include residual strength, residual tangent modulus, and residual secant modulus corresponding to a shear strain of 0.04. These data show that the degradation of the shear strength and modulus of the lamina is significant. This is an expected result because the shear properties are matrix controlled. Typical fatigue failures of $[\pm 45]_s$ laminates are illustrated in Figure 14.

UNNOTCHED AND NOTCHED LAMINATE STATIC TESTS

Characterization of the static properties of the $[0/0/45/-45]_s$ laminate consisted of determination of the laminate elastic properties (Young's modulus and Poisson's ratio) and of the notched and unnotched laminate strengths.

Static properties of the unnotched $[0/0/45/-45]_s$ laminates are summarized in Table 9. Examples of the static failures of the unnotched $[0/0/45/-45]_s$ laminate are shown in Figure 15.

Static properties of the notched $[0/0/45/-45]_s$ laminate are summarized in Table 10. The notched laminate contains a central circular notch of diameter 0.25 inches (6.35 mm) in a 3.81 cm wide coupon. The average static strength of the notched laminate is approximately sixty (60) percent of the unnotched strength. Also, the ultimate strain for the two laminates are identical when the strain of the notched laminate is measured at the edge of the notch. Typical static failures of the notched laminate are shown in Figure 16. Note that the failures occur by a transverse propagation of the notch.

NOTCHED LAMINATE FATIGUE TESTS

The notched laminates were subjected to two different amplitudes of sinusoidal fatigue loadings; namely, S = 0.8 and S = 0.667. The residual strength and stiffness characteristics of the laminate were determined at various stress cycle intervals. In addition, fatigue damage in the vicinity of the notch was also monitored.

Maximum Stress Equal to 80% of Ultimate Static Notched Strength

Test results for notched laminates subjected to a sinusoidal fatigue loading of maximum amplitude equal to eighty (80) percent of the static ultimate notched strength are summarized in Table 11. These results show that while the modulus of the notched laminate is virtually unchanged by the fatigue loading either at 50,000 or 500,000 cycles, the average residual strength increases from the static strength of 0.452 GN/m^2 to 0.496 GN/m^2 at 50,000 cycles, to 0.521 GN/m^2 at 500,000 cycles, and to 0.526 GN/m^2 at 1.5×10^6 cycles. Recalling that the unnotched laminate strength was 0.752 GN/m^2, the net section strength of a 1.5 inch (38.1 mm) width test specimen containing a 0.25 inch (6.35 mm) circular hole would be 0.627 GN/m^2. Hence, after 50,000 cycles at S = 0.8, the residual strength of the laminate is seventy-nine (79) percent of net section

strength, while after 500,000 cycles the residual strength has increased to eighty-four (84) percent of net section strength. Average ultimate strain at the edge of the notch has increased from 0.0067 for the static unnotched strength test to 0.00694 after 50,000 cycles, to 0.00718 after 500,000 cycles, and to 0.00724 after 1.5 x 10^6 cycles.

This increase in the residual strength and the ultimate strain at the edge of the notch as a function of fatigue cycles supports the contention that axial fatigue damage alleviates the stress concentration and that cyclic loading softens the material in the vicinity of the notch. The effect of such a softening is to reduce the stiffnesses as well as the strengths. This is consistent with the concept of wearout.

Maximum Stress Equal to 67% of Ultimate Static Notched Strength

Residual strength results for notched laminates subjected to a sinusoidal fatigue loading of maximum stress equal to sixty-seven (67) percent of notched static strength are summarized in Table 12. The test results again show that the residual strength of the notched laminate exceeds the notched static strength. After ten (10) million cycles at S = 0.67, the average residual strength is eighty-six (86) percent of the static net section strength. In addition, the average ultimate strain measured at the edge of the notch after ten (10) million cycles is 0.00765 or fourteen (14) percent greater than the static ultimate strains.

A typical residual strength test failure mode is illustrated in Figure 17. Note that failure occurs by a transverse propagation of the notch even though considerable visual axial damage has occurred in the 0° layers during fatigue.

SURFACE AXIAL DAMAGE GROWTH

The nature of the fatigue damage in the vicinity of the notch can be characterized as a form of axial cracking of the two surface 0° layers followed by delamination of the 0° layers in the region of the projection of the notch diameter. In an

attempt to quantify the rate of damage, the crack length in the 0° layer was monitored. Figure 18 shows the crack length at various cycle levels. Typical growth rate data were obtained by monitoring growth in the four quadrants and both sides of the circular notch. Both average length, as well as maximum and minimum length data, are presented in Figure 19 for S = 0.8 and in Figure 20 for S = 0.667.

Delamination of the 0° layers in the vicinity of the notch follows the axial cracking in the 0° layers. Figure 21 shows "C" scan results which reveal the extent of delamination. The fatigue failure specimen 4CLI exhibited significant delamination prior to failure. The delaminated specimen is shown in Figure 22. For this specimen, the failure mode is different from the notched static tests (Figure 16) and the residual strength tests (Figure 17).

DETERMINATION OF AXIAL CRACK GROWTH BY AN X-RAY TECHNIQUE

It has been observed in Reference 2 that axial crack propagation (denoted by ζ in Figure 2) occurs in notched Boron/epoxy laminates both for static and fatigue loadings. For the present case, a through-the-thickness axial crack can propagate only if the ± 45° fibers fracture in the region of the shear strain concentration at the notch tip. Consequently, in order to determine whether the ± 45° fibers have failed or not, an X-Ray technique (similar to that in Reference 10) was employed. The tests were conducted at the NASA Langley Research Center on the notched $[0_2/\pm 45]_s$ Boron/epoxy laminates (S = 0.8, R = 0.1 at 25Hz) supplied by Materials Sciences Corporation. Figure 23 illustrates the surface damage growth (in-plane shear failure of 0° surface layers and subsequent delamination from the 45 layers) at 1.5×10^6 cycles. This damage growth is similar to that observed in other specimens (Figure 18). The X-Ray pictures in the region of shear strain concentration for this specimen are shown in

Figure 24. It is evident that there are only a few scattered - 45° fiber failures. For a different stacking sequence ($[45/0/-45/0]_S$) and S-level (0.667) in Reference 10, the 45° fiber failures were more pronounced for the same notch size.

ANALYSIS/EXPERIMENT CORRELATION STUDY

The primary objective of the current effort is to evaluate the analytical model for fatigue failure, developed in Reference 1, by comparing the analytical predictions with observed experimental phenomena. This quasi-heterogeneous, mini-mechanics model is a simple approach to the rather complex problem of fracture and fatigue of notched composite laminates. It avoids the study of extreme detail such as that associated with a micro-mechanical analysis of the heterogeneous material. At the same time, it combines physically realistic failure modes with engineering assumptions which make the analysis tractable.

The data required for this model are of two types: those which can be measured directly, such as changes in the lamina strength and stiffness characteristics with number of load cycles, and those which cannot be measured directly, such as the characteristic dimension, 'm', of the average stress concentration region. Obtaining the first type of data does not present any significant problems. However, definition of the parameter, 'm', is not a straightforward task. An approach to determine 'm' in a semi-empirical fashion is to utilize a limited static fracture data for the laminate to 'tune' the model.

The following specific tasks were performed for the analysis/experiment correlation study:

(i) Investigation of the feasibility of utilizing experimental lamina fatigue data to predict effectively the degraded laminate properties as a function of number of cycles.

(ii) Determination of analysis parameters, such as the overstressed region 'm', from the static experimental data for notched $[0/\pm 45]_s$ Boron/epoxy laminates.

(iii) Monitoring, analytically, the progressive behavior of the notched $[0_2/\pm 45]_s$ Boron/epoxy laminates in tension/tension fatigue for the purposes of determining lifetime, damage propagation, residual strength, and mode of fatigue failure.

(iv) Correlation of analytical predictions and observed experimental fatigue response of the notched $[0/\pm 45]_s$ Boron/epoxy laminates.

UNNOTCHED AND NOTCHED LAMINATE STATIC TEST DATA CORRELATION

Inherent in any laminate analysis problem is the capability to compute the effective properties (strength as well as stiffness) of a laminate. While the determination of laminate stiffness is rather straightforward, there is always some uncertainty associated with the failure stresses. A first ply failure criterion, though commonly used, must be used with caution. In the present investigation, the maximum stress criterion is used for the computation of tensile (σ_x^t) and in-plane shear ($\tau°$) strengths and ultimate shear strain (γ_{ult}). This criterion states that the laminate fails when any stress component in a lamina of the laminate attains its maximum allowable value. The failure is considered to be an ultimate failure of the laminate if the applied stress, at which a stress component (axial, transverse, or shear) reaches its ultimate value in any lamina, is greater than the applied failure stress as obtained from a 'netting' analysis wherein the transverse and shear moduli of all lamina are assumed to be zero. Alternatively, the failure is termed as a yield type failure if the 'netting' analysis failure stress is greater than the applied stress at which a stress component in any lamina reaches its ultimate value. Generally, if the first stress to reach the limit value is in the fiber direction of a lamina, the failure is catastrophic with no load-carrying capacity beyond

initial failure. If, on the other hand, the stress component to reach its ultimate value first is either the normal stress transverse to the fiber direction or the in-plane shear stress, the laminate will possess load-carrying capacity at a reduced modulus beyond initial failure.

For the laminate in question ($[0_2/\pm 45]_s$ Boron/epoxy), utilization of this failure criterion gives a good agreement with the experimental data for the unnotched tensile strength. This is obvious from Table 9, wherein the analytical prediction of σ_x^t (0.715 GN/m^2) is within 5% of the experimental value (0.752 GN/m^2). This can be attributed to the initial fiber failure in the 0° layers. As far as the in-plane shear strength ($\tau°$) and ultimate shear strain (γ_{ult}) are concerned, it should be recalled that the shear stress-strain response in the failure analysis is assumed to be elastic, perfectly-plastic (no experiments were conducted to obtain the shear stress-strain behavior of the laminate). Consequently, if the initial (first ply) failure for an in-plane shear loading is a fiber failure (which is not the case in the present laminates), then the shear stress strain response can be regarded as elastic with $\gamma_{ult} = \tau°/G_{xy}$. However, if the initial failure is a matrix type failure (transverse tension in ± 45° layers in the present case), then the value of G_{xy} is taken to be the initial tangent shear modulus; and the shear strength, $\tau°$ and the strain of failure γ_{ult} are obtained from the 'netting' analysis. In summary, the pertinent laminate properties E_x, E_y, ν_{xy}, G_{xy}, σ_x^t, $\tau°$, and γ_{ult} are obtained from laminate analysis and the static unnotched tests.

In the absence of a simple capability to define the parameter 'm', the notched $[0_2/\pm 45]_s$ Boron/epoxy laminate tests were conducted for the purposes of determining that parameter as well as notched strength. Also, these tests were used for observing the static mode of failure. The notch was in the form of a circular hole, 0.64 cm in diameter in a 3.81 cm wide coupon. The notch size to laminate width ratio (0.1666) indicates

that the finite size effect will not be an important factor in the analysis. The static failure analysis for axial/transverse propagation of the notch has been described in a previous section and is illustrated schematically in Figure 25. This figure should be read in conjunction with Figure 3.

Having defined the laminate properties and the notch size, the FATLAM I computer code is used to obtain a value of 'm' corresponding to the experimental notched strength of 0.45 GN/m^2 (Table 10) and the analytical value of σ_x^t (Table 9). The variation of notch tip overstress σ_{SCFM} with applied laminate stress σ is shown in Figure 26 for the notched laminate. The point F, whose coordinates are σ_x^t (0.715 GN/m^2) and σ (0.45 GN/m^2), represents the failure point. Suppose m* (number of Boron fibers in the overstressed region) is arbitrarily chosen to be 12. For this value, the axial crack propagation failure stress σ_A will exceed the experimental failure value of σ = 0.45 GN/m^2 while for a transverse propagation (corresponding to σ_x^t = 0.715 GN/m^2), the σ_T value is less than σ = 0.45 GN/m^2. Additionally, for an axial crack propagation mode, the peak value of σ_{SCFM}, as denoted by point P should be at all times less than σ_x^t = 0.715 GN/m^2. If, for another value of m* = 7 (< 12), the point P' is below σ_x^t (0.715 GN/m^2) as shown in the figure, then the failure stress σ_A will be less than σ = 0.45 GN/m^2. Thus, the only possible mode of failure predicted for σ = 0.45 GN/m^2 is transverse crack propagation across the specimen. The σ_{SCFM} vs σ variation for m* = 21 (m = 0.212 cm) passes through the failure point F. This value of m* is used subsequently in the fatigue analysis.

NOTCHED LAMINATE FATIGUE TEST DATA CORRELATION

With the determination of all the analysis parameters and the lamina fatigue data, the fatigue analysis of the notched $[0_2/\pm 45]_s$ Boron/epoxy laminates can now be performed. The analysis procedure utilizes the methodology described earlier and in Reference 1 and incorporates the modification to consider

the spatial variation of degraded properties. The approach is illustrated schematically in Figure 27. The modified version of FATLAM I computer code (FATLAM IA) is used in conjunction with a laminate analysis code.

The lamina experimental fatigue test data (see Tables 6 and 8) are converted to a S-N and residual strength/modulus - N curve format. These curves are shown in Figure 28 for the longitudinal tension and in Figure 29 for in-plane shear. In both these figures, the S - N curves were obtained from a least square fit. In Figure 28, the longitudinal tension data generated during the present program appears to be rather unconservative and a preliminary fatigue analysis indicated that for S = 0.8, the notched specimen would fail ar about N = 100 to 1000 cycles. Since this prediction is contrary to the experimental observations, it was decided to discard these data as not representative of the 0° plies and instead, to use the data in Reference 11. The Avco/Narmco 5505 Boron/epoxy specimens in Reference 11 had an unnotched tensile strength of approximately 1.27 GN/m^2 which compares well with the strength in Table 3. The S - N curves obtained from the data in Reference 11 are also shown in Figure 28. A possible reason for the poor experimental results for the [0] fatigue specimens is the misalignment of the fibers with respect to the load axis. The residual strength/modulus - N curves for the data of Reference 11 are drawn in an approximate fashion.

The transverse tension fatigue data (Table 7) generated during this program also exhibited considerable scatter mainly because of the fragile nature of the test specimen. As a result, the degradation for the transverse tension properties was assumed to be similar to the in-plane shear properties since both are matrix dominated. This choice is supported by the data of Figure 29 which show that the S - N curve for [90] tension tests for Boron/epoxy from Reference 11 is similar to the in-plane shear S - N curve.

The stress states in the different layers in a $[0_2/\pm 45]_s$ laminate are shown in Table 13 for both the overstressed region, (predominantly axial tensile stress) and the shear region (predominantly in-plane shear stress). It is seen that lamina fatigue data for longitudinal and transverse compression are required. These data are not available at the present time. This deficiency in the data is particularly significant for those 45° layers, within the shear region, which are subjected to compression along the fiber axis and tension in the transverse direction. In the event of transverse tension degradation or failure in this layer, the compression modulus and strength cannot be predicted reliably. Furthermore, transverse cracking will induce interlaminar stresses and hence, the determination of compressive fatigue properties from [0] laminates will not suffice. For the purposes of the present investigation, the degradation for the longitudinal compression modulus and strength and transverse compression strength is taken to be the same as that for in-plane shear. This choice is based upon the established relation between compressive strength and shear modulus.

Maximum Stress Equal to 80% of Static Notched Strength

The tension/tension fatigue tests for S = 0.8 were conducted with a maximum stress value of 0.36 GN/m^2 and R = 0.1. With this maximum value of the applied laminate stress, a fatigue analysis was performed with and without spatial variation of degraded properties.

Fatigue Failure

Laminae properties for the $[0_2/\pm 45]_s$ laminate are presented in Table 14. The first row shows the initial static properties (N = 1). These properties are used in the FATLAM I computer code to predict laminate stress distributions in the hole region without

considering the modified analysis of Appendix A (a characteristic dimension based on m* = 21 was utilized). These laminate stresses were used to predict layer stresses which are presented in the top row of Table 15 in the form of ratios of actual layer stress component to ultimate layer stress component, S_{11}, S_{22}, and S^e_{12}. The axial stress is uncoupled from the transverse and in-plane shear stresses and the interaction between in-plane shear and transverse stresses is considered by means of an "effective" S^e_{12} as in Equation (2).

Subsequently, an ΔN value is chosen (ΔN = 999 in this case) and it is assumed that the layer stresses do not change significantly for cycling from 1 to 1000 cycles. For this new value of N (1000 cycles), the residual (degradation) factors for each layer are determined for the moduli and strength from the residual property curves of Figures 28 and 29. These are tabulated in Table 15. These residual factors are used to determine new laminae properties in the overstressed and shear regions in Table 14 for N = 1000. The new layer properties are used for another cycle of the FATLAM I program. Repeated application of this procedure leads to the results shown in Tables 14 and 15.

Note that in Table 15, the S_{22} value for the -45° layer in the shear region is greater than 1 (at N = 1) and thus, a transverse tension failure is predicted. For this situation, the residual transverse and in-plane shear properties are arbitrarily assumed to be 1/10th of the lamina properties at N = 1. Also, as discussed above, the residual factor for the longitudinal compression modulus and strength is taken to be 0.85, which the residual factor for the shear modulus in the region of axial overstress.

When the above procedure is repeated for additional increments of N, it is observed that at about 500,000 cycles (see Table 15) the 0° layers fail in in-plane shear in the shear

region. The growth of an axial in-plane shear crack increases the interlaminar shear stresses and hence, the tendency of the 0° surface layers to delaminate from the subsurface ±45° layers. This delamination phenomena has been observed in the fatigue tests. Indeed, it appears to be the dominant mechanism of damage propagation. Since the present analysis does not account for the effects of interlaminar stresses, progressive delamination of the 0° layers from the ±45° layers cannot be predicted quantitatively at this time. In addition, those 45° layers which are loaded in compression within the shear transfer region have "failed" in transverse tension at the start of the loading. Hence, the wearout in the 45° layers cannot be determined from test data for longitudinal compression fatigue which are obtained on laminae which had not experienced transverse tension damage or failure. The present experiments for the $[0_2/\pm 45]_s$ notched laminates indicate that the ±45° fibers in the shear region do not fail, except in limited regions, thus inhibiting the growth of a through-the-thickness axial crack. Calculations made above using the wearout rates in Figures 28 and 29 tend to confirm this.

The progressive wearout of the laminate properties is shown in Table 16. At N = 500,000 cycles, the residual unnotched tension strength, σ_x^t, has reduced to 0.637 GN/m^2 (from 0.715 GN/m^2) while the maximum axial overstress at the notch root, σ_{SCFM}, has changed only slightly to 0.571 GN/m^2 (Table 15). Thus, the condition for a transverse fracture in fatigue ($\sigma_{SCFM} > \sigma_x^t$) is being approached.

The same laminate was then analyzed using the revised procedure which includes the modification* to consider the spatial variation of degraded properties. An important difference

---

*The FATLAM I computer code has been modified to the FATLAM IA code which incorporates the changes in the analysis as described in Appendix A.

that is observed between these results, which are presented in Tables 17 and 18, and those in Tables 14 and 15 is that the in-plane shear failure in the 0° layers in the shear region is advanced by almost a decade and occurs before N = 50,000 cycles. Another change is that the laminate axial stress in the overstress region drops more rapidly with N, than it does when spatial variation of properties has not been included. For example, the maximum axial stress at 500,000 cycles is 0.558 GN/m^2 in Table 18 as compared with 0.571 GN/m^2 in Table 15. The predicted unnotched laminate strength at this point is 0.637 GN/m^2 for both analyses at 500,000 cycles. Thus, it is to be expected that the modified analysis will predict a longer lifetime prior to transverse crack propagation.

Residual Notched Strength

The previous calculations defined fatigue failure by determining the time (number of cycles) at which the maximum laminate stress became equal to the local residual laminate strength. At any time prior to this, there remains the question of what additional load, above the applied fatigue load, could be sustained by the laminate. This is the problem of residual strength of the notched laminate.

Computations of residual strength have been made by taking the residual laminae and laminate properties from Tables 18 and 19 and using them in the FATLAM IA computer code. The residual laminate stiffnesses and strengths are tabulated in Table 19. The ratios, E_R and G_R, which define the residual to initial laminate extensional and shear stiffnesses are summarized in Table 20. These reduced stiffnesses are used in the highly stressed regions as discussed earlier (see Figure 5). The resulting calculated residual notched strength values, as a function of number of cycles, are also shown in Table 20. The notched

laminate residual strength is predicted to increase slightly up to about N = 50,000 cycles and decrease for N = 500,000 cycles. The experimental data (Table 11) also show an increase at N = 50,000 cycles; however, it is a larger increase than predicted. Further, the experiments show a continued increase up to and beyond 500,000 cycles. In this context, it should be noted that the analytical predictions can only be as accurate as the lamina fatigue data.

The relative importance of the degradation of extensional and shear properties also requires consideration. Thus, if the same calculations are repeated with the assumption that there is no degradation of extensional properties, the results are changed as shown in the last column of Table 20. For this case, there is a continued increase in the residual strength up to N = 500,000 cycles. In the table, for $E_R = 1$, a decrease in the value of G_R increases the residual strength. This increase does not correlate quantitatively with the results in Table 11, although the trend is the same. Referring to Figure 21, which shows the extend of the 0° surface layer delamination, it is clear that the shear stiffness in the region of delamination should be less than that in the undelaminated regions. However, unless the extent of delamination is known, the variation of the shear stiffness in the x-direction cannot be accurately determined. Consideration of such discrete regions of increasing shear stiffnesses along the x-axis will tend to reduce the notch tip stress concentration factor and as a result, the predictions of residual strength will be higher. In fact, a factor which also influences the residual notched strength is the growth of the inelastic length α. The larger the value of α, the lower is the maximum value of the stress concentration factor (SCF). The SCF is represented by the slope σ_{SCFM}/σ_x in Figure 3. Thus, for a given value of σ_x^t, the σ_T value will increase with increasing α; that is, the residual notched strength will increase.

The calculations presented in Table 20 are based on the assumption that the interlaminar delamination between the 0° and ±45° layers results primarily in the degradation of the shear properties in the region of the projection of notch diameter. However, referring to Figure 21, which shows the extent of delamination, it becomes apparent that the longitudinal modulus in that region has also degraded significantly because the 0° surface layers are no longer effective. In fact, the laminate in the delaminated region is a $[\pm 45]_s$ laminate with a much lower longitudinal modulus than the original $[0_2/\pm 45]_s$ laminate. Thus, in order to calculate the stress redistribution, the failure model should be able to consider varying properties in the core region (see Fig. 2) as a function of the axial coordinate. This capability does not exist at the present time. An approximation to the actual behavior can be made, however. Since the longitudinal stiffness in the delaminated region is negligible as compared to that of the laminate, the debonded region can be effectively considered as a notch. Hence, the failure analysis is performed for a laminate with a notch shape as indicated by the "C" scans in Figure 21. Such a failure analysis for rectangular shaped notch which considers the finite size effect has been developed in Reference 12.

Specifically, for S = 0.8, the notch geometry is determined from Figure 19, which shows the variation of axial crack length vs. number of cycles, for N = 50,000 and 500,000 cycles. The corresponding laminae properties are taken from Table 17. The resulting residual strengths are shown in Table 21. Note that the increase in the residual strength is higher than that in Table 20 and comparable to the experimentally obtained values. The drop in the residual strength at N = 500,000 cycles from that at N = 50,000 cycles is once again attributed to the reduction in σ_x^t and the uncertainty associated with the [0] laminate tension/tension residual property data.

Maximum Stress Equal to 67% of Static Notched Strength

The tension/tension fatigue tests for S = 0.67 were conducted with a maximum stress value of 0.3 GN/m^2 and R = 0.1. A fatigue analysis was subsequently performed and the results are tabulated in Tables 22 and 23. The conclusions of the analysis are essentially similar to the case of S = 0.8, except that the laminae failures (such as the 0° in-plane shear failure in the region of shear-strain concentration) are delayed in time. Table 24 indicates the wearout of the laminate properties while the residual notched strength as a function of N is shown in Table 25. The residual strength registers a marginal increase at N = 10,000 cycles and decreases with increasing N. For the case when the delaminated region is effectively modeled as a rectangular hole, the size of which is obtained from Figure 20 for N = 5×10^5 and 1.5×10^6 cycles, the residual strengths are tabulated in Table 26. Once again, these values are higher than those in Table 25.

Results from Tables 11, 12, 21, and 26 are summarized in Figure 30 (the average experimental value for S = 0.8 at N = 1.5×10^6 cycles does not consider the fatigue failure data point in Table 11). The experimental values for S = 0.8 and 0.667 approach the net section strength with increasing N. The predicted values also show an initial increase followed by a subsequent decrease. This decrease is primarily due to the wearout of the laminate longitudinal properties as obtained from the data in Figure 28.

CONCLUDING REMARKS

The failure model for predicting through-crack growth and ultimate failure of notched fiber-composite laminates under fatigue loading (Ref. 1) has been modified and compared with limited experimental data. The modifications made to the fatigue failure model permit the treatment of spatial variation of degraded properties. Modification of the fatigue failure model and correlation of the experimental/analytical results were the principal aims of the current effort.

The fatigue failure model was modified to treat spatial variation of degraded properties by assuming the material in the vicinity of the notch degrades uniformly, while the remainder of the laminate retains its virgin properties. This piecewise model of material degradation represents the physical phenomena without requiring a complicated analysis.

The following experiments were performed in an attempt to verify the fatigue model for notched Boron/epoxy laminates:

(i) longitudinal tensile static and fatigue tests (life, residual stiffness, and strength) of unnotched $[0]_8$, $[90]_8$, and $[\pm 45]_{2s}$.

(ii) static tests of unnotched and notched laminates: $[0_2/\pm 45]_s$.

(iii) fatigue tests of notched laminates $[0_2/\pm 45]_s$ (life, damage propagation, and residual strength for 0.8 and 0.67 of notched ultimate strength).

The transverse and the longitudinal data from (i) were considered unreliable for different reasons. The transverse test data from the $[90]_8$ laminates were excessively scattered. In the absence of good transverse data, the transverse property degradation was assumed to be proportional to axial-shear-property degradation.

The longitudinal test data from the $[0]_8$ were considered to be abnormally low, possibly due to fiber misalignment. For the purposes of analytical prediction, the longitudinal data in

Reference 11 was used in lieu of the longitudinal data generated during this program.

In accordance with the modified fatigue model, laminate fatigue behavior was predicted from lamina fatigue data. Predictions were compared with the experimental notched-laminate fatigue data for $[0_2/\pm 45]_s$ Boron/epoxy laminates containing a 0.635 cm diameter circular hole. The specific phenomena of interest are:

(i) the initiation of fatigue damage and its growth as a function of load cycles;

(ii) fatigue life and mode of failure; and

(iii) the residual strength after a predetermined number of cycles and the corresponding mode of failure.

Certain of the predicted phenomena were observed experimentally. Principal among these is the increase in residual strength after fatigue loading, and both axial and transverse damage growth.

Correlation of theory and experiment was hampered by the following factors:

(i) delamination of the 0° surface layers in the region of the longitudinal projection of the notch diameter;

(ii) lack of statistically significant data base for lamina fatigue properties in general; and

(iii) absence of lamina axial compression fatigue data in particular.

The principal deficiency appears to be the lack of a capability to predict growth of delaminations. Therefore, the interplay of stacking sequence and various failure modes (transverse, axial, and off-axis through-cracks and delaminations) should be investigated analytically and experimentally in detail.

APPENDIX A

GOVERNING EQUATIONS FOR FAILURE MODEL WITH SPATIAL VARIATION OF DEGRADED PROPERTIES

Referring to Figures 2 and 5 in the main text and Reference 3, the equations of equilibrium in the various regions of shear stress transfer are as follows:

REGION OF IN-PLANE SHEAR DAMAGE (AXIAL CRACK)

Equilibrium of the center core and adjacent overstressed regions in the x-direction gives:

$$n\ k\ h\ E_{x_o} \frac{d^2\ U_0}{dx^2} = 0 \qquad \text{(A1)}$$

$$m\ j\ h\ E_{x_o} \frac{d^2\ U_1}{dx^2} - \left(\frac{G_{xy_o}\, jh}{m} + \frac{G'_{90}\ j_{90} h}{m} \right) (U_1 - U_2) = 0 \qquad \text{(A2)}$$

where

$$U_2 = \sigma_g \frac{x}{E_{x_o}} \S \qquad \text{and}$$

$$G'_{90} = \frac{V_f E_f}{2} \left(\frac{h^*}{\ell} \right)^2 \left\{ 1 + \kappa \frac{E_f}{4G_f} \left(\frac{h^*}{\ell} \right)^2 \right\}$$

It is obvious that the gross laminate properties are used in the above equations. The last term in equation (A2) represents the modified shear stiffness of the 90 degree layers in the laminate and is derived in Reference 3 assuming that the fibers are clamped at two points separated by a length m which is the assumed region of shear transfer (see Figure A-1). The modified shear modulus G_{90} is the sum of the shear modulus of the 90 degree lamina (G_{12}) and the contribution of the fiber bending stiffness in the 90 degree layers over a length m (G'_{90}). As m increases,

§ Subscript 'o' represents laminate properties at N = 1 while 'n' represents properties at N > 1.

the fiber bending stiffness decreases and G_{90} approaches the conventional value of G_{12} for the 90 degree laminate. In $[0/\pm\theta]$ laminates with $0° \leq \theta \leq 45°$, the bending stiffness of the fibers in $\pm\theta$ layers is negligible.

Equations (A1) and (A2) are rewritten as:

$$n^* \; j \; A_f \; E_{xf_o} \frac{d^2 \; U_0}{dx^2} = 0 \tag{A3}$$

$$E_R \, m^* \; j \; A_f \; E_{xf_o} \frac{d^2 \; U_1}{dx^2} - \left(\frac{G_{xy_o} \; j \; A_f}{m^* d^2 \; V_f} + \frac{G'_{90} \; j_{90} A_f}{m^* d^2 \; V_f} \right) (U_1 - U_2) = 0 \tag{A4}$$

where

$E_R = E_{x_n} / E_{x_o}$ and

E_{x_n} = laminate longitudinal modulus at $N > 1$.

The above differential equations are nondimensionalized by assuming

$$U_{0,1} = \sigma_{gf} \left(\frac{V_f \; m^*}{E_{xf_o} \; G_{xy_o}} \right)^{\frac{1}{2}} u_{0,1} \; d \tag{A5}$$

and

$$x = \left(\frac{E_{xf_o} V_f \; m^*}{G_{xy_o}} \right)^{\frac{1}{2}} \xi \; d \; . \tag{A6}$$

Thus, we have

$$n^* \; \frac{d^2 \; u_0}{d\xi^2} = 0 \tag{A7}$$

$$m^* E_R \; \frac{d^2 \; u_1}{d\xi^2} - (1 + r) \; (u_1 - \xi) = 0 \tag{A8}$$

where $r = \dfrac{j_{90}}{j} \dfrac{G'_{90}}{G_{xy_o}}$.

The solutions of equations (A7) and (A8) are

$$u_0 = C_1$$

$$u_1 = \xi + C_2 \left(e^{\Delta\xi} - e^{-\Delta\xi}\right) \qquad 0 \le \xi \le \zeta \tag{A9}$$

where $\Delta = \left(\frac{1 + r}{m^* E_R}\right)^{\frac{1}{2}}$ and C_1 and C_2 are constants.

The boundary conditions $\frac{du_0}{d\xi}(\xi = 0) = 0$ and $u_1(\xi = 0) = 0$ have already been considered.

INELASTIC REGION

The following governing equations are derived for x-direction equilibrium in the inelastic zone (shear stress in shear region $= \tau^\circ$, shear strain $\le \gamma_{ult}$)

$$n^* j A_f E_{xf_o} \frac{d^2 U_0}{dx^2} - 2j h \tau^\circ - 2 \frac{G'_{90} j_{90} A_f}{m^* d^2 V_f} (U_0 - U_1) = 0 \tag{A10}$$

$$E_R m^* j A_f E_{xf_o} \frac{d^2 U_1}{dx^2} + j h \tau^\circ - \frac{G'_{90} j_{90} A_f}{m^* d^2 V_f} (U_1 - U_0)$$

$$- \left(\frac{G_{xy_o} j A_f}{m^* d^2 V_f} + \frac{G'_{90} j_{90} A_f}{m^* d^2 V_f} \right) (U_1 - U_2) = 0 \tag{A11}$$

where τ° = yield (failure) shear stress of the laminate at the current value of N.

In addition to the preceeding nondimensionalization of the displacements and the coordinates $U_{0,1}$, the yield shear stress τ° is nondimensionalized in the following manner:

$$\tau^\circ = \sigma_{gf} \left(\frac{G_{xy_o} V_f}{E_{xf_o} m^*} \right)^{\frac{1}{2}} \bar{\tau}_y \, . \tag{A12}$$

where $\bar{\tau}_y$ is the nondimensional shear stress.

Equations (A10) and (A11) appear in nondimensionalized form as:

$$n^* \frac{d^2 u_0}{d\xi^2} - 2\bar{\tau}_y - 2r\,(u_0 - u_1) = 0 \qquad \text{(A13)}$$

$$E_R\, m^* \frac{d\, u_1}{d\xi^2} + \bar{\tau}_y - r(u_1 - u_0) - (1 + r)\,(u_1 - \xi) = 0 \qquad \text{(A14)}$$

The solutions for equations (A13) and (A14) are:

$$\left.\begin{aligned} u_0 &= \xi - \frac{\bar{\tau}_y}{r} + C_3\, e^{\gamma_1 \xi} + C_4\, e^{-\gamma_1 \xi} + C_5\, e^{\gamma_2 \xi} + C_6\, e^{-\gamma_2 \xi} \\ u_1 &= \xi + B_1\,(C_3 e^{\gamma_1 \xi} + C_4\, e^{-\gamma_1 \xi}) + B_2 (C_5\, e^{\gamma_2 \xi} + C_6\, e^{-\gamma_2 \xi}) \end{aligned}\right\} \zeta \le \xi \le \alpha \qquad \text{(A15)}$$

where

$$\gamma_{1,2} = \left\{ \frac{2r\,(m' + n^*) + n^*}{2m'\, n^*} \pm \frac{1}{2m'\, n^*} \left[\left(2r(m' + n^*) + n^* \right)^2 - 8r\, m'\, n^* (1 + r) \right]^{\frac{1}{2}} \right\}^{\frac{1}{2}}$$

$m' = m^* E_R$,

and $B_{1,2} = 1 - \frac{n}{2r}\, \gamma_{1,2}^2$.

It is evident that the above solutions are not valid for $r = 0$, as in the case of a laminate with no 90 degree layers. If $r = 0$, the solutions assume the form:

$$\left.\begin{aligned} u_0 &= \frac{\bar{\tau}_y}{n^*}\, \xi^2 + C_3\, \xi + C_4 \\ u_1 &= \xi + \bar{\tau}_y + C_5\, e^{\Delta \xi} + C_6 e^{\Delta \xi} \end{aligned}\right\} \zeta \le \xi \le \alpha \qquad \text{(A16)}$$

C_3, C_4, C_5 and C_6 are constants of integration.

ELASTIC REGION

In the elastic region, the equations of equilibrium are:

$$n^* \frac{d^2 u_0}{d\xi^2} + 2(G_R + r)(u_1 - u_0) = 0 \qquad \text{(A17)}$$

$$m^* \frac{d^2 u_1}{d\xi^2} - (G_R + r)(u_1 - u_0) + (1 + r)(\xi - u_1) = 0 \qquad \text{(A18)}$$

where

$G_R = G_{xy_n}/G_{xy_o}$ and G_{xy_n} = laminate in-plane shear modulus for $N > 1$.

The solutions of equations A17 and A18 are:

$$\left.\begin{aligned} u_0 &= \xi + C_7 e^{-\beta_1 \xi} + C_8 e^{-\beta_2 \xi} \\ u_1 &= \xi + B_3 C_7 e^{-\beta_1 \xi} + B_4 C_8 e^{-\beta_2 \xi} \end{aligned}\right\} \alpha \le \xi \qquad \text{(A19)}$$

where

$$\beta_{1,2} = \left[\frac{(m^* + Qn^*)(G_R + r)}{m^* n^*} \pm \frac{(G_R + r)}{m^* n^*} \left\{ (m^* + Qn^*)^2 - \frac{2m^* n^* (1 + r)}{(G_R + r)} \right\}^{1/2} \right]^{1/2},$$

$$Q = (1 + G_R + 2r)/2(G_R + r),$$

$$B_{3,4} = 1 - n^* \beta_{1,2}^2 / 2(G_R + r)$$

and C_7 and C_8 are constants of integration. In order to ensure

finite stresses at ∞, terms involving positive exponentials have been eliminated from the displacements in equation A19. This boundary conditions of the problem are (ζ is nondimensional distance from notch to axial crack tip; and α is nondimensional distance from notch to beginning of elastic zone - the "inelastic length"):

$$\left.\begin{aligned} u_1\ (\xi = 0) &= 0 \\ \frac{d\,u_0}{d\xi}\ (\xi = 0) &= 0 \end{aligned}\right\} \qquad \text{(A20)}$$

$$\left.\begin{aligned} u_0\ (\xi = \zeta^-) &= u_0\ (\xi = \zeta^+) \\ \frac{d\,u_0}{d\xi}\ (\xi = \zeta^-) &= \frac{d\,u_0}{d\xi}\ (\xi = \zeta^+) \\ u_1\ (\xi = \zeta^-) &= u_1\ (\xi = \zeta^+) \\ \frac{d\,u_1}{d\xi}\ (\xi = \zeta^-) &= \frac{d\,u_1}{d\xi}\ (\xi = \zeta^+) \end{aligned}\right\} \qquad \text{(A21)}$$

$$\left.\begin{aligned} u_0\ (\xi = \alpha^-) &= u_0\ (\xi = \alpha^+) \\ \frac{d\,u_0}{d\xi}\ (\xi = \alpha^-) &= \frac{d\,u_0}{d\xi}\ (\xi = \alpha^+) \\ u_1\ (\xi = \alpha^-) &= u_1\ (\xi = \alpha^+) \\ \frac{d\,u_1}{d\xi}\ (\xi = \alpha^-) &= \frac{d\,u_1}{d\xi}\ (\xi = \alpha^+) \end{aligned}\right\} \qquad \text{(A22)}$$

$$\frac{d\,u_0}{d\xi}\ (\xi \to \infty) = \frac{d\,u_1}{d\xi}\ (\xi \to \infty) = 1 \qquad \text{(A23)}$$

and

$$u_0 \ (\xi = \alpha^+) - u_1 \ (\xi = \alpha^+) = \bar{\tau}_y \quad . \tag{A24}$$

The boundary conditions of Equations A20 and A23 have already been used. Hence, there remain a total of nine boundary conditions and nine unknowns which consist of the eight constants C_1, C_2, C_3, C_4, C_5, C_6, C_7, C_8 and the nondimensional yield shear stress $\bar{\tau}_y$.

REFERENCES

1. McLaughlin, P. V., Jr., Kulkarni, S. V., Huang, S. N., and Rosen, B. W., Fatigue of Notched Fiber Composite Laminates, Part I: Analytical Model, NASA CR-132747, March, 1975.

2. Durchlaub, E. C., and Freeman, R. B., Design Data for Composite Structure Safelife Prediction, AFML-TR-73-225, March, 1974.

3. Kulkarni, S. V., and Rosen, B. W., Design Data for Composite Structure Safelife Prediction: Analysis Evaluation, TFR/2221, Materials Sciences Corporation, August, 1973; also reference 2.

4. Zweben, C. H., Fracture Mechanics and Composite Materials: A Critical Analysis, ASTM STP 521, 1973; also Materials Sciences Corporation Report, 1972.

5. Rosen, B. W., and Zweben, C. H., Tensile Failure Criteria for Fiber Composite Materials, NASA CR-2057, 1972.

6. Waddoups, M. E., et al., Macroscopic Fracture Mechanics of Advanced Composite Materials, J. Composite Materials, Vol. 5, 1971, pp. 446-454.

7. Whitney, J. M., and Nuismer, R. J., Stress Fracture Criteria for Laminated Composites Containing Stress Concentrations, J. Composite Materials, Vol. 8, 1974, pp. 253-265.

8. Hashin, Z., and Rotem, A., A Fatigue Failure Criterion for Fiber Reinforced Materials, J. Composite Materials, Vol. 7, 1973, pp. 448-464.

9. Rosen, B. W., A Simple Procedure for Experimental Determination of the Longitudinal Shear Modulus of Unidirection Composites, J. Composite Materials, Vol. 6, 1972, pp. 552-554.

10. Roderick, G. L., and Whitcomb, J. D., X-Ray Method Shows Fiber Fail During Fatigue of Boron/Epoxy Laminates, J. Composite Materials, Vol. 9, 1975, pp. 391-393.

REFERENCES (Continued)

11. Hofer, K. E., et al., Development of Engineering Data on the Mechanical and Physical Properties of Advanced Composite Materials, AFML-TR-72-205, Part II, February, 1974.

12. Quarterly Progress Reports I & II, Evaluation of Fracture in Notched Composite Laminates, NASA Contract NAS2-9069 with Materials Sciences Corporation, 1976.

Laminate	No. of Plies	Test Section			
		Length		Width	
		(in)	(cm)	(in)	(cm)
$[0]_8$	8	6.0	15.24	0.5	1.27
$[90]_8$	8	6.0	15.24	1.0	2.54
$[45/-45/45/-45]_s$	8	6.0	15.24	1.0	2.54
$[0/0/45/-45]_s$	8	9.0	22.86	1.5	3.81

Table 1. Various Test Specimen Geometries

Test Specimen	Longitudinal Gage	Transverse Gage	Location
$[0]_8$	1	1	midspan
$[90]_8$	1	0	midspan
$[45/-45/45/-45]_s$	1	1	midspan
$[0/0/-45/45]_s$	1	1	midspan
$[0/0/-45/45]_s$ (Notched)	2*	1	quarterspan

* Notched laminates contained a gage at the edge of the notch

Table 2. Location and Orientation of Strain Gages for Different Specimens

Specimen	Laminate	σ_{11}^{t} §	E_{11} §	$\varepsilon_{11} \times 10^{-3}$	ν_{12}
1-1-5	$[0]_8$	1.21	219.2	5.5	0.21
1-1-6	$[0]_8$	1.31	206.8	6.2	0.17
1-1-8	$[0]_8$	1.24	227.5	5.35	0.20
	Avg.	1.25	217.8	5.68	0.19

§ GN/m^2

Table 3. Boron/Epoxy Lamina Longitudinal Tension Properties

Specimen	Laminate	σ_{22}^{t} §	E_{22} §(tan.)	E_{22} §(sec.)	$\varepsilon_{22} \times 10^{-3}$
2BC1	$[90]_8$	0.054	23.23	17.51	3.07
2BC3	$[90]_8$	0.053	25.44	18.54	2.90
2BC4	$[90]_8$	0.053	22.06	17.24	3.04
	Avg.	0.053	23.58	17.76	3.40

§ GN/m^2

Table 4. Boron/Epoxy Lamina Transverse Tension Properties

Specimen	Laminate	τ_{12}° §	G_{12} §(tan.)	G_{12} §(sec.)	γ_{12}
3BL1	$[45/-45/45/-45]_s$	0.066	5.79	1.48	0.045
3BL2	$[45/-45/45/-45]_s$	0.081	6.20	1.59	0.051
3BL3	$[45/-45/45/-45]_s$	0.073	5.93	1.48	0.049
	Avg.	0.073	5.97	1.52	0.049

§ GN/m^2

Table 5. Boron/Epoxy Lamina In-Plane Shear Properties from $[\pm 45]_s$ Laminate Tension Tests

Specimen	S	N, Cycles	σ_{11}^{t} § Residual Strength	E_{11} § Residual Modulus
1R-1-2	0.80	440	FF*	FF
1-1-3T	0.80	100	FF	FF
1R-2-4	0.80	160	FF	FF
1R-1-8	0.80	100	1.16	199.3
1R-1-3	0.80	100	1.16	202.7
1R-1-6	0.80	100	1.18	206.8
1R-1-7	0.80	200	1.21	210.3
1R-1-1	0.80	200	1.18	208.9
1-1-4	0.75	440	FF	FF
1R-2-5	0.65	235,660	FF	FF
1-1-2	0.65	950	FF	FF
1R-2-6	0.65	20,000	1.22	213.7
1R-1-5	0.65	20,000	1.25	210.3
1R-2-2	0.65	20,000	1.08	224.1
1R-2-3	0.65	2,000	1.10	223.4
1R-2-7	0.65	2,000	1.08	212.4
1R-1-4	0.65	2,000	1.32	231.7
1-1-1	0.55	11,700	FF	FF
1-1-7	0.55	11,330,210	1.10	182.0

§ GN/m^2

*FF - Fatigue Failure

Table 6. Boron/Epoxy Lamina Longitudinal Tension/Tension Fatigue Properties

Specimen	S	N, Cycles	σ_{22}^{t} § Residual Strength	E_{22} § Tangent Modulus	E_{22} § Secant*** Modulus
2BL3	0.80	110	FF*	FF	FF
2BR1	0.80	1,200	FF	FF	FF
2ACR1	0.80	7,930	FF	FF	FF
2ACL1	0.65	20,000	0.0379	22.5	17.5
2AL1	0.65	10,800	0.0537**	21.6	18.6
2AL4	0.65	12,820	0.0592**	19.9	17.3
2ACL3	0.65	2,000	0.0542	27.9	19.1
2AL2	0.65	2,000	0.0580	27.6	19.5
2ACR4	0.65	2,000	0.0490	31.4	21.6
2ACL4	0.55	2,489,640	FF	FF	FF
2AR1	0.55	43,190	FF	FF	FF
2BC2	0.55	49,980	FF	FF	FF
2BL4	0.55	7,831	0.0536**	25.7	18.8
2BL1	0.55	5,011	0.0522**	31.5	21.4
2AL3	0.55	20,000	0.0589	24.1	19.5
2ACR3	0.55	2,000	0.0548	37.6	20.5
2ACL2	0.55	2,000	0.0537	26.2	17.0
2ACR2	0.55	2,000	0.0577	32.1	24.0

§ GN/m^2

* FF - Fatigue failure

** Residual strength after fatigue failure

*** Corresponding to the ultimate value of ε_{22}

Table 7. Boron/Epoxy Lamina Transverse Tension/Tension Fatigue Properties

Specimen	S	N, Cycles	$\tau_{12}^{\circ\,\S}$ Residual Strength	$G_{12}^{\S}$ Tangent Modulus	$G_{12}^{\S}$ Secant** Modulus
3AR2	0.80	2,890	FF*	FF	FF
3BC2	0.80	13,040	FF	FF	FF
3BR3	0.80	14,450	FF	FF	FF
3AR4	0.65	25,050	FF	FF	FF
3AC4	0.65	18,060	FF	FF	FF
3BR1	0.65	4,740	FF	FF	FF
3AC2	0.65	20,000	0.0688	4.87	1.52
3AC3	0.65	2,000	0.0716	5.70	1.58
3AR1	0.65	2,000	0.0585	5.69	1.42
3BC3	0.65	2,000	0.0743	6.14	1.55
3AR3	0.52	3,523,720	FF	FF	FF
3BR2	0.52	103,750	FF	FF	FF
3BL4	0.52	11,120	FF	FF	FF
3AL1	0.52	20,850	FF	FF	FF
3AC1	0.52	10,000	0.0678	5.33	1.52
3AL2	0.52	10,000	0.0769	5.81	1.54
3BC4	0.52	10,000	0.0574	5.61	1.35
3AL3	0.52	100,000	0.0771	5.00	1.54
3BC1	0.52	100,000	0.0688	5.76	1.40
3AL4	0.52	100,000	0.0572	4.06	1.27

§ GN/m^2

* FF - Fatigue failure

** Secant modulus corresponding to $\gamma_{12} = 0.04$

Table 8. Boron/Epoxy Lamina In-Plane Shear Fatigue Properties

Specimen		E_x § Modulus	ν_{xy} Poisson's Ratio	ε_x^t Ultimate Strain	σ_x^t § Ultimate Strength
4CCL1		125.4	0.72	0.0073	0.830
4CR1		138.6	0.68	0.0062	0.752
4ACR1		115.1	0.70	0.0069	0.748
4BR1		113.75	0.66	0.0065	0.680
	Avg.	123.0	0.69	0.0067	0.752
	Anal.	123.3	0.66		0.715

§ GN/m^2

Table 9. Unnotched $[0_2/\pm45]$ Boron/Epoxy Laminate Tension Properties

Specimen		§ Modulus	Poisson's Ratio	Ultimate Strain		§ Ultimate Strength (Notched)
				Notch Edge	Remote	
4BCL1		123.9	0.58	0.0067	0.0036	0.454
4ACL2		122.0	0.65	0.0069	0.0038	0.440
4CL2		135.1	0.70	0.0061	0.0036	0.464
	Avg.	127.0	0.64	0.0066	0.0037	0.452

§ GN/m^2

Table 10. Notched (.635 cm Diameter Circular Hole) $[0_2/\pm45]_s$ Boron/Epoxy Laminate Tension Properties

Specimen	N, Cycles	Residual Strength §	Ultimate Strain		Modulus §
			Notch Edge	Remote	
4ACL1	50,000	0.468	0.00680	0.0042	122.3
4ACR2	50,000	0.527	0.00707	0.0042	128.9
4BL1	50,000	0.493	0.00695	0.0042	122.7
		Avg. 0.496	0.00694	0.0042	
4BL2	500,000	0.545	0.0067	0.0047	118.6
4CCL2	500,000	0.560	0.00735	0.0046	133.0
4DR3	500,000	0.458	0.0075	0.0046	103.9
		Avg. 0.521	0.00718	0.0046	
4CR2	1,500,000	0.570	0.00854	0.0049	120.0
4AR1	1,500,000	0.490	0.00690	0.0045	120.0
4CCR1**	1,500,000	0.520	-	-	-
		Avg. 0.526	0.00724	0.0047	
4CL1	1,500,000	FF*	FF		FF

§ GN/m^2

* FF - Fatigue failure

** Tested at NASA Langley Research Center

Table 11. Notched $[0_2/\pm45]_s$ Boron/Epoxy Laminate Tension/Tension Fatigue Properties (S=.8)

Specimen	N, Cycles	Residual § Strength	Ultimate Strain		Modulus §
			Notch Edge	Remote	
4DR2	500,000	0.438	0.00655	0.0046	104.1
4AL2	500,000	0.499	0.0071	0.0044	120.6
4BCR2	500,000	0.502	0.0070	0.0044	126.4
		Avg. 0.48	0.00688	0.0044	
4DL1	1,500,000	0.465	0.00715	0.0046	104.1
4BC2	1,500,000	0.492	0.00755	0.0044	116.0
4BCR1	1,500,000	0.533	0.00725	0.0046	123.4
		Avg. 0.496	0.00731	0.0045	
4AR2	10,000,000	0.534	0.00690	0.0045	115.1
4DL2	10,000,000	0.558	0.00885	0.0055	106.8
4AL1	10,000,000	0.535	0.0072	0.005	112.4
		Avg. 0.542	0.00765	0.005	

§ GN/m^2

Table 12. Notched $[0_2/\pm45]_s$ Boron/Epoxy Laminate Tension/Tension Fatigue Properties (S=.667)

Lamina Location	0° Layer			+45° Layer			-45° Layer		
	σ_{11}	σ_{22}	σ_{12}	σ_{11}	σ_{22}	σ_{12}	σ_{11}	σ_{22}	σ_{12}
Overstressed Region	t*	c**	---	t	t	✓	t	t	✓
Shear § Region	---	---	✓	t	c	---	c	t	---

*t - tension
**c - compression
§ - second and fourth quadrants

Table 13. Stress States in Different Layers of the $[0_2/\pm45]_s$ Laminate in the Overstressed and Shear Regions

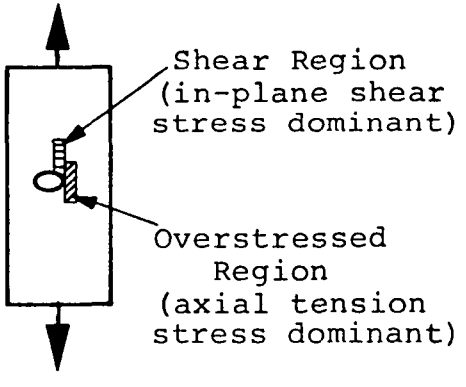

Lamina Location	0° Layer									Fatigue Cycles, N
					Ultimate Strength Values					
	E_{11}	E_{22}	ν_{12}	G_{12}	long. ten.	trans. ten.	long. compr.	trans. compr.	in-plane shear	
overstressed region	217.8	23.58	.19	5.97	1.25	.053	2.481	.31	.073	1 (S=.8)
shear region	217.8	23.58	.19	5.97	1.25	.053	2.481	.31	.073	
overstressed region	217.8	23.58	.19	5.97	1.25	.053	2.481	.31	.073	1,000 (S=.8)
shear region	217.8	21.22	.19	5.37	1.25	.0498	2.232	.291	.0686	
overstressed region	217.8	23.58	.19	5.97	1.21	.053	2.481	.31	.073	50,000 (S=.8)
shear region	217.8	20.75	.19	5.25	1.25	.047	2.183	.276	.065	
overstressed region	217.8	23.58	.19	5.97	1.19	.053	2.481	.31	.073	500,000 (S=.8)
shear region	217.8	2.358	.19	.597	1.25	.005	1.786	.223	.007	

Table 14. Variation of Laminae Properties as a Function of Fatigue Cycles (Moduli and Strength Values are in GN/m^2)

Lamina Location	45° Layer									
					Ultimate Strength Values					
	E_{11}	E_{22}	ν_{12}	G_{12}	long. ten.	trans. ten.	long. compr.	trans. compr.	in-plane shear	Fatigue Cycles, N
overstressed region	217.8	23.58	.19	5.97	1.25	.053	2.481	.31	.073	1 (S=.8)
shear region	217.8	23.58	.19	5.97	1.25	.053	2.481	.31	.073	
overstressed region	217.8	20.04	.19	5.07	1.25	.0477	2.10	.279	.0657	1,000 (S=.8)
shear region	217.8	23.58	.19	5.97	1.25	.053	2.481	.31	.073	
overstressed region	217.8	19.34	.19	4.90	1.25	.038	2.03	.223	.053	50,000 (S=.8)
shear region	217.8	23.58	.19	5.97	1.25	.053	2.481	.31	.073	
overstressed region	217.8	23.58	.19	.597	1.25	.005	2.03	.223	.007	500,000 (S=.8)
shear region	217.8	23.58	.19	5.97	1.25	.053	2.481	.31	.073	

Table 14 (contd.). Variation of Laminae Properties as a Function of Fatigue Cycles (Moduli and Strength Values are in GN/m^2)

Laminate Location	-45° Layer									
					Ultimate Strength Values					
	E_{11}	E_{22}	ν_{12}	G_{12}	long. ten.	trans. ten.	long. compr.	trans. compr.	in-plane shear	Fatigue Cycles, N
overstressed region	217.8	23.58	.19	5.97	1.25	.053	2.481	.31	.073	1 (S=.8)
shear region	217.8	23.58	.19	5.97	1.25	.053	2.481	.31	.073	
overstressed region	217.8	20.04	.19	5.07	1.25	.0477	2.10	.279	.0657	1,000 (S=.8)
shear region	185.13	2.358	.19	.597	1.25	.005	2.23	.279	.007	
overstressed region	217.8	19.34	.19	4.9	1.25	.038	2.03	.223	.053	50,000 (S=.8)
shear region	178.6	2.358	.19	.597	1.25	.005	1.786	.223	.007	
overstressed region	217.8	2.358	.19	.597	1.25	.005	2.03	.223	.007	500,000 (S=.8)
shear region	178.6	2.358	.19	.597	1.25	.005	1.786	.223	.007	

Table 14 (contd.). Variation of Laminae Properties as a Function of Fatigue Cycles (Moduli and Strength Values are in GN/m^2)

Laminate Stress Type	Maxm. Stress (Force/m)	0° layer						Fatigue Cycles, N (S=.8)
		S_{11}	Residual Factor for E_{11}^{t}	Residual Factor for σ_{11}^{t}	S_{12}^{e} or S_{22}	Residual Factor for G_{12}, E_{22}^{c}	Residual Factor for $\tau_{12}, \sigma_{22}^{c}$	
Axial	.572 (.000581)	.8	NC*	NC	.167	NC	NC	1-1000
Shear	.231 (.000235)	-	NC	NC	.58	.9	.94	
Axial	.571 (.00058)	.807	NC	.97	.174	NC	NC	1000-50,000
Shear	.22 (.000224)	-	NC	NC	.56	.88	.89	
Axial	.5715 (.000581)	.809	NC	.95	.174	NC	NC	50,000-500,000
Shear	.2188 (.000222)	-	NC	NC	.55	.1**	.1**	
Axial	.571 (.00058)	.853	NC	.93	.21	NC	NC	500,000-1.5×10^{6}
Shear	.2146 (.000218)	-	NC	NC	-	.1	.1	

*No change
**In-plane shear failure

Table 15. Variation of Degradation or Residual Factors as a Function of Fatigue Cycles

Laminate Stress Type	Maxm. Stress (Force/m)	+45° layer						Fatigue Cycles, N (S=.8)
		S_{11}	Residual Factor for E_{11}^{t}	Residual Factor for σ_{11}^{t}	S_{12}^{e} or S_{22}	Residual Factor for $G_{12}, E_{22}^{t,c}$	Residual Factor for $\tau_{12}, \sigma_{22}^{t,c}$	
Axial	.572 (.000581)	.139	NC *	NC	.7	.85	.9	1-1000
Shear	.231 (.000235)	.616	NC	NC	.234	NC	NC	
Axial	.571 (.00058)	.135	NC	NC	.62	.82	.72	1000-50,000
Shear	.22 (.000224)	.624	NC	NC	.234	NC	NC	
Axial	.5715 (.000581)	.134	NC	NC	.61	.1 **	.1**	50,000-500,000
Shear	.2188 (.000222)	.637	NC	NC	.248	NC	NC	
Axial	.571 (.00058)	.11	NC	NC	-	.1	.1	500,000-1.5×10^{6}
Shear	.2146 (.000218)	.675	NC	NC	.27	NC	NC	

*No change
**Transverse tension/shear failure

Table 15 (contd.). Variation of Degradation or Residual Factors as a Function of Fatigue Cycles

Laminate Stress Type	Maxm. Stress (Force/m)	-45° layer						Fatigue Cycles, N (S=.8)
		S_{11}	Residual Factor for $E_{11}^{t,c}$	Residual Factor for $\sigma_{11}^{t,c}$	S_{12}^{e} or S_{22}	Residual Factor for G_{12}, E_{22}^{t}	Residual Factor for $\tau_{12}, \sigma_{22}^{t}$	
Axial	.572 (.000581)	.139	NC	NC	.7	.85	.9	1-1000
Shear	.231 (.000235)	.31	.85	.85	>1	.1**	.1**	
Axial	.571 (.00058)	.135	NC	NC	.62	.82	.72	1000-50,000
Shear	.22 (.000224)	.289	.82	.82	-	.1	.1	
Axial	.5715 (.000581)	.134	NC	NC	.61	.1 §	.1 §	50,000-500,000
Shear	.2188 (.000222)	.285	.82	.82	-	.1	.1	
Axial	.571 (.00058)	.11	NC	NC	-	.1	.1	500,000-1x5x10^6
Shear	.2146 (.000218)	.306	.82	.82	-	.1	.1	

* No change
** Transverse tension failure
§ Transverse tension/shear failure

Table 15 (contd.). Variation of Degradation or Residual Factors as a Function of Fatigue Cycles

Laminate Location	E_x	E_y	ν_{xy}	G_{xy}	σ_x^t	$\tau°$	γ_{ult}	Fatigue Cycles, N (S=.8)
overstressed region	123.3	39.68	.66	32.15	.715	--	--	1
shear region	123.3	39.68	.66	32.15	--	.3125	.0115	
overstressed region	122.0	38.63	.67	31.85	.707	--	--	1,000
shear region	118.8	34.1	.7	28.92	--	.3125	.0125	
overstressed region	121.8	38.43	.677	31.80	.683	--	--	50,000
shear region	118.8	33.65	.7	28.43	--	.3125	.0127	
overstressed region	115.2	33.39	.74	30.40	.637	--	--	500,000
shear region	115.6	25.08	.857	26.09	--	.3125	.0127	

Table 16. Degradation of Laminate Properties as a Function of Fatigue Cycles (Moduli and Strength Values are in GN/m^2)

Lamina Location	0° Layer									Fatigue Cycles, N
					Ultimate Strength Values					
	E_{11}	E_{22}	ν_{12}	G_{12}	long. ten.	trans. ten.	long compr.	trans. compr.	in-plane shear	
overstressed region	217.8	23.58	.19	5.97	1.25	.053	2.481	.31	.073	1 (S=.8)
shear region	217.8	23.58	.19	5.97	1.25	.053	2.481	.31	.073	
overstressed region	217.8	23.58	.19	5.97	1.25	.053	2.481	.31	.073	1000 (S=.8)
shear region	217.8	20.98	.19	5.31	1.25	.0493	2.20	.288	.0679	
overstressed region	217.8	23.58	.19	5.97	1.25	.053	2.481	.31	.073	50,000 (S=.8)
shear region	217.8	2.358	.19	.597	1.25	.005	2.20	.288	.007	
overstressed region	217.8	23.58	.19	5.97	1.187	.053	2.481	.31	.073	500,000 (S=.8)
shear region	217.8	2.358	.19	.597	1.25	.005	2.20	.288	.007	

Table 17. Variation of Laminae Properties As Function of Fatigue Cycles (Moduli and Strength Values are in GN/m^2)

Lamina Location	45° Layer									Fatigue Cycles, N
					Ultimate Strength Values					
	E_{11}	E_{22}	ν_{12}	G_{12}	long. ten.	trans. ten.	long compr.	trans. compr.	in-plane shear	
overstressed region	217.8	23.58	.19	5.97	1.25	.053	2.481	.31	.073	1 (S=.8)
shear region	217.8	23.58	.19	5.97	1.25	.053	2.481	.31	.073	
overstressed region	217.8	20.04	.19	5.07	1.25	.0477	2.109	.279	.0657	1000 (S=.8)
shear region	217.8	23.58	.19	5.97	1.25	.053	2.481	.31	.073	
overstressed region	217.8	19.33	.19	4.89	1.25	.038	2.03	.22	.0526	50,000 (S=.8)
shear region	217.8	23.58	.19	5.97	1.25	.053	2.481	.31	.073	
overstressed region	217.8	2.358	.19	.597	1.25	.005	2.03	.22	.007	500,000 (S=.8)
shear region	217.8	23.58	.19	5.97	1.187	.053	2.481	.31	.073	

Table 17 (contd.). Variation of Laminae Properties As Function of Fatigue Cycles (Moduli and Strength Values are in GN/m^2)

Lamina Location	-45° Layer									
					Ultimate Strength Values					
	E_{11}	E_{22}	ν_{12}	G_{12}	long. ten.	trans. ten.	long compr.	trans. compr.	in-plane shear	Fatigue Cycles, N
overstressed region	217.8	23.58	.19	5.97	1.25	.053	2.481	.31	.073	1 (S=.8)
shear region	217.8	23.58	.19	5.97	1.25	.053	2.481	.31	.073	
overstressed region	217.8	20.04	.19	5.07	1.25	.0477	2.109	.279	.0657	1000 (S=.8)
shear region	185.13	2.358	.19	.597	1.25	.005	2.109	.279	.007	
overstressed region	217.8	19.33	.19	4.89	1.25	.038	2.03	.22	.0526	50,000 (S=.8)
shear region	178.6	2.358	.19	.597	1.25	.005	2.03	.22	.007	
overstressed region	217.8	2.358	.19	.597	1.25	.005	2.03	.22	.007	500,000 (S=.8)
shear region	178.6	2.358	.19	.597	1.25	.005	2.03	.22	.007	

Table 17 (contd.). Variation of Laminae Properties as Function of Fatigue Cycles (Moduli and Strength Values are in GN/m^2)

Laminate Stress Type	Maxm. Stress (Force/m)	0° layer						Fatigue Cycles, N (S=.8)
		S_{11}	Residual Factor for E_{11}^t	Residual Factor for σ_{11}^t	S_{12}^e or S_{22}	Residual Factor for G_{12}, E_{22}^c	Residual Factor for τ_{12}, σ_{22}^c	
Axial	.572 (.000581)	.8	NC*	NC	.167	NC	NC	1-1000
Shear	.231 (.000235)	-	NC	NC	.58	.9	.94	
Axial	.5652 (.000574)	.8	NC	NC	.172	NC	NC	1000-50,000
Shear	.2419 (.000246)	-	NC	NC	.61	.1**	.1**	
Axial	.558 (.000567)	.79	NC	.95	.17	NC	NC	50,000-500,000
Shear	.253 (.000257)	-	NC	NC	-	.1	.1	
Axial								500,000-1.5×10^6
Shear								

*No change
**In-plane shear failure

Table 18. Variation of Degradation or Residual Factors as a Function of Fatigue Cycles

Laminate Stress Type	Maxm. Stress (Force/m)	+45° layer						Fatigue Cycles, N (S=.8)
		S_{11}	Residual Factor for E_{11}^{t}	Residual Factor for q_{11}^{t}	S_{12}^{e} or S_{22}	Residual Factor for $G_{12}, E_{22}^{t,c}$	Residual Factor for $\tau_{12}, q_{22}^{t,c}$	
Axial	.572 (.000581)	.139	NC*	NC	.7	.85	.9	1-1000
Shear	.231 (.000235)	.616	NC	NC	.234	NC	NC	
Axial	.5652 (.000574)	.134	NC	NC	.62	.82	.72	1000-50,000
Shear	.2419 (.000246)	.7	NC	NC	.266	NC	NC	
Axial	.558 (.000567)	.13	NC	NC	.59	.1**	.1**	50,000-500,000
Shear	.253 (.000257)	.796	NC	.95	.31	NC	NC	
Axial								500,000-1.5×10^{6}
Shear								

*No change
**Transverse tension/shear failure

Table 18 (contd.). Variation of Degradation or Residual Factors as a Function of Fatigue Cycles

Laminate Stress Type	Maxm. Stress (Force/m)	-45° layer						Fatigue Cycles, N (S=.8)
		S_{11}	Residual Factor for $E_{11}^{t,c}$	Residual Factor for $\sigma_{11}^{t,c}$	S_{12}^{e} or S_{22}	Residual Factor for G_{12}, E_{22}^{t}	Residual Factor for $\tau_{12}, \sigma_{22}^{t}$	
Axial	.572 (.000581)	.139	NC*	NC	.7	.85	.9	1-1000
Shear	.231 (.000235)	.31	.85	.85	>1	.1**	.1**	
Axial	.5652 (.000574)	.134	NC	NC	.62	.82	.72	1000-50,000
Shear	.2419 (.000246)	.318	.82	.82	>1	.1	.1	
Axial	.558 (.000567)	.13	NC	NC	.59	.1***	.1***	50,000-500,000
Shear	.253 (.000257)	.362	.82	.82	-	.1	.1	
Axial								500,000-1.5×10^6
Shear								

*No change
**Transverse tension failure
***Transverse tension/shear failure

Table 18 (contd.) Variation of Degradation or Residual Factors as a Function of Fatigue Cycles

Laminate Location	E_x	E_y	ν_{xy}	G_{xy}	σ_x^t	$\tau°$	γ_{ult}	Fatigue Cycles, N (S=.8)
overstressed region	123.3	39.68	.66	32.15	.715	--	--	1
shear region	123.3	39.68	.66	32.15	--	.3125	.0115	
overstressed region	122.0	38.63	.67	31.85	.708	--	--	1,000
shear region	118.8	34.1	.7	28.89	--	.3125	.0125	
overstressed region	121.78	38.42	.677	31.80	.706	--	--	50,000
shear region	115.6	25.08	.857	26.09	--	.3125	.0127	
overstressed region	115.25	33.39	.74	30.40	.637	--	--	500,000
shear region	115.6	25.08	.857	26.09	--	.3125	.0127	

Table 19. Degradation of Laminate Properties as a Function of Fatigue Cycles (Moduli and Strength Values are in GN/m^2)

No. of Cycles, N	E_R	G_R	Residual Notched Strength (S=.8) GN/m^2
1	1	1	.45
1,000	.989	.9	.45 (.455*)
50,000	.987	.812	.46 (.465*)
500,000	.934	.812	.41 (.465*)

*With no degradation of E_x (E_R=1) and σ_x^t

Table 20. Variation of E_R, G_R, and Residual Strength with Number of Fatigue Cycles

No. of Cycles, N	Measured Axial Crack Length, cm	σ_x^t, GN/m^2	Residual Strength, GN/m^2	
			Analysis	Experiment
50,000	.75	.706	.521	.496
500,000	1.875	.637	.471	.521

Table 21. Residual Notched Strength for S=0.8 by Approximating the Axially Delaminated Region as a Rectangular Hole

Lamina Location	0° Layer									Fatigue Cycles, N
					Ultimate Strength Values					
	E_{11}	E_{22}	ν_{12}	G_{12}	long. ten.	trans. ten.	long compr.	trans. compr.	in-plane shear	
overstressed region	217.8	23.58	.19	5.97	1.25	.053	2.481	.31	.073	1
shear region	217.8	23.58	.19	5.97	1.25	.053	2.481	.31	.073	(S=.667)
overstressed region	217.8	23.58	.19	5.97	1.25	.053	2.481	.31	.073	10,000
shear region	217.8	21.92	.19	5.55	1.25	.05	2.30	.294	.069	(S=.667)
overstressed region	217.8	23.58	.19	5.97	1.25	.053	2.481	.31	.073	500,000
shear region	217.8	20.75	.19	5.25	1.25	.039	2.18	.229	.054	(S=.667)
overstressed region	217.8	23.58	.19	5.97	1.25	.053	2.481	.31	.073	1.5×10^6
shear region	217.8	2.358	.19	.597	1.25	.005	2.18	.229	.007	(S=.667)

Table 22. Variation of Laminae Properties as a Function of Fatigue Cycles (Moduli and Strength Values are in GN/m^2)

Lamina Location	45° Layer									
					Ultimate Strength Values					
	E_{11}	E_{22}	ν_{12}	G_{12}	long. ten.	trans. ten.	long compr.	trans. compr.	in-plane shear	Fatigue Cycles, N
overstressed region	217.8	23.58	.19	5.97	1.25	.053	2.481	.31	.073	1 (S=.667)
shear region	217.8	23.58	.19	5.97	1.25	.053	2.481	.31	.073	
overstressed region	217.8	20.51	.19	5.19	1.25	.048	2.158	.285	.067	10,000 (S=.667)
shear region	217.8	23.58	.19	5.97	1.25	.053	2.481	.31	.073	
overstressed region	217.8	20.04	.19	5.07	1.25	.032	2.10	.192	.045	500,000 (S=.667)
shear region	217.8	23.58	.19	5.97	1.25	.053	2.481	.31	.073	
overstressed region	217.8	2.358	.19	.597	1.25	.005	2.10	.192	.007	1.5×10^6 (S=.667)
shear region	217.8	23.58	.19	5.97	1.25	.053	2.481	.31	.073	

Table 22 (contd.). Variation of Laminae Properties as a Function of Fatigue Cycles (Moduli and Strength Values are in GN/m^2)

Lamina Location	-45° Layer									Fatigue Cycles, N
					Ultimate Strength Values					
	E_{11}	E_{22}	ν_{12}	G_{12}	long. ten.	trans. ten.	long compr.	trans. compr.	in-plane shear	
overstressed region	217.8	23.58	.19	5.97	1.25	.053	2.481	.31	.073	1
shear region	217.8	23.58	.19	5.97	1.25	.053	2.481	.31	.073	(S=.667)
overstressed region	217.8	20.51	.19	5.19	1.25	.048	2.158	.285	.067	10,000
shear region	189.4	2.358	.19	.597	1.25	.005	2.158	.285	.007	(S=.667)
overstressed region	217.8	20.04	.19	5.07	1.25	.032	2.10	.192	.045	500,000
shear region	185.1	2.358	.19	.597	1.25	.005	2.10	.192	.007	(S=.667)
overstressed region	217.8	2.358	.19	.597	1.25	.005	2.10	.192	.007	1.5×10^6
shear region	185.1	2.358	.19	.597	1.25	.005	2.10	.192	.007	(S=.667)

Table 22 (contd.). Variation of Laminae Properties as a Function of Fatigue Cycles (Moduli and Strength Values are in GN/m^2)

Laminate Stress Type	Maxm. Stress (Force/m)	0° Layer						Fatigue Cycles, N (S=.667)
		S_{11}	Residual Factor for E_{11}^{t}	Residual Factor for σ_{11}^{t}	S_{12}^{e} or S_{22}	Residual Factor for G_{12}, E_{22}^{c}	Residual Factor for $\tau_{12}, \sigma_{22}^{c}$	
Axial	.477 (.000485)	.667	NC*	NC	.14	NC	NC	1-10,000
Shear	.193 (.000.96)	-	NC	NC	.49	.93	.95	
Axial	.471 (.0004785)	.664	NC	NC	.14	NC	NC	10,000-500,000
Shear	.2 (.000203)	-	NC	NC	.519	.88	.74	
Axial	.471 (.0004785)	.664	NC	NC	.14	NC	NC	500,000-$1.5x10^6$
Shear	.2 (.000204)	-	NC	NC	.519	.1**	.1**	
Axial	.468 (.0004754)							$1.5x10^6$-10^7
Shear	.209 (.000213)							

* No change
** In-plane shear failure

Table 23. Variation of Degradation or Residual Factors as a Function of Fatigue Cycles

Laminate Stress Type	Maxm. Stress (Force/m)	+45° Layer						Fatigue Cycles, N (S=.667)
		S_{11}	Residual Factor for E_{11}^{t}	Residual Factor for q_{11}^{t}	S_{12}^{e} or S_{22}	Residual Factor for $G_{12}, E_{22}^{t,c}$	Residual Factor for $\tau_{12}, q_{22}^{t,c}$	
Axial	.477 (.000485)	.116	NC*	NC	.6	.87	.92	1-10,000
Shear	.193 (.000196)	.514	NC	NC	.185	NC	NC	
Axial	.471 (.0004785)	.111	NC	NC	.533	.85	.62	10,000-500,000
Shear	.2 (.000203)	.576	NC	NC	.212	NC	NC	
Axial	.471 (.0004785)	.111	NC	NC	.533	.1**	.1**	500,000-1.5×10^{6}
Shear	.2 (.000204)	.576	NC	NC	.212	NC	NC	
Axial	.468 (.0004754)							1.5×10^{6}-10^{7}
Shear	.209 (.000213)							

* No change
** Transverse Tension/Shear Failure

Table 23 (contd.). Variation of Degradation or Residual Factors as a Function of Fatigue Cycles

Laminate Stress Type	Maxm. Stress (Force/m)	-45° Layer						Fatigue Cycles, N (S=.667)
		S_{11}	Residual Factor for $E_{11}^{t,c}$	Residual Factor for $\sigma_{11}^{t,c}$	S_{12}^{e} or S_{22}	Residual Factor for G_{12}, E_{22}^{t}	Residual Factor for $\tau_{12}, \sigma_{22}^{t}$	
Axial	.477 (.000485)	.116	NC	NC	.6	.87	.92	1-10,000
Shear	.193 (.000196)	.258	.87	.87	>1	.1	.1	
Axial	.471 (.0004785)	.111	NC	NC	.533	.85	.62	10,000-500,000
Shear	.2 (.000203)	.263	.85	.85	--	.1	.1	
Axial	.471 (.0004785)	.111	NC	NC	.533	.1	.1	500,000-1.5×10^{6}
Shear	.2 (.000204)	.263	.85	.85	--	.1	.1	
Axial	.468 (.0004754)							1.5×10^{6}-10^{7}
Shear	.209 (.000213)							

* No change
** Transverse Tension Failure
§ Transverse Tension/Shear Failure

Table 23 (contd.). Variation of Degradation or Residual Factors as a Function of Fatigue Cycles

Laminate Location	E_x	E_y	ν_{xy}	G_{xy}	σ_x^t	$\tau°$	γ_{ult}	Fatigue Cycles (S=.667)
overstressed region	123.3	39.68	.66	32.15	.715	--	--	1
shear region	123.3	39.68	.66	32.15	--	.3125	.0115	
overstressed region	122.22	38.77	.67	31.89	.708	--	--	10,000
shear region	119.0	34.65	.698	29.28	--	.3125	.0125	
overstressed region	122.0	38.63	.675	31.85	.707	--	--	500,000
shear region	118.8	33.93	.7	28.85	--	.3125	.0125	
overstressed region	115.2	33.39	.74	30.40	.669	--	--	1.5×10^6
shear region	115.6	25.08	.857	26.09	--	.3125	.0125	

Table 24. Degradation of Laminate Properties as a Function of Fatigue Cycles (Moduli and Strength Values are in GN/m^2)

No. of Cycles, N	E_R	G_R	Residual Notched Strength (S=.667) GN/m^2
1	1	1	.45
10,000	.989	.912	.455
500,000	.989	.897	.45
$1.5x10^6$	.934	.826	.432

Table 25. Variation of E_R, G_R, and Residual Strength with Number of Fatigue Cycles

No. of Cycles, N	Measured Axial Crack Length, cm	σ_x^t, GN/m^2	Residual Strength, GN/m^2	
			Analysis	Experiment
500,000	0.8	0.707	0.48	0.489
$1.5x10^6$	1.2	0.669	0.465	0.496

Table 26. Residual Notched Strength for S=0.667 by Approximating the Axially Delaminated Region as a Rectangular Hole

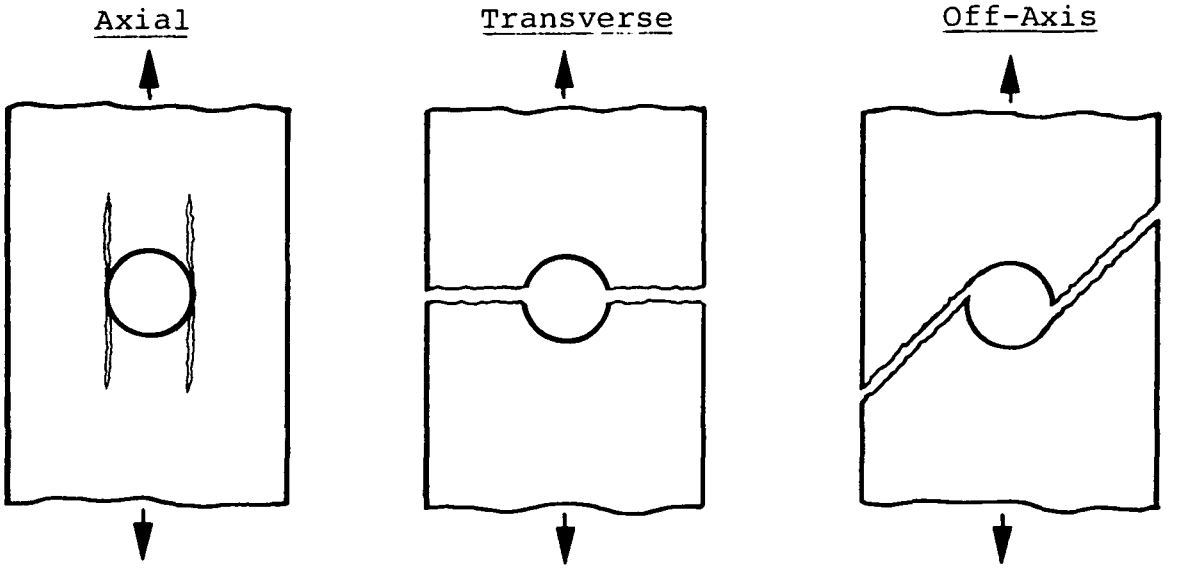

[0] Static, Fatigue

$[0_2/\pm45]_s$ Fatigue

$[0_2/\pm45]_s$ Static (for larger notch sizes)

$[\pm45]_s$ Static

$[0/90]_s$ Static

$[0_2/\pm45]_s$ Static

$[0/\pm45/90]_s$ Static

$[\pm45]_s$ Fatigue

Figure 1. Observed Static and Fatigue Failure Modes in Notched Boron/Epoxy Laminates (Ref. 2)

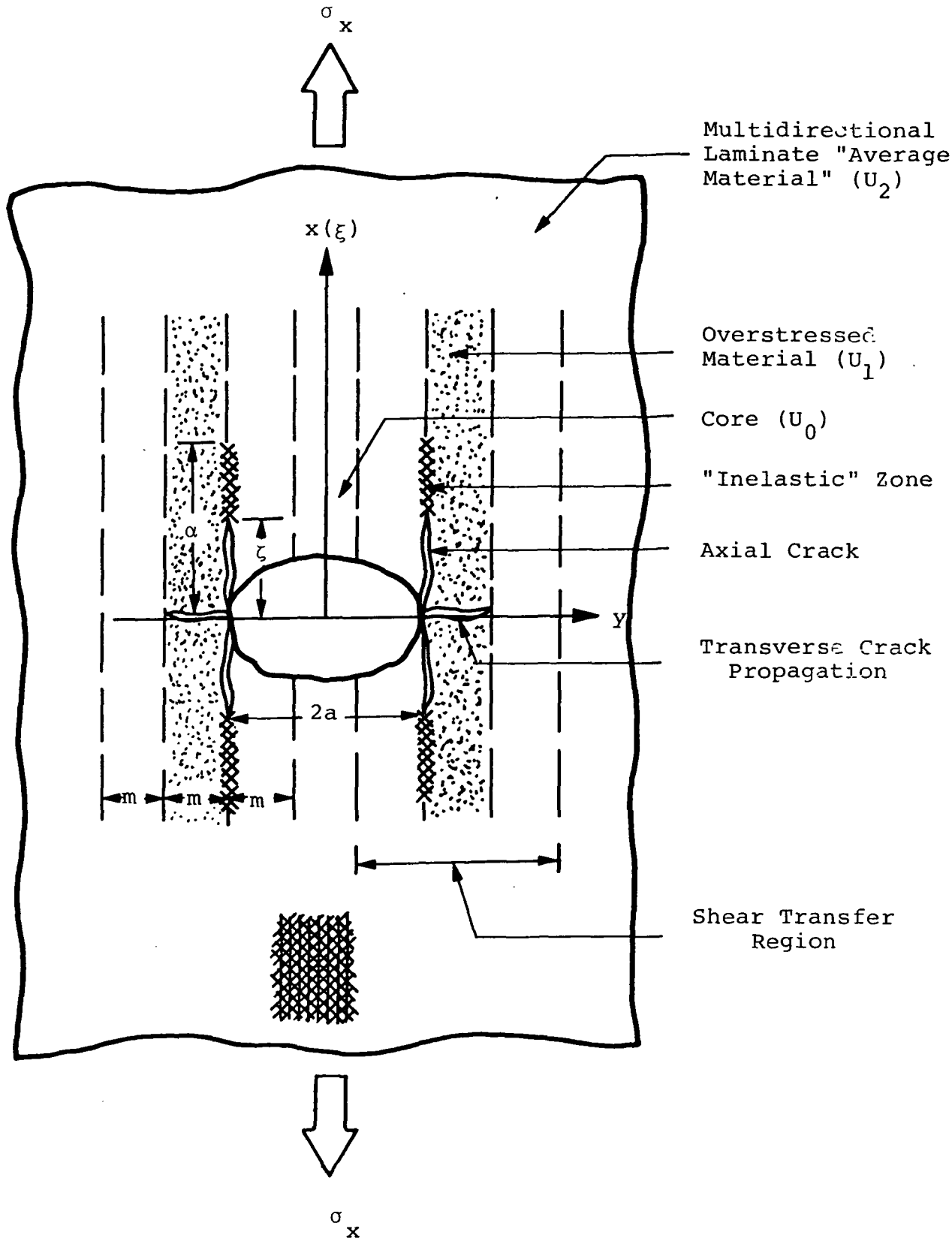

Figure 2. Mini-Mechanics Model for a Notched Laminate

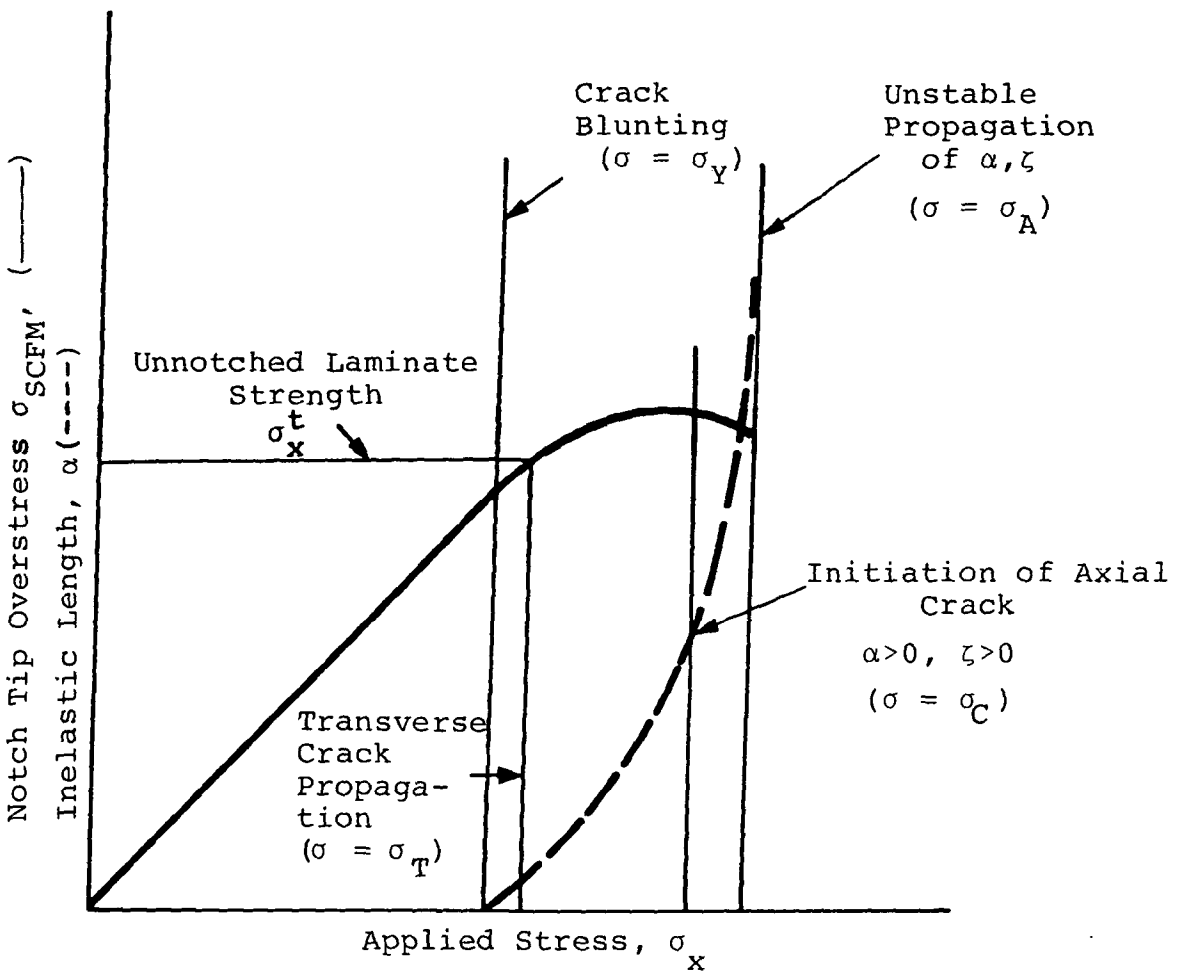

Figure 3. Crack Growth as a Function of Applied Stress

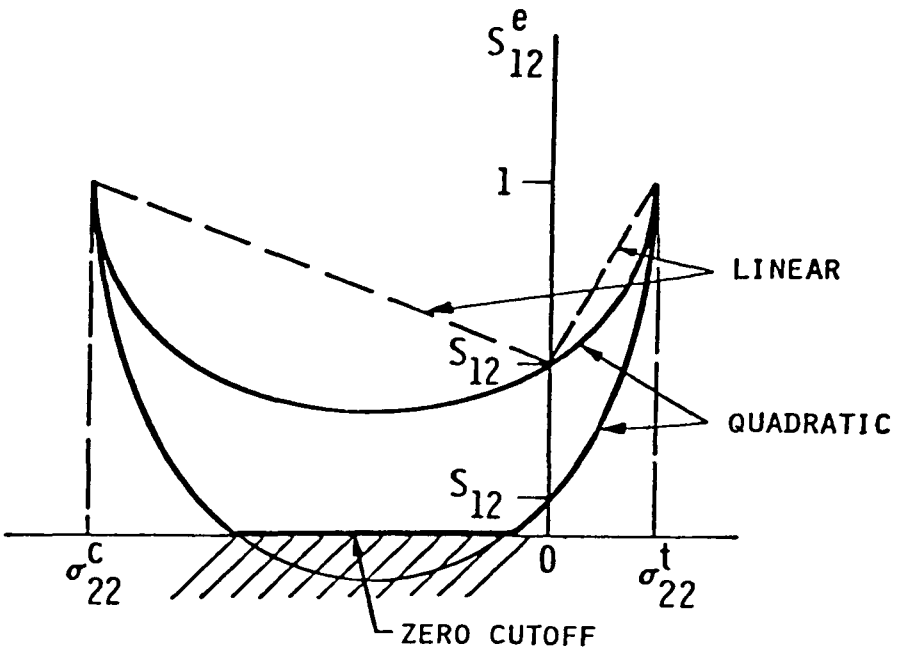

Figure 4. "Effective" Shear Stress in Fatigue Due to Transverse Tension

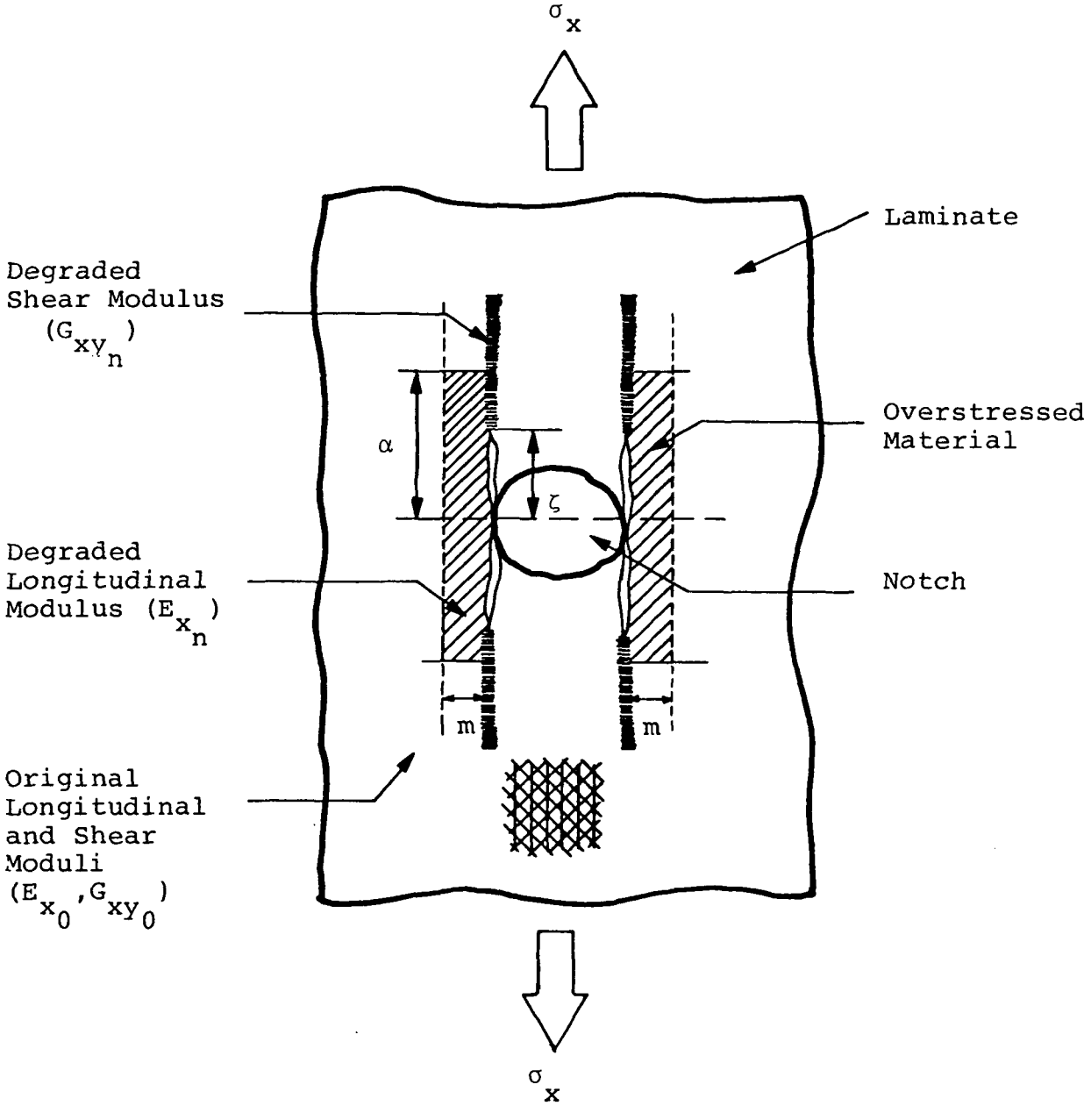

Figure 5. Degraded Modulus and Strength Regions in a Notched Laminate after Fatigue Cycling

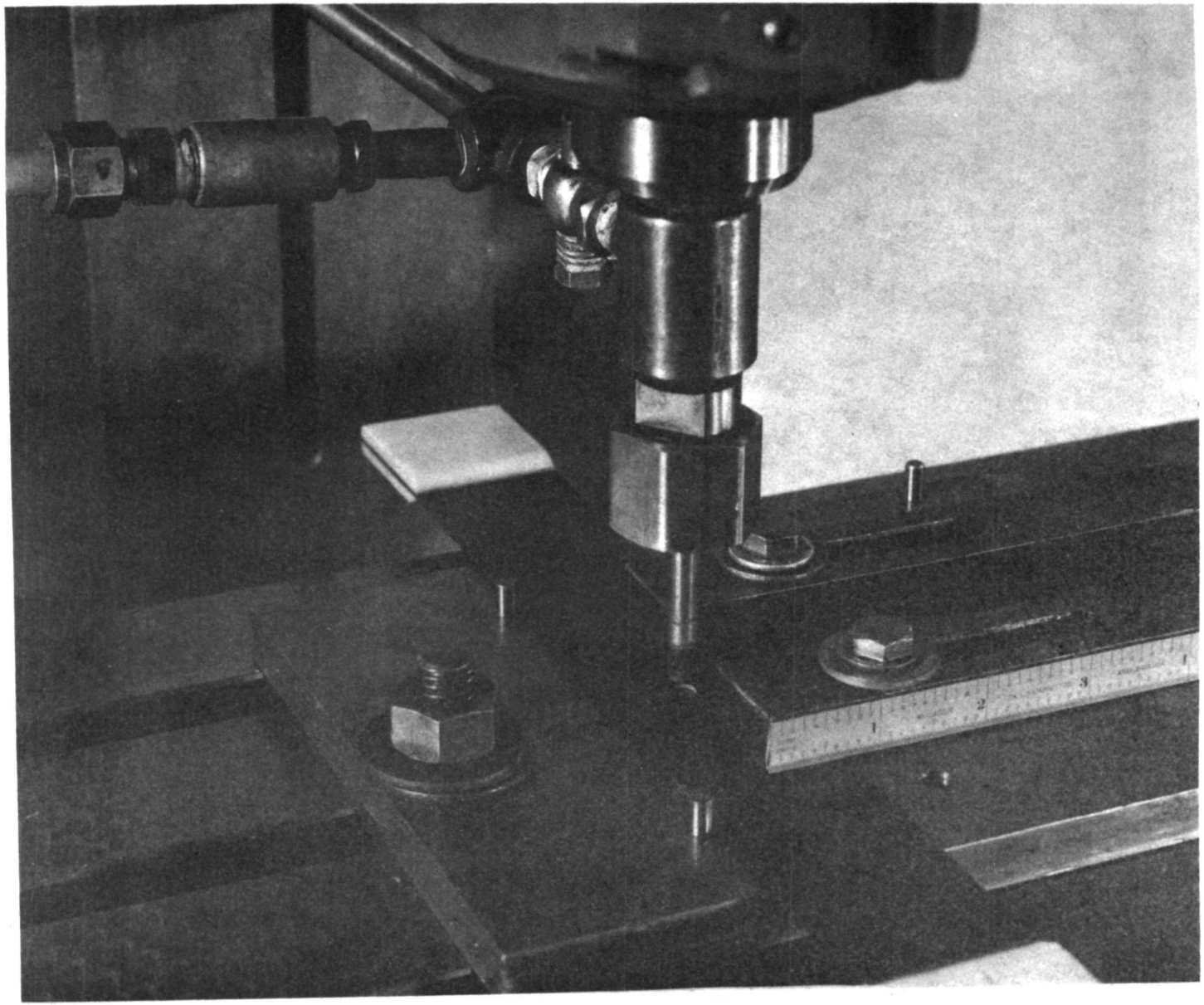

Figure 6. Notch Machining Apparatus

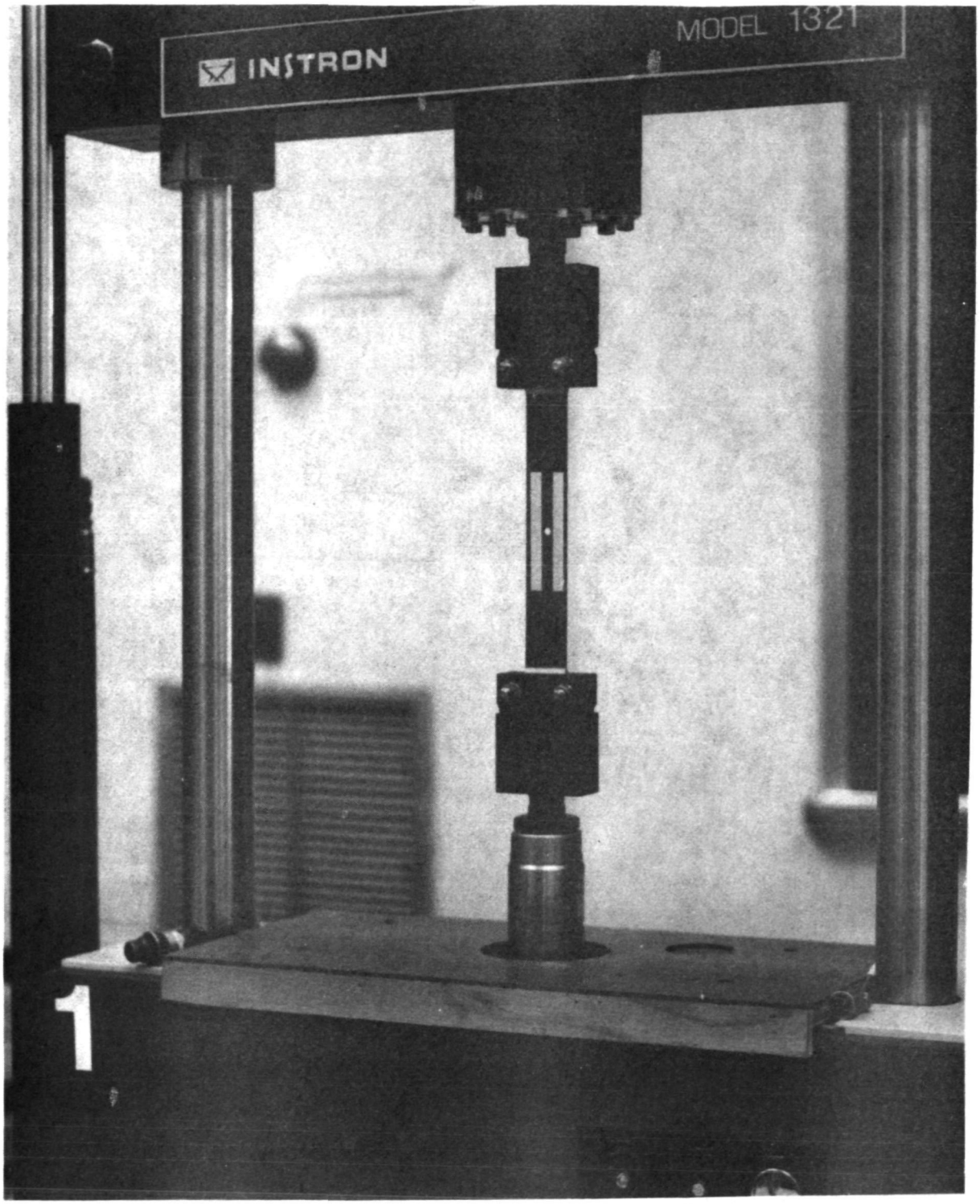

Figure 7. Specimen Grip Configuration

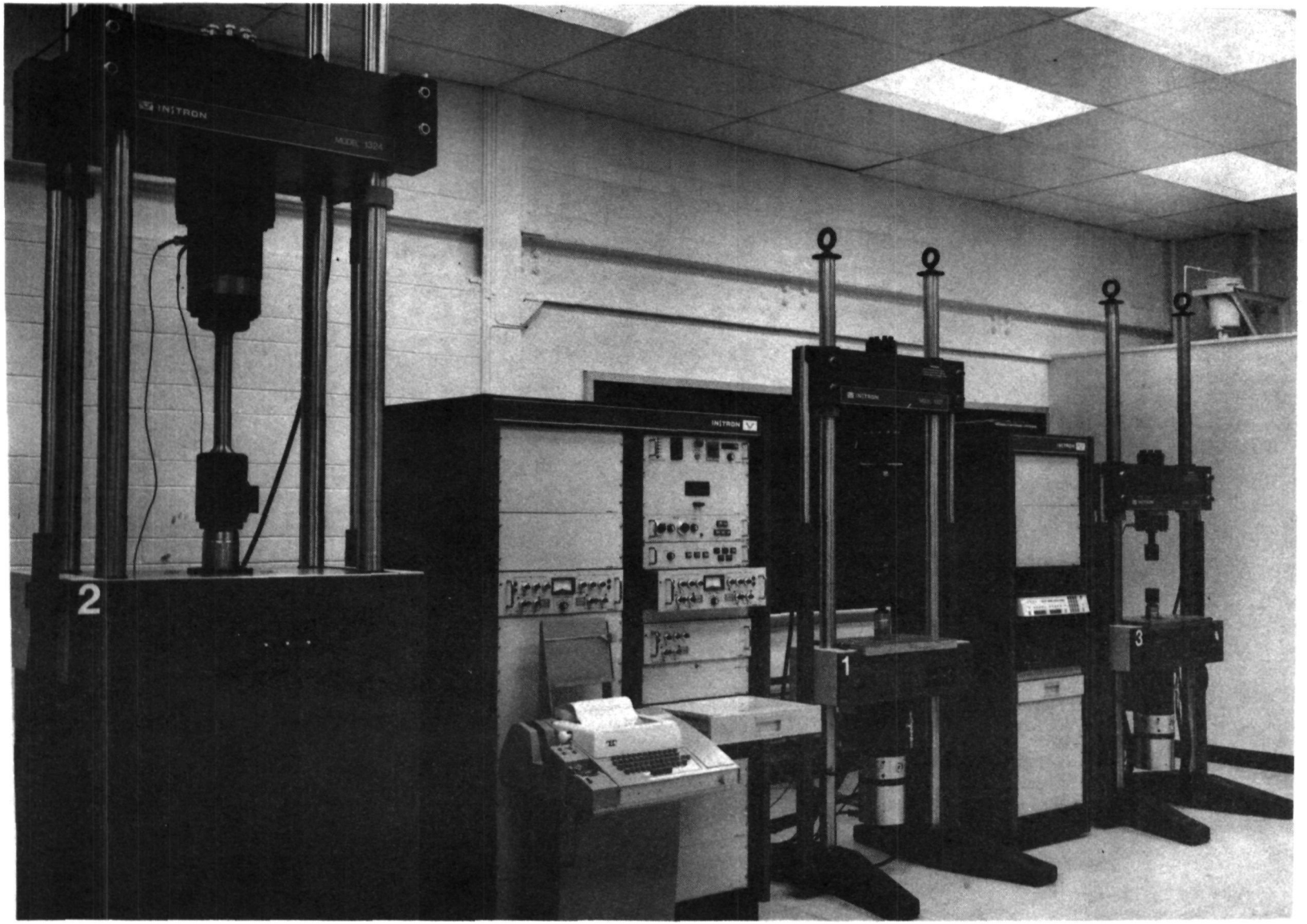

Figure 8. Servo-Hydraulic Test System

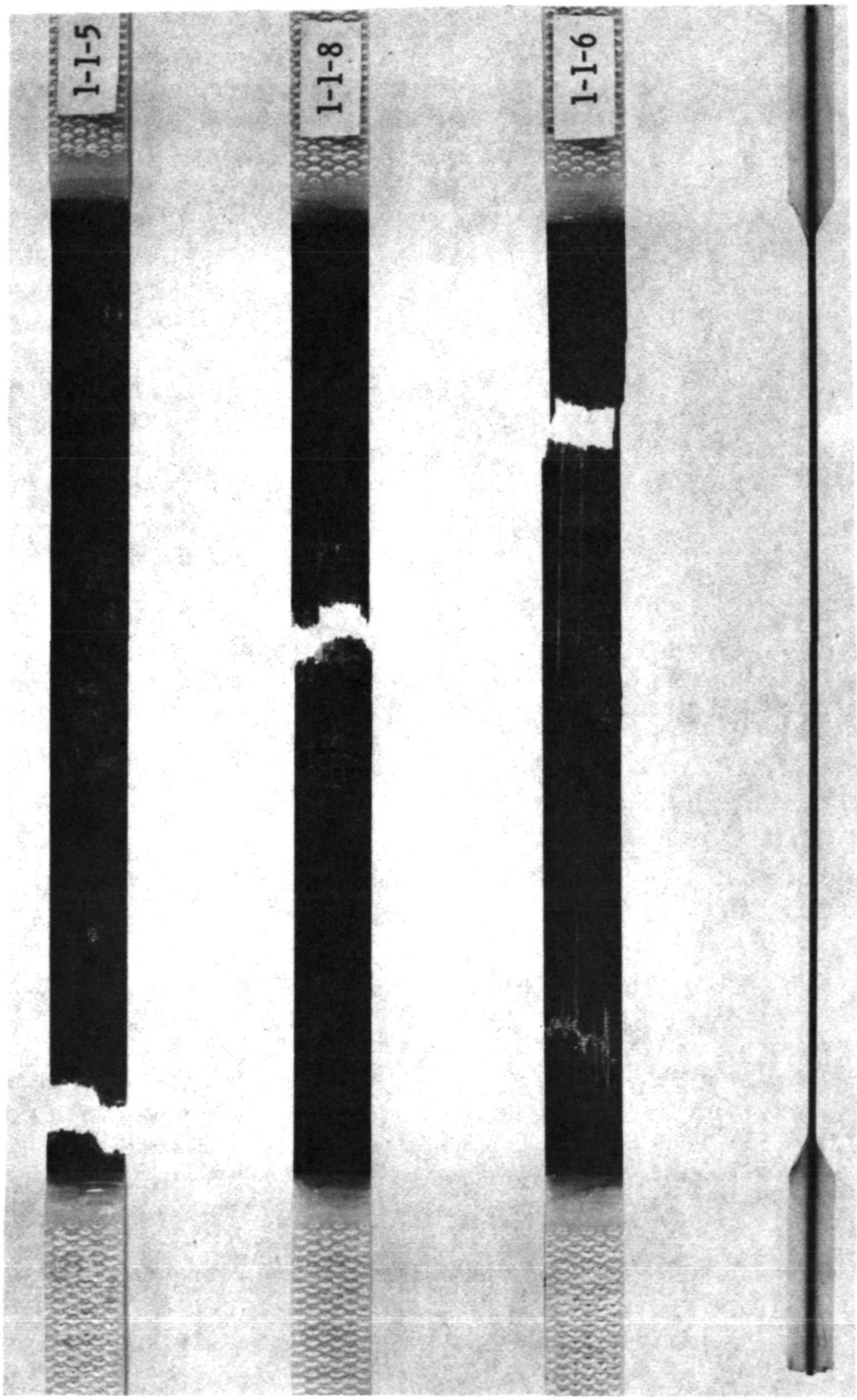

Figure 9. Typical Failures of [0] Boron/Epoxy Laminates Subjected to Longitudinal Tension Loading

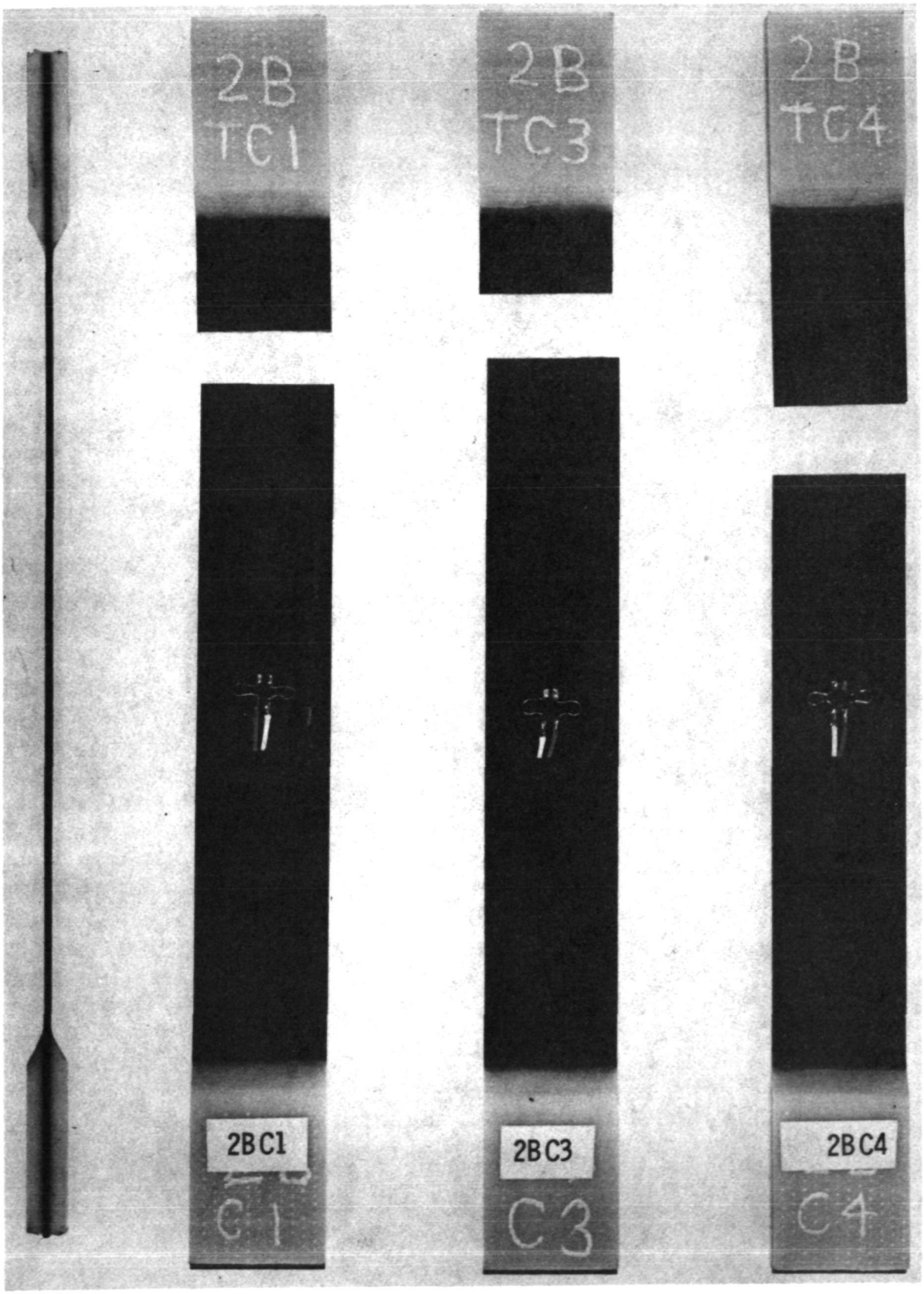

Figure 10. Typical Failures of [90] Boron/Epoxy Laminates Subjected to Longitudinal Tension Loading

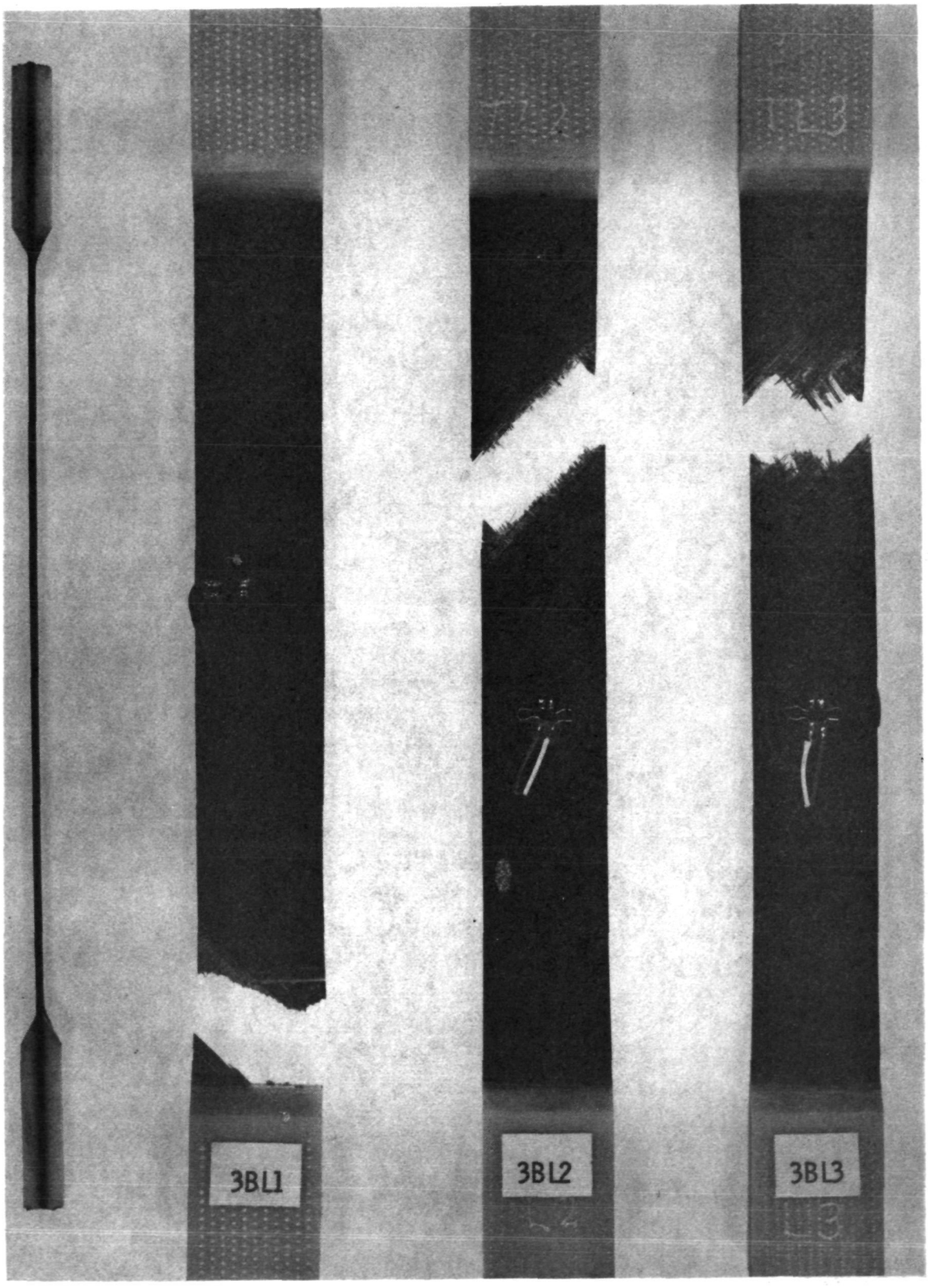

Figure 11. Typical Failures of $[\pm 45]_s$ Boron/Epoxy Laminates Subjected to Longitudinal Tension Loading

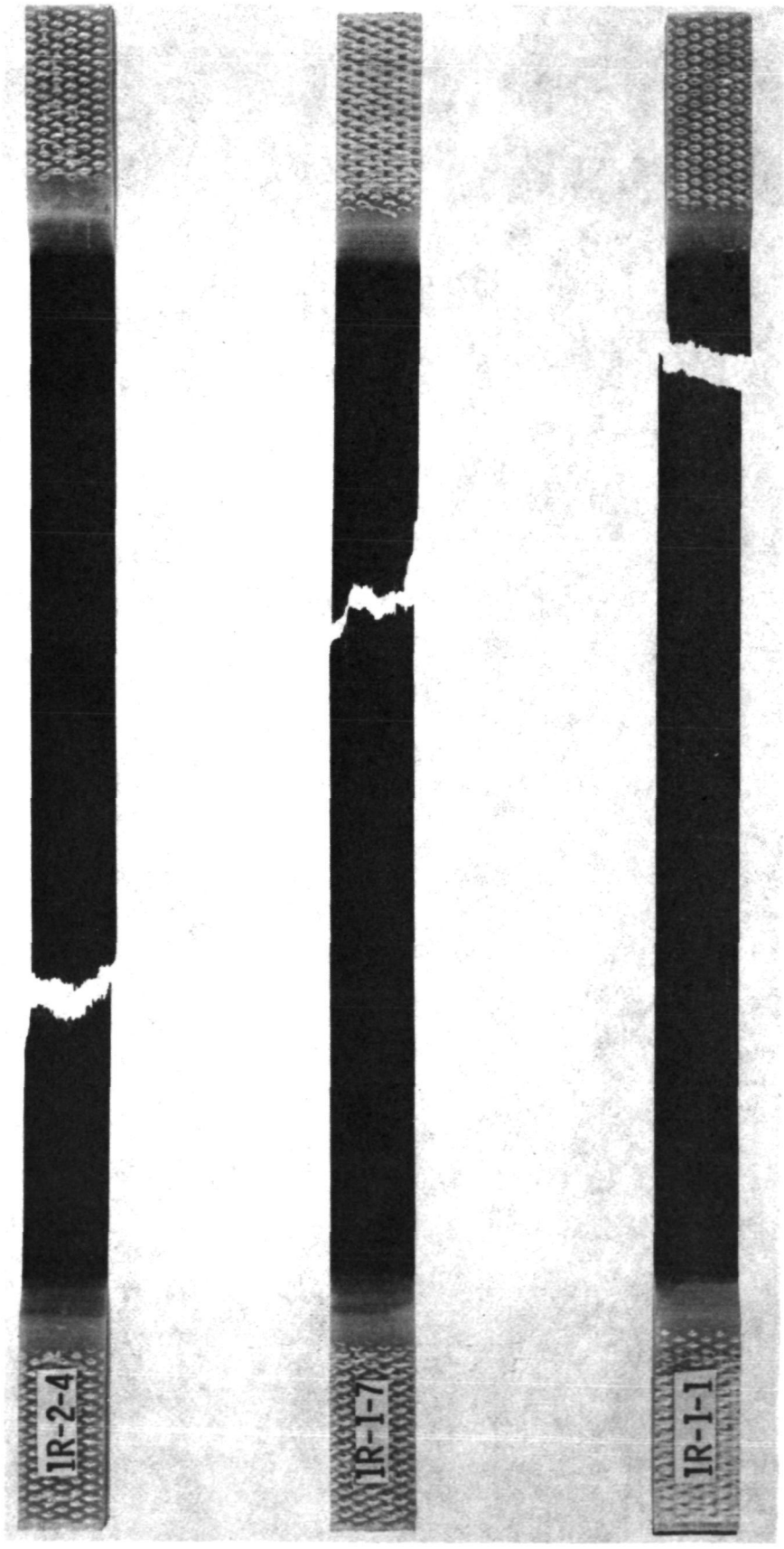

Figure 12. Typical Failures of [0] Boron/Epoxy Laminates Subjected to Longitudinal Tension/Tension Fatigue Loading

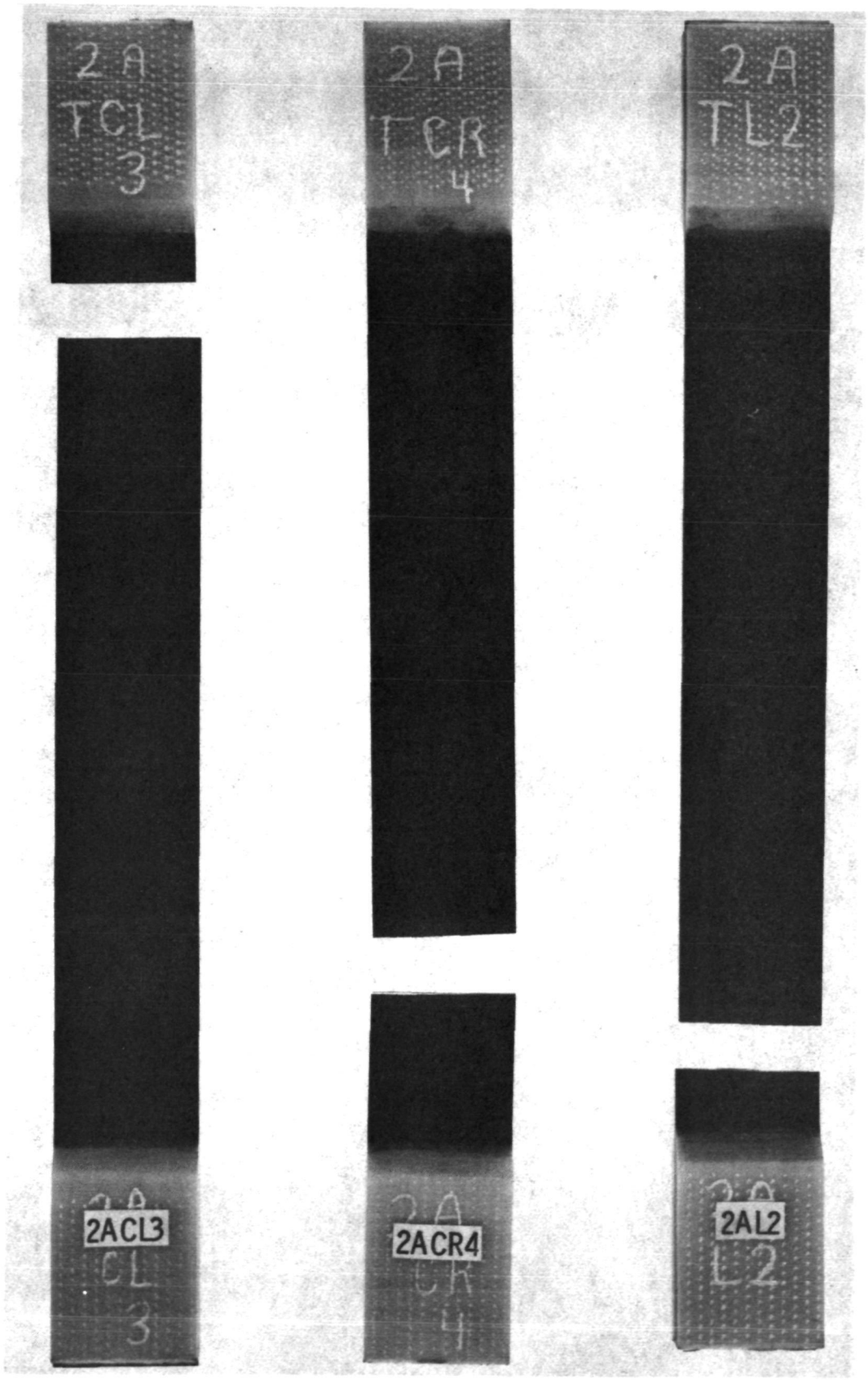

Figure 13. Typical Failures of [90] Boron/Epoxy Laminates Subjected to Longitudinal Tension/Tension Fatigue Loading

Figure 14. Typical Failures of $[\pm 45]_s$ Boron/Epoxy Laminates Subjected to Longitudinal Tension/Tension Fatigue Loading

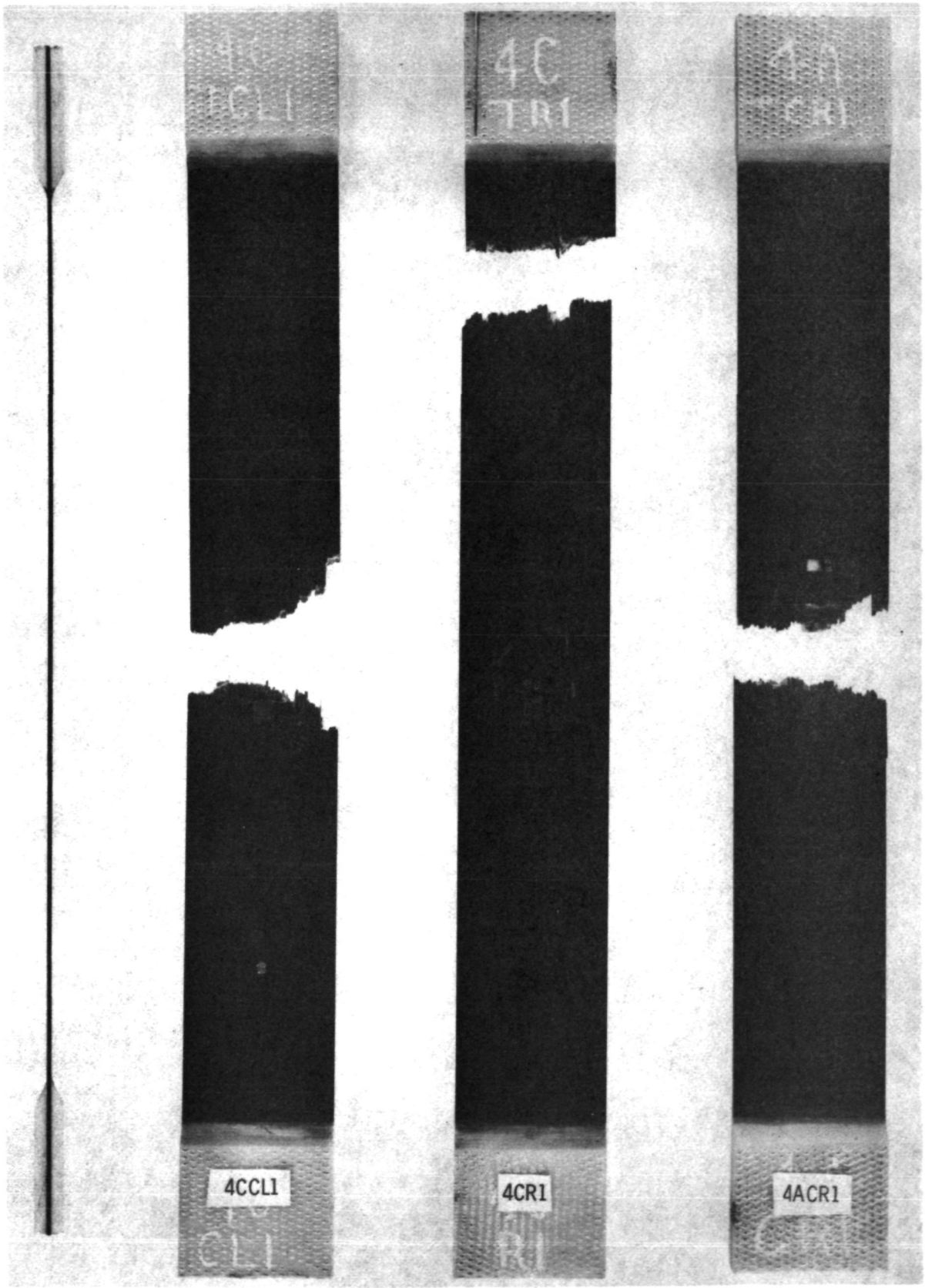

Figure 15. Typical Failures of $[0_2/\pm 45]_s$ Boron/Epoxy Laminates Subjected to Longitudinal Tension Loading

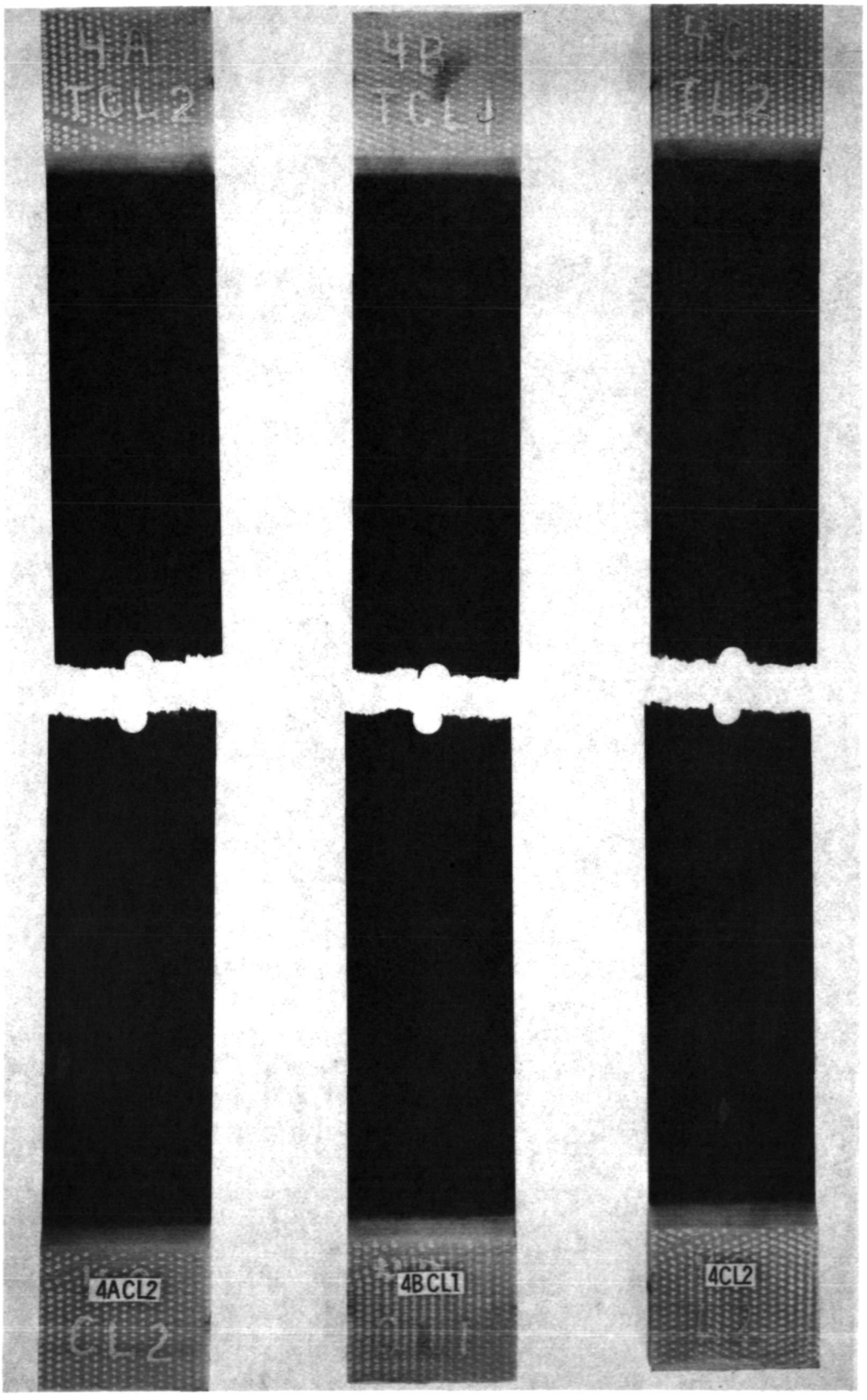

Figure 16. Typical Failures of Notched (0.64 cm. Circular Hole in a 3.81 cm Wide Coupon) $[0_2/\pm 45]_s$ Boron/Epoxy Laminate Subjected to Longitudinal Tension Loading

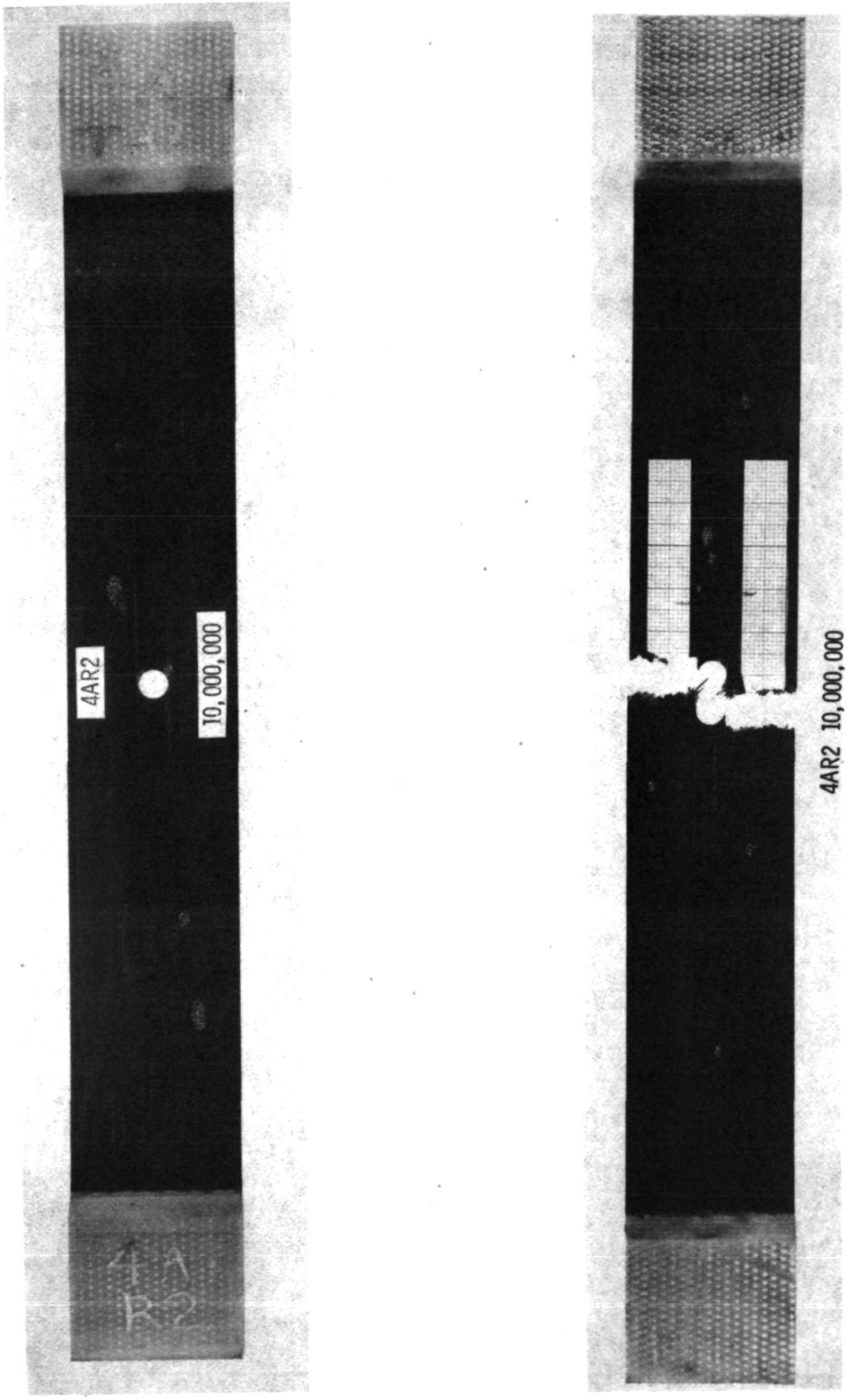

(a) Fatigue Damage (b) Residual Strength Test

Figure 17. Axial Fatigue Damage Growth and Residual Strength Test Failure Mode for a $[0_2/\pm45]_s$ Boron/Epoxy Laminate Subjected to Tension/Tension Fatigue Loading (S=.667)

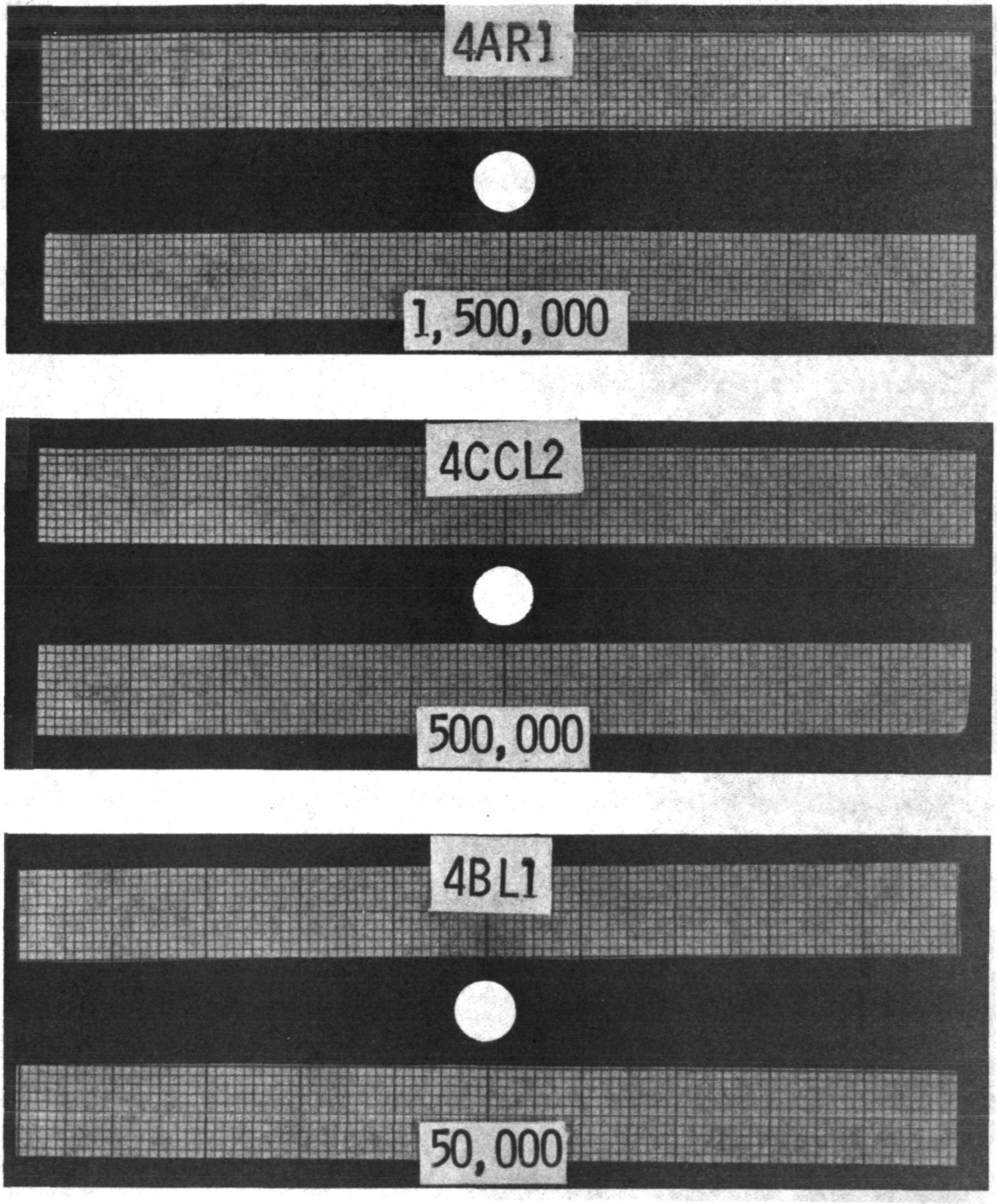

Figure 18. Axial Damage Growth for Different Fatigue Cycles for a $[0_2/\pm 45]_S$ Boron/Epoxy Laminate Subjected to Longitudinal Tension/Tension Fatigue Loading (S=.8)

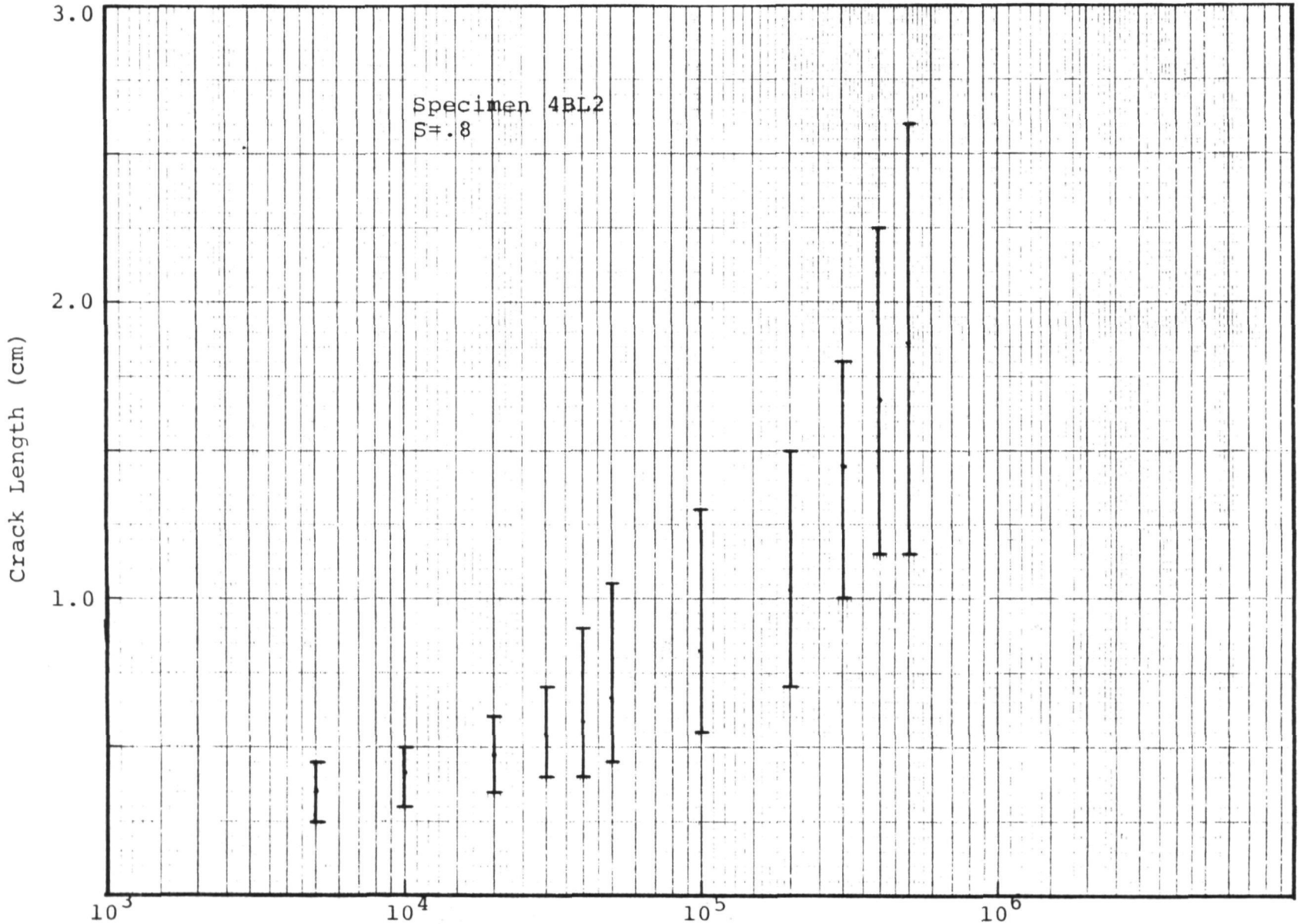

Figure 19. Axial Crack Length in 0° Surface Layers as a Function of Fatigue Cycles (S=.8)

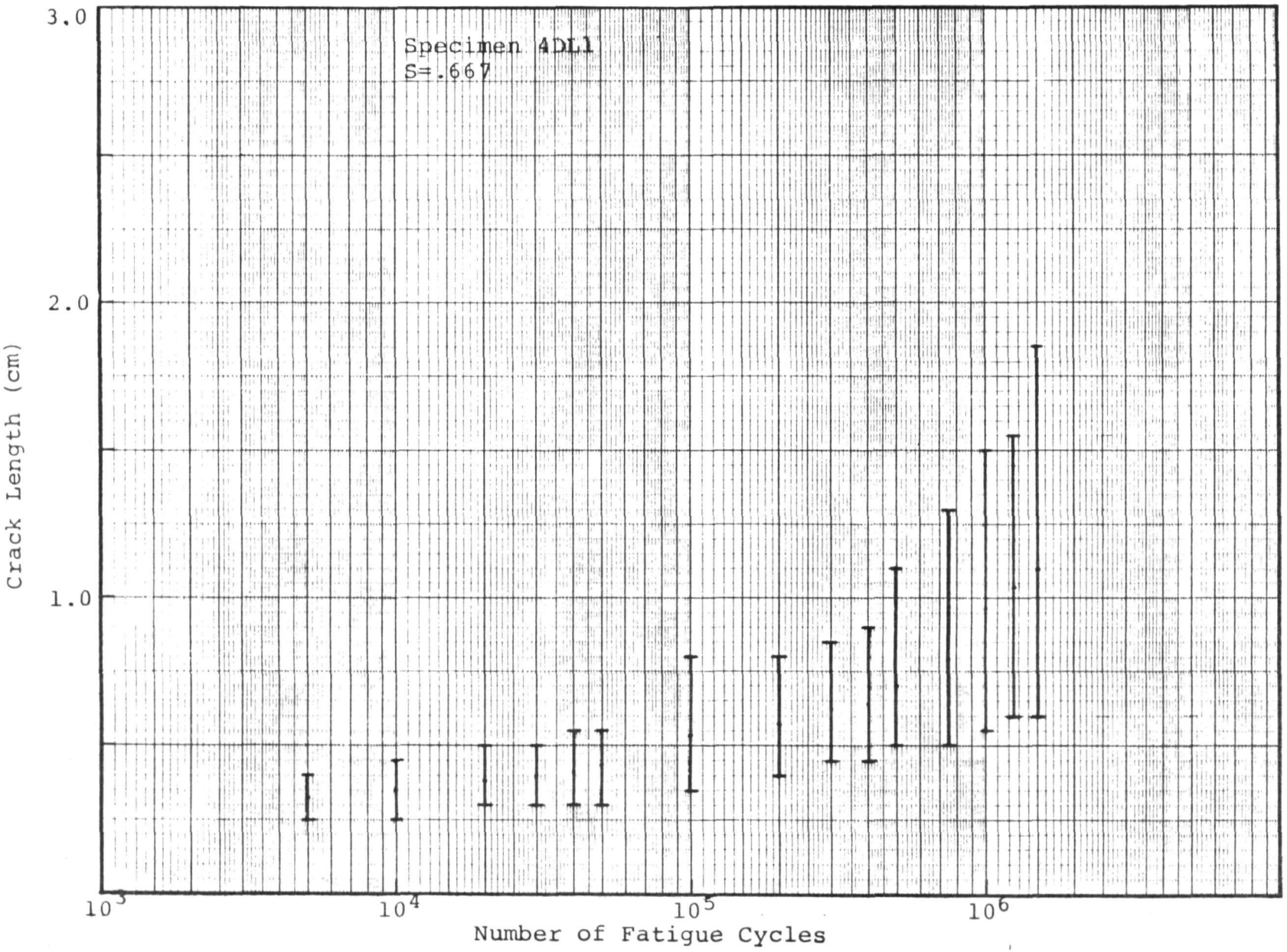

Figure 20. Axial Crack in 0° Surface Layers as a Function of Fatigue Cycles (S=.667)

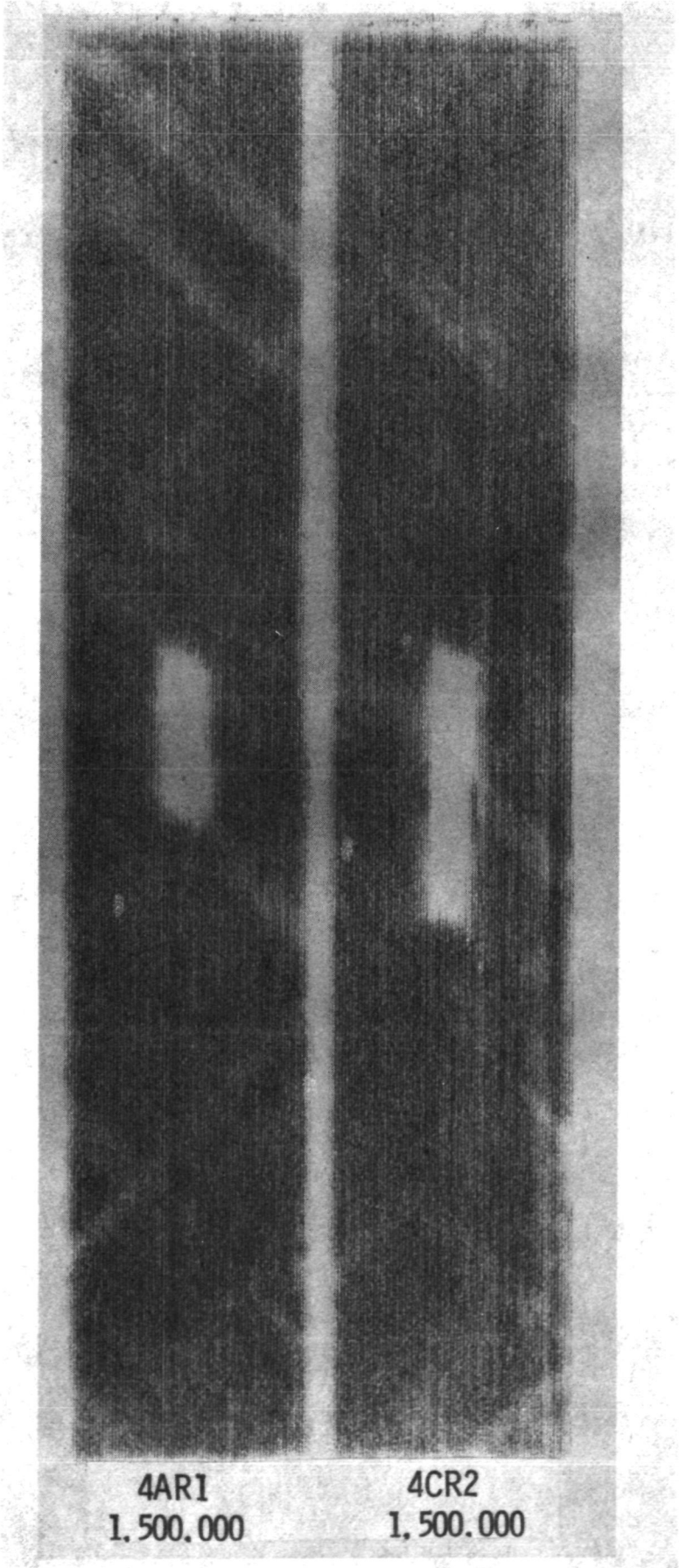

Figure 21. Typical "C" Scans Revealing Extent of Delamination Between 0° Surface Layers and ±45° Subsurface Layers in a Notched $[0_2/\pm45]_s$ Boron/Epoxy Laminate

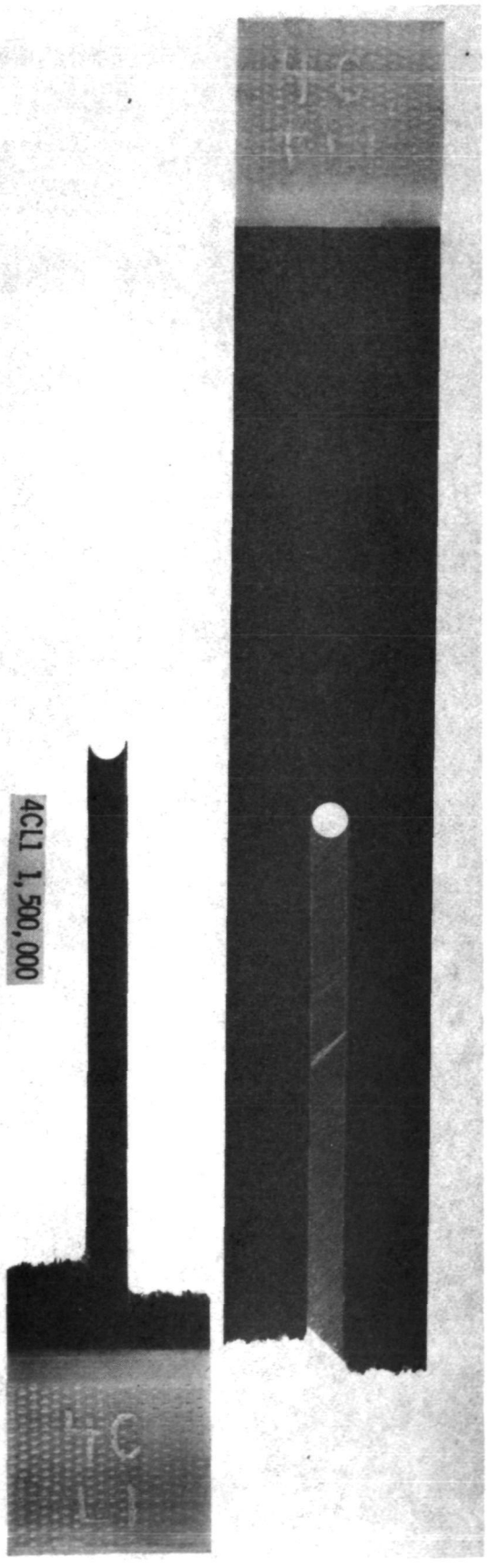

Figure 22. Fatigue Failure of a Notched $[0_2/\pm45]_s$ Boron/Epoxy Laminate Showing Delamination of the 0° Layers from the Laminate (S=.8)

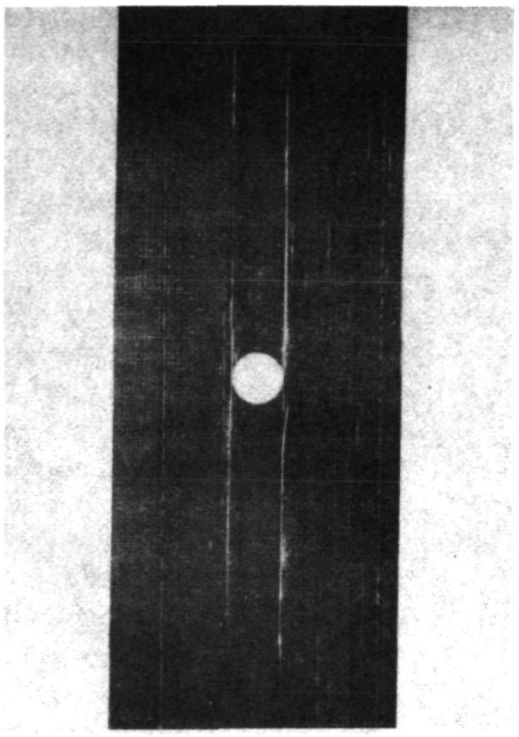

Front
(1.5 x 10^6 Cycles)

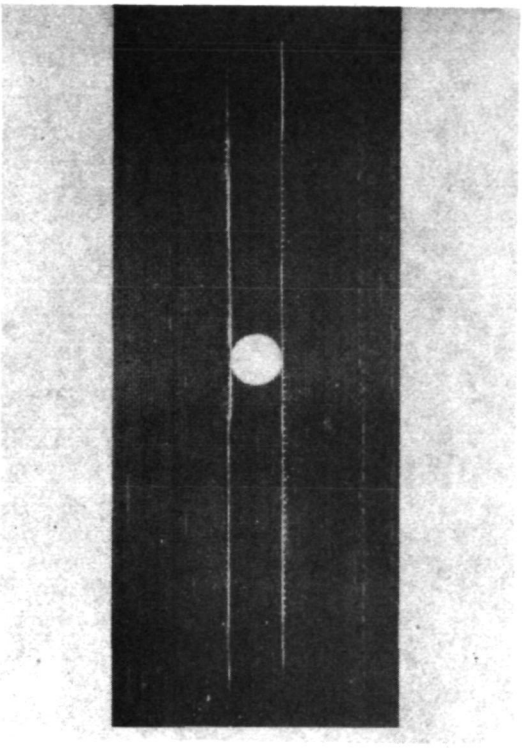

Back
(1.5 x 10^6 Cycles)

Figure 23. Axial Fatigue Damage Growth for a $[0_2/\pm45]_s$ Boron/Epoxy Laminate Subjected to Tension/Tension Fatigue Loading (S=.8); Courtesy G. L. Roderick, US AAMRDL, Langley Directorate

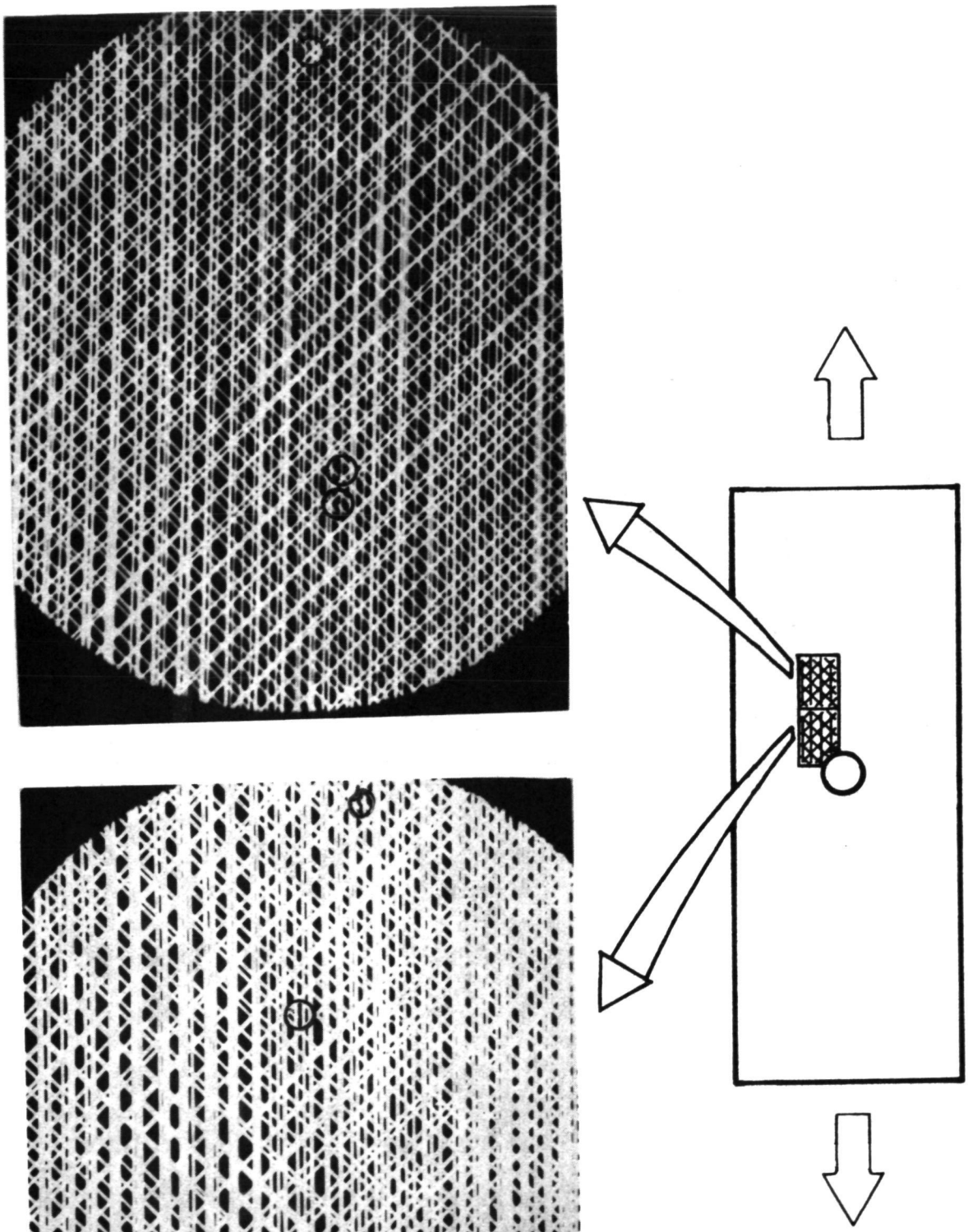

Figure 24. X-Ray Pictures Illustrating -45° Fiber Breaks at $N=1.5 \times 10^6$ for S=.8 (courtesy, G.L. Roderick, US AAMRDL, NASA Langley Research Center)

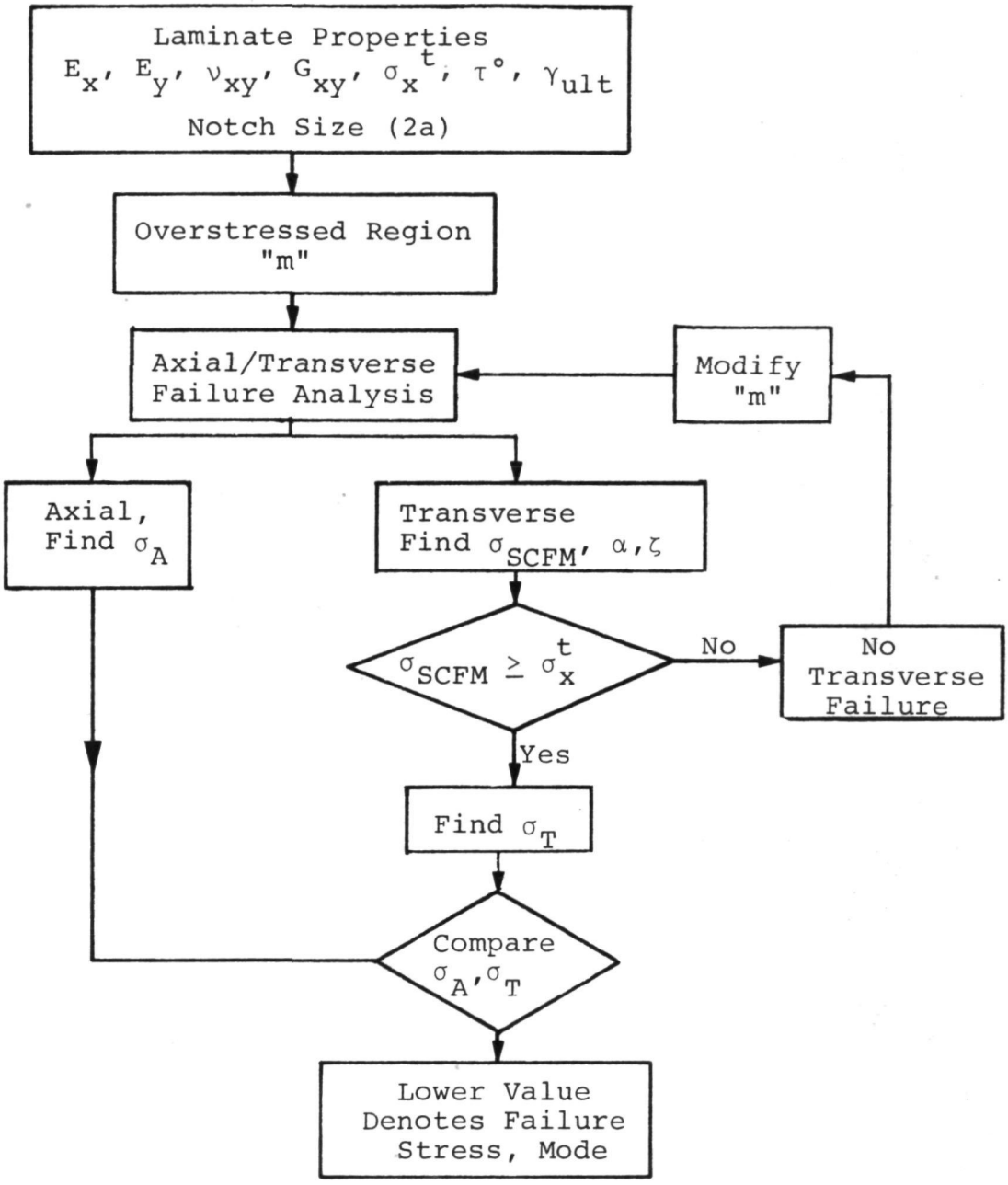

Figure 25. Static Failure Analysis Procedure for Axial/ Transverse Cracking

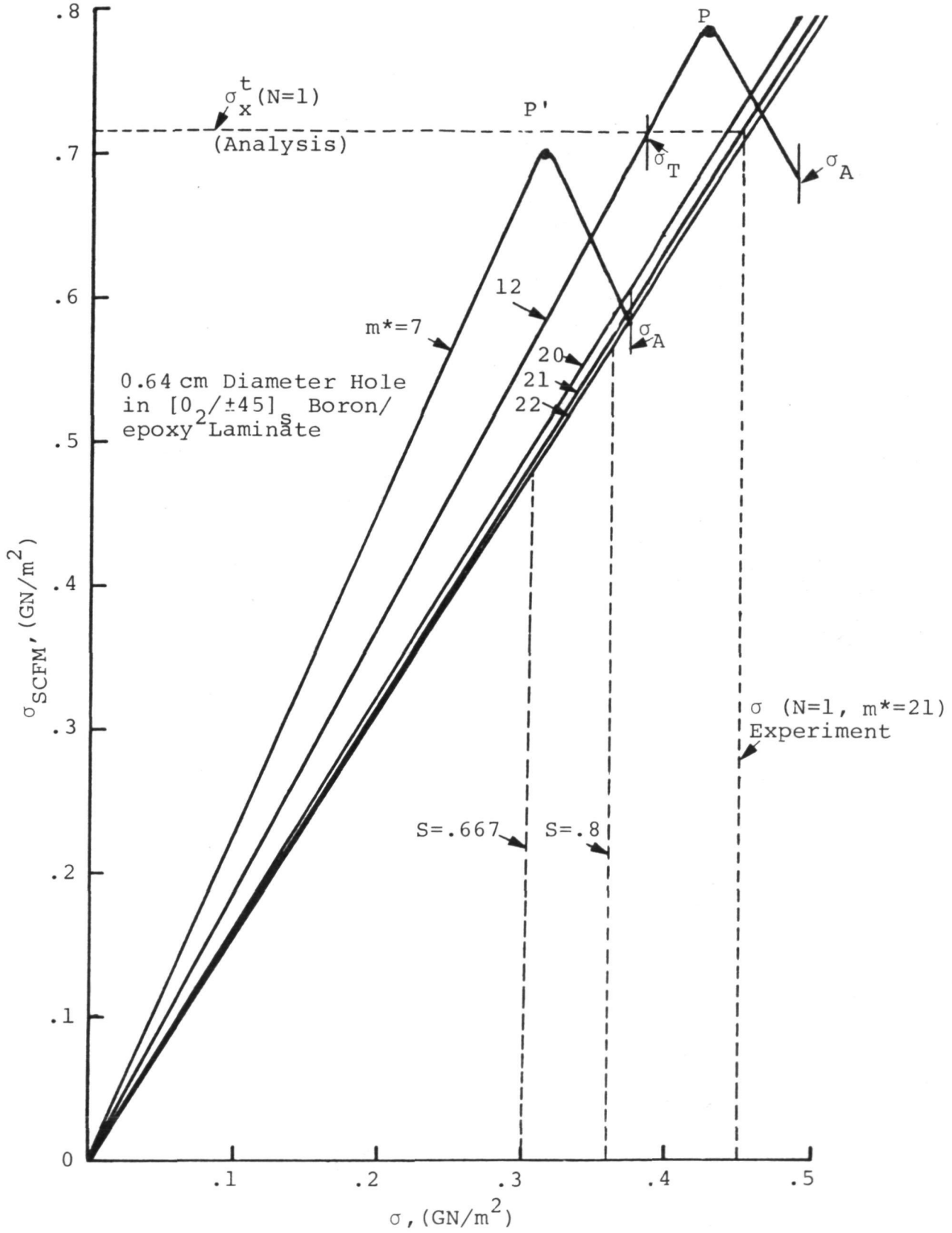

Figure 26. Variation of Notch Tip Overstress with Applied Stress for Different Values of m*

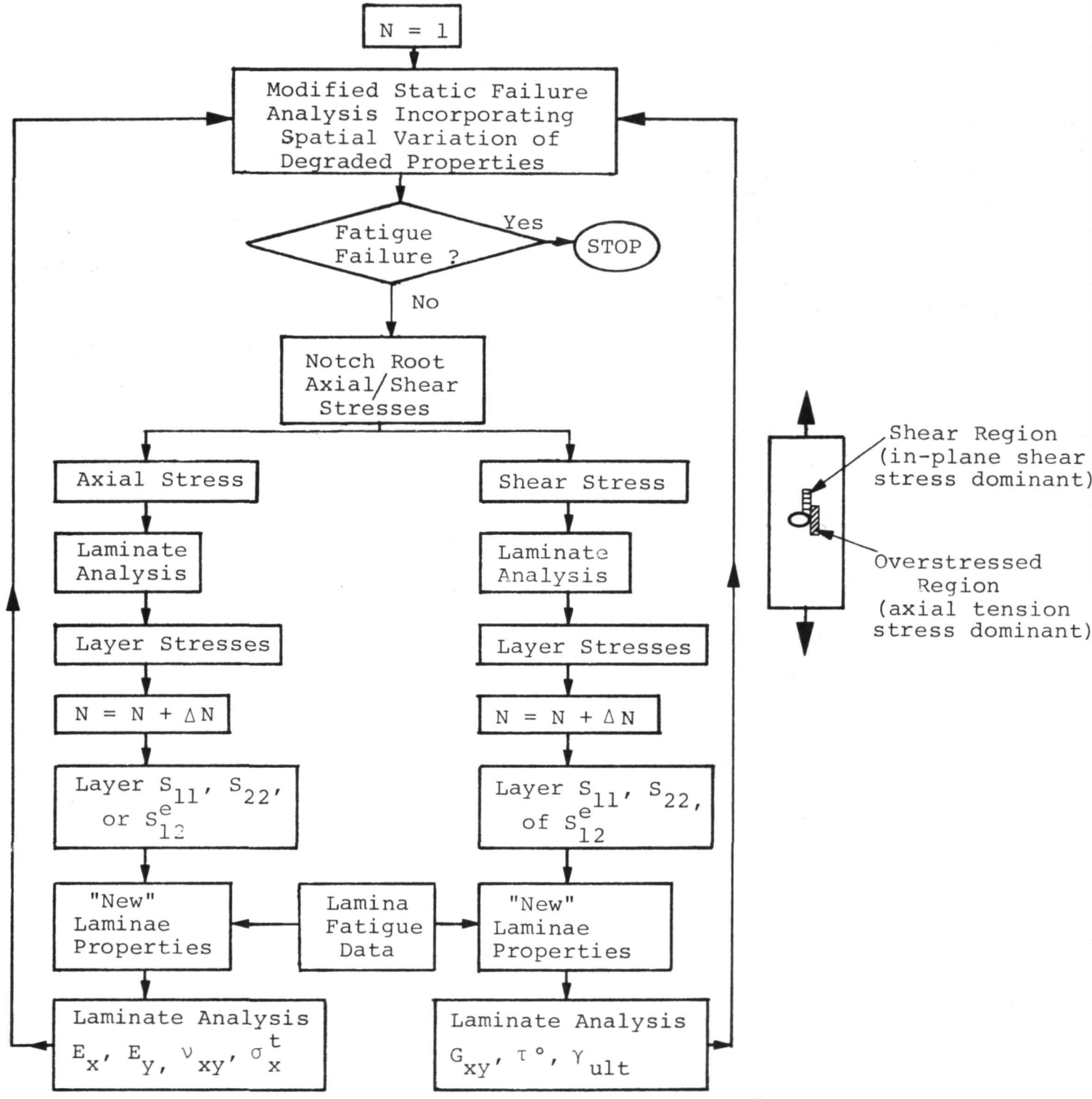

Figure 27. Fatigue Analysis Procedure

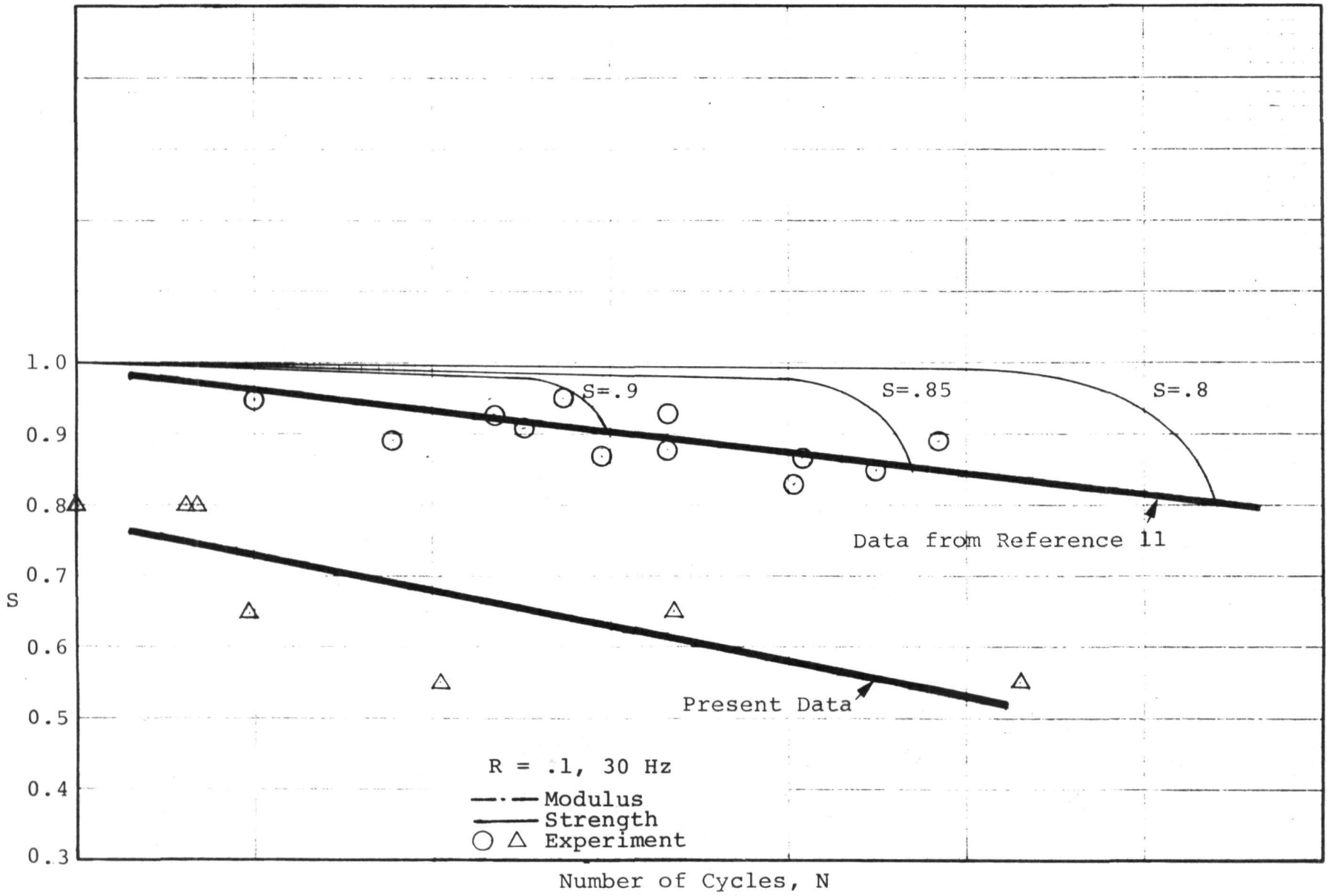

Figure 28. Unnotched [0] Boron/epoxy Laminate Longitudinal Tension/Tension Fatigue Data

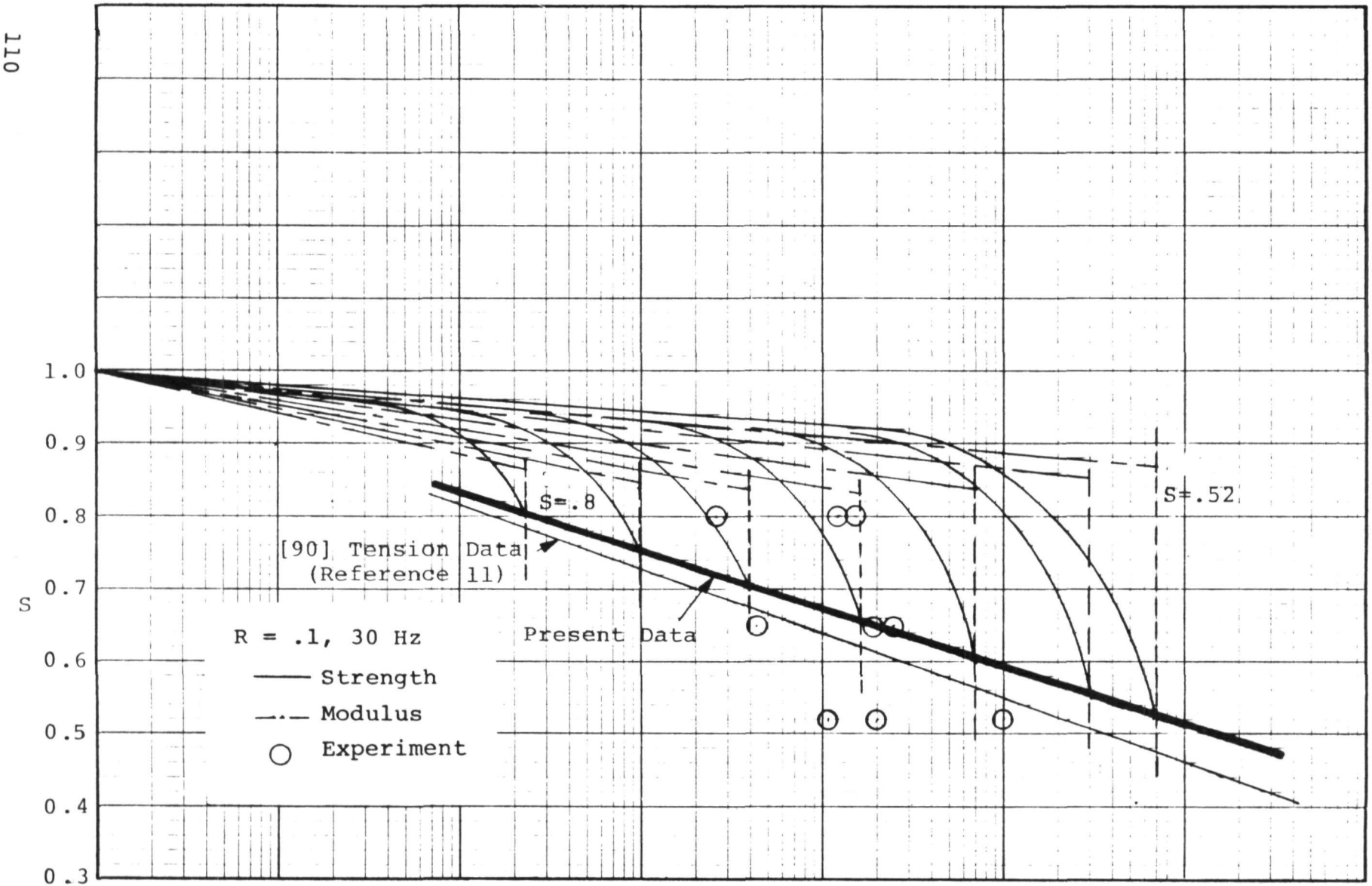

Figure 29. Unnotched $[\pm 45]_s$ Boron/epoxy Laminate In-Plane Shear Fatigue Data

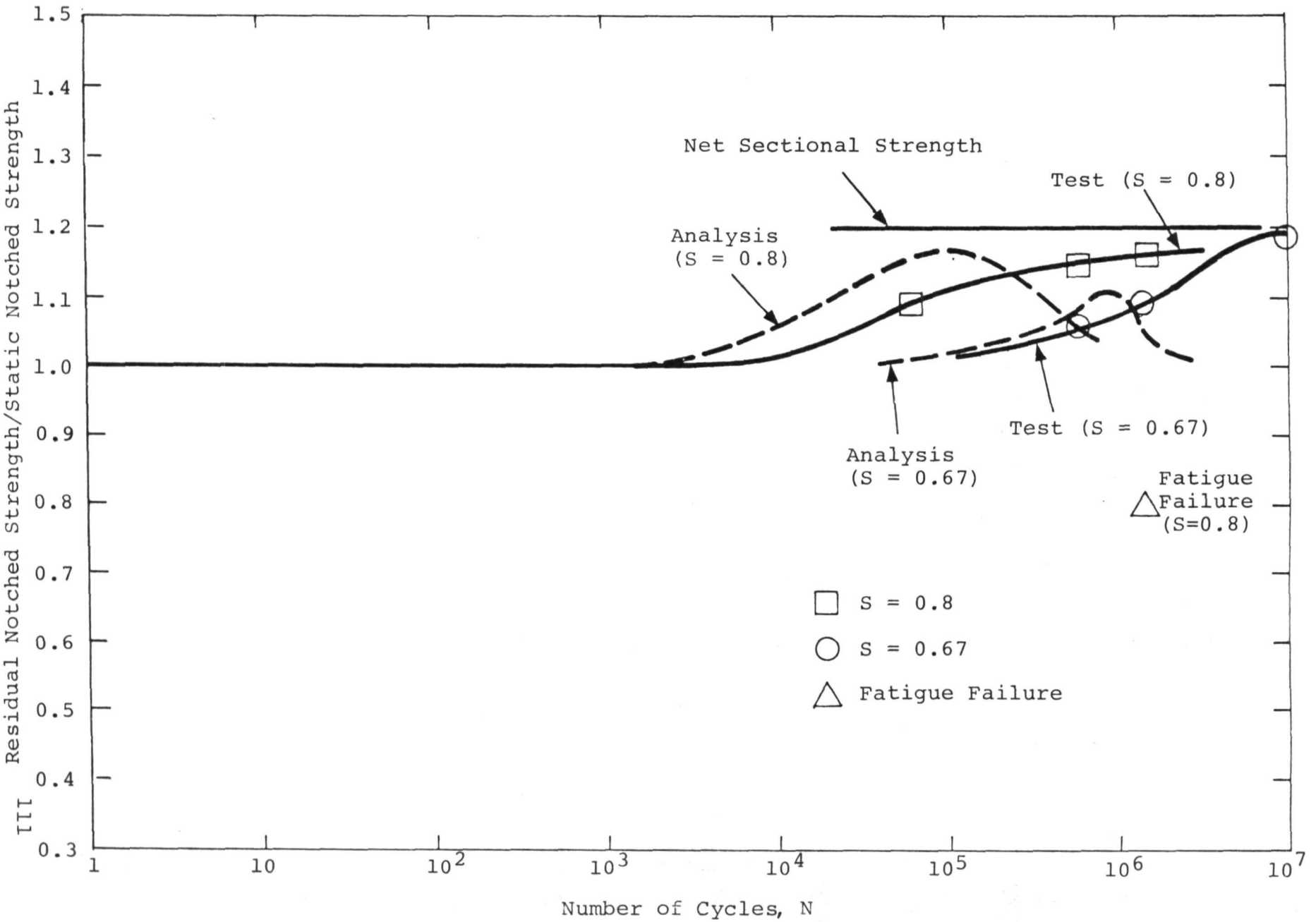

Figure 30. Variation of Residual Strength with Number of Cycles

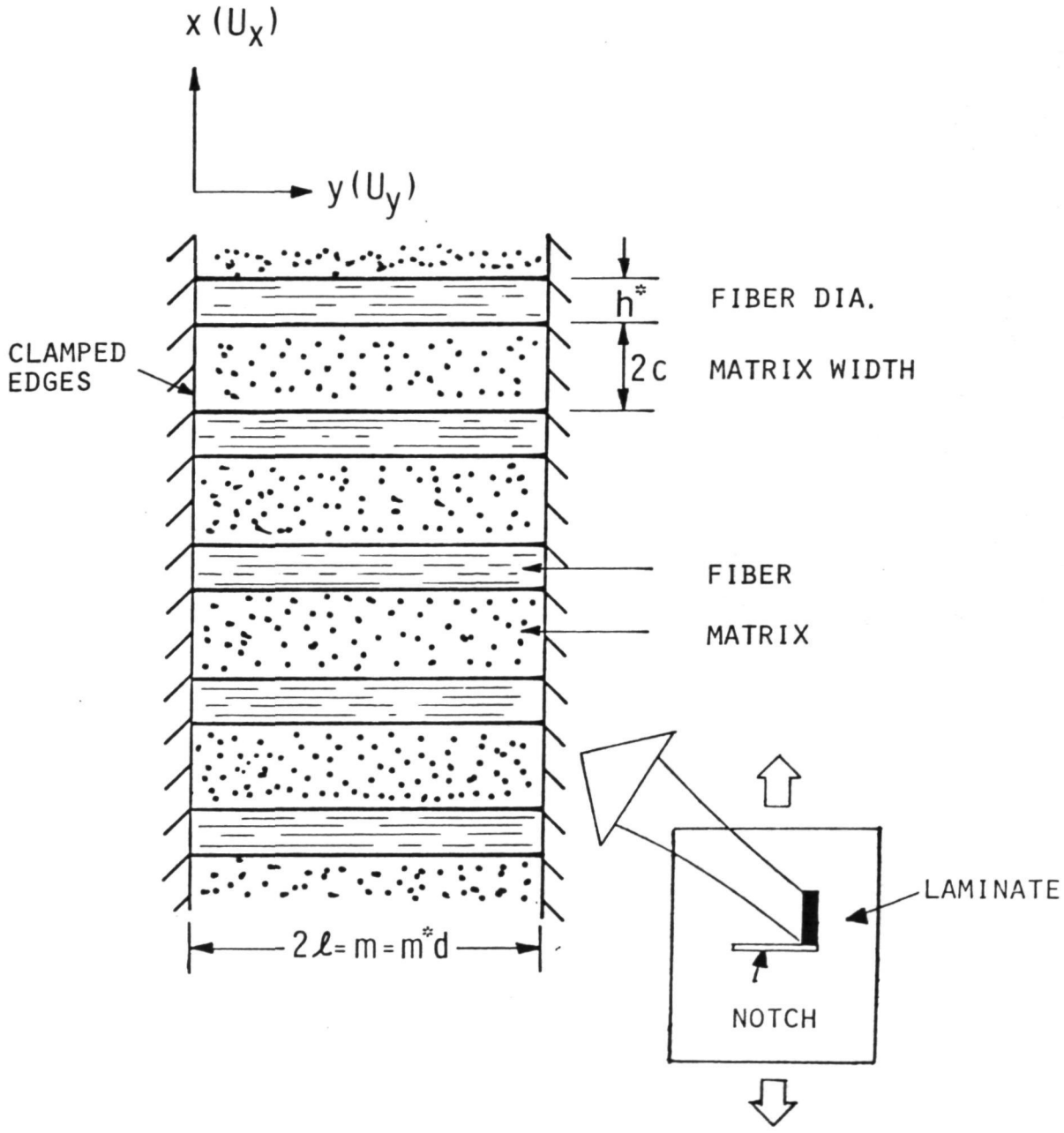

Figure A-1. [90] Lamina Boundary Conditions in the Shear Region for Calculating Modified Shear Modulus